Université de Valenciennes et du Hainaut-Cambrésis

Thèse de doctorat

Pour obtenir le grade de Docteur de l'Université de

VALENCIENNES ET DU HAINAUT-CAMBRESIS

Discipline, spécialité selon la liste des spécialités pour lesquelles l'Ecole Doctorale est accréditée :
Electronique

Présentée et soutenue par

Yamen ISSA.

Le 02/12/2013, à Valenciennes

Ecole doctorale :
Sciences Pour l'Ingénieur (SPI)

Equipe de recherche, Laboratoire :
Institut d'Electronique, de Micro-Electronique et de Nanotechnologie/Département d'Opto-Acousto-Electronique (IEMN/DOAE)

Contributions to Cooperative Diversity in Multiple Access UWB Systems

JURY

Président du jury
- BENSRHAIR, Abdelaziz. Professeur des Universités. INSA de Rouen, LITIS.

Rapporteurs
- VUONG, Tan-Phu. Professeur des Universités. Université de Grenoble INP, IMEP-LAHC.
- MEGHDADI, Vahid. Maître de Conférences HDR. Université de Limoges, ENSIL, Xlim.

Examinateurs
- BERBINEAU, Marion. Directrice de Recherche. IFSTTAR LEOST, Villeneuve d'ascq.
- SIMON, Éric. Maître de Conférences. Université de Lille 1, IEMN-TELICE.

Directeur de thèse
- DAYOUB, Iyad. Maître de Conférences HDR, Université de Valenciennes, IEMN-DOAE.

Université de Valenciennes et du Hainaut-Cambrésis

N°d'ordre : 13/28

Thèse de doctorat

Pour obtenir le grade de Docteur de l'Université de

VALENCIENNES ET DU HAINAUT-CAMBRESIS

Spécialité :
Electronique

Présentée et soutenue par
Yamen ISSA

Ecole Doctorale :
Sciences pour l'Ingénieur (SPI)

Equipe de recherche, Laboratoire :
Institut d'Electronique, de Micro-Electronique et de Nanotechnologie/Département d'Opto-Acousto-Electronique (IEMN/DOAE)

Contributions to Cooperative Diversity in Multiple Access UWB Systems

Soutenue le : 02/12/2013, à l'IEMN-DOAE (Valenciennes)

JURY

Rapporteurs
- VUONG, Tan-Phu. Professeur des Universités. Université de Grenoble INP, IMEP-LAHC.
- MEGHDADI, Vahid. Maître de Conférences HDR. Université de Limoges, ENSIL, Xlim.

Examinateurs
- BENSRHAIR, Abdelaziz. Professeur des Universités. INSA de Rouen, LITIS.
- BERBINEAU, Marion. Directrice de Recherche. IFSTTAR LEOST, Villeneuve d'ascq.
- SIMON, Eric. Maître de Conférences. Université de Lille 1, IEMN-TELICE.

Directeur de thèse
- DAYOUB, Iyad. Maître de Conférences HDR, Université de Valenciennes, IEMN-DOAE.

I dedicate this work to my father Afif, who always stands by my side,

To my wife Rasha, for her unconditional support and endless love,

To my family who supported me in the hardest times,

To my beloved son Rayan.

Acknowledgements

The work for this thesis was not only a very rich scientific experience, but also a great human experience for me. From one part, this work led me to experience the positive aspects of scientific research and deepen my knowledge in the communication field. On the other hand, it allowed me to integrate a teamwork and live a friendly and very rich culture. For that, this thesis could not have been accomplished without the help and collaboration of many people. I take this opportunity to extend my sincere gratitude and appreciation to all those who made this Ph.D thesis possible.

First and foremost, I would like to express my deepest gratitude to my research guide Dr. Iyad Dayoub who helped me through the most difficult times and introduced me to this exciting field of science. I am grateful to him for his dedicated advices, inspiration, encouragement, continuous support and valuable help throughout my Ph.D. His integral view on research and his great efforts for providing high-quality work, has made a deep impression on me. During our course of interaction, I have learnt extensively from him in scientific research as well as in practical life.

My special words of thanks should also go to Mr. Walaa Hamouda, professor at Concordia University in QC., for his support, guidance, scientific discussion and encouragement. His cooperation, motivation and support have accelerated my researches and kept me going ahead.

Also, I thank IEMN-DOAE laboratory members, Professor Jamal Assaad - director, professors of the laboratory and the secretary, for receiving me as a Ph.D. student. Thank you all for both the financial and technical help. Special thanks to my friends and colleagues in IEMN with whom I spent the most of my time.

I would like to take this opportunity to thank the University of Tishreen in Syria for granting me the scholarship that allowed me to continue my studies in France and especially to Dr. Hassan Abbas and Dr. Jamal Khalifeh, professors at the University of Tishreen for their support during my studies.

I must also thank the project CISIT for the financial support in the last year of my thesis.

Finally, and most importantly, I would like to thank my reviewing committee members for accepting to dedicate their time and effort to examine this work.

Title

Contributions to Cooperative Diversity in Multiple Access UWB Systems

Abstract

Wireless networks continue to gain popularity over wired networks while their users do not stop to grow their demands for high data rates. The new researches in this field try to meet these demands with the new orientation of the industry towards low cost, low power consumption and multifunctional small devices. Therefore, designer and researchers face a compromise between these goals and the required quality of service (QoS). In wireless network, multipath fading severely corrupts the link performance. Indeed, as a signal propagates through a wireless channel, it incurs random fluctuations in time, reflections, and attenuation due to the wireless link nature and the arbitrarily movement of the users. Multiple input multiple output (MIMO) system is an effective countermeasure to combat multipath effects and to provide spatial diversity to the receiver. But it requires the implementation of physically separated antennas in order to have independent fading effects. Theoretically, MIMO systems increase the capacity of wireless links compared to systems with single transmit or receive antenna (SISO). In the same context, ultra wideband (UWB) technology offers unique qualities such as the unlicensed re-utilization of the allocated spectrum. This technology can underlay existing radio systems using signal with low power and quasi flat power spectral densities (PSD). In addition, UWB signals occupy wide bandwidth leading to fine time resolution which can be employed for localization applications as well as a high capacity and data rates. All these advantages make this technology a very interesting choice for low and high rate communication in different applications. Motivated by the aim to answer to the new demands in the field of wireless communication while preserving simplicity, low cost, and low power consumption; we propose to use cooperative diversity in conjunction with UWB technology in wireless networks. Cooperative diversity is indeed an alternative of the well-known diversity techniques where instead of installing multiple antennas on each node, these nodes can share their antennas to relay each other's signal in such a way that they form a virtual antenna array (virtual MIMO system). To show the benefits of the proposed solution, we study an UWB system with cooperation schemes in multipath environment using decode-and-forward (FD) relaying protocol. Next, we compare the bit error performance of the proposition with the case of non-cooperative UWB communication in same environment. We consider, respectively, time hopping pulse position modulation (TH-PPM) and direct sequence binary phase shift keying (DS-BPSK) systems. Due to the high number of multipath components (MPCs) in UWB channel, we refer to use partial Rake (P-Rake) receiver

in our simulation. We analytically analyze the decision variable at the output of Rake receiver and present simulation results of the BER performance of these two systems under different UWB channel considering the IEEE 802.15.4a standard, more precisely, residential and office line-of-sight (LOS) and non-line-of-sight (NLOS) channel environments. Our results show that the relay cooperation significantly improves the performance of the two systems under different scenarios, and that the diversity gain increases proportionally with the number of cooperative relays. Increasing the number of fingers in a RAKE receiver will enhance the systems performance but will, unfortunately, increase the complexity of the design. In order to remedy this problem, we can use selective Rake (S-RAKE) receiver, which combines the best MPCs of the received signal. In presence of multiple access interference (MAI), our results show that the overall system performance degrades significantly, but the benefit of cooperation is still moderately effective. The performance in this case is limited in terms of attainable diversity that the source-relay link becomes worse when MAI is present. Hence, if better reliability is achieved at the relay nodes, the diversity may be improve, or may even be maintained. In light of this, we propose to employ antenna selection at the relay receiver in order to improve the reliability of the source-relay link. We assume that the relay node is equipped with multiple antennas and the receiver selects the best antenna which corresponds to the best sub-channel between the source and the relay out of the available sub-channels. The proposal based on the principle of antenna selection can maintain a good performance in the presence of AMI. The consequence of this is that, while leveraging the benefits of the available antennas at the relay, the number of radio frequency (RF) chains is reduced to the number of selected antennas, which leads to reduced cost and complexity.

Keywords: *Cooperative diversity, cooperative networks, sensor networks, UWB, virtual MIMO, antennas selection, Rake receiver.*

Titre

Contributions à la diversité coopérative dans les systèmes ULB à accès multiple

Résumé

Les réseaux sans fil continuent à gagner en popularité sur les réseaux filaires, tandis que leurs utilisateurs ne cessent pas de croître leurs demandes pour des débits élevés. Les nouvelles recherches dans ce domaine tentent de répondre à ces demandes avec la nouvelle orientation de l'industrie vers les petits appareils multifonctionnels à faible coût et à faible consommation d'énergie. Par conséquent, le concepteur et les chercheurs sont confrontés à un compromis entre ces objectifs et la qualité de service (QoS) requise. Dans les systèmes radio mobiles, l'évanouissement dû aux multi-trajets sévèrement corrompt la performance de la liaison de communication. En effet, lorsqu'un signal radio se propage à travers un canal sans fil, il subit des fluctuations aléatoires, des réflexions et d'atténuation due à la nature de la liaison sans fil et la mobilité arbitraire des utilisateurs. Le système (multiple-input multiple-output MIMO) est une contre-mesure pour lutter contre l'évanouissement dû aux multi-trajets qui permit d'introduire la pleine diversité spatiale. Mais, souvent l'intégration d'antennes multiples au niveau de l'émetteur ou du récepteur est coûteuse. Théoriquement, les systèmes MIMO augmentent la capacité du canal sans fil par rapport aux systèmes avec une seule entrée et une seule sortie (single-input single-output SISO). Dans le même contexte, la technologie ultra-large bande (ULB) offre des qualités uniques telles que la réutilisation libre sans licence du spectre attribué. Cette technologie peut coexister avec les systèmes radio existants grâce à l'utilisation de signaux impulsionnels de faible densité spectrale de puissance (PSD). En outre, les signaux ULB occupent une large bande passante menant à la résolution temporelle fine qui peut être utilisé pour des applications de localisation ainsi qu'une grande capacité et hauts débits. Tous ces avantages font que la technologie ULB devient un choix très intéressant pour les communications et la transmission de données à bas et à haut débit. Pour répondre aux nouvelles exigences dans le domaine de la communication sans fil, tout en préservant la simplicité, faible coût et faible consommation d'énergie, nous proposons d'utiliser la diversité coopérative en conjonction avec la technologie ULB. En effet, la diversité coopérative est une alternative des techniques de diversité spatiale bien connues. Mais, à la place de l'installation de plusieurs antennes sur chaque nœud, ces nœuds peuvent partager les antennes des autres nœuds qui se trouvent dans le voisinage pour relayer le signal de la source de telle sorte qu'ils forment un réseau d'antennes virtuelle (système MIMO virtuel). Pour montrer l'utilité de la solution proposée, nous étudions un système ULB coopératif dans environnement à trajets multiples en utilisant le protocole de

coopération decode-and-forward (FD). Ensuite, nous comparons la performance de la proposition en termes de taux d'erreur binaire (TEB) avec le cas d'un système ULB non-coopératif dans le même environnement. Par la suite, nous considérons, respectivement, une technique d'accès multiple par saut temporel avec une modulation de la position d'impulsion (time hopping pulse position modulation TH-PPM) et une technique d'accès multiple par séquence directe et une modulation de phase à deux états (direct sequence binary phase shift keying DS-BPSK). En raison du nombre élevé de trajets multiples dans le canal ULB, un récepteur Rake partielle (P-Rake) est utilisé à la réception. Nous analysons analytiquement la variable de décision à la sortie du récepteur Rake et présentons des résultats de simulation de la performance en termes de TEB pour les deux systèmes proposés sous différents canaux ULB compte tenu de la norme IEEE 802.15.4a, plus précisément, les environnements résidentiels et de bureaux à ligne directe (line-of-sight LOS) et sans ligne directe (non-line-of-sight NLOS). Nos résultats montrent que la coopération avec des relais améliore significativement les performances de ces systèmes dans différents scénarios, et que le gain de diversité augmente proportionnellement avec le nombre de relais. L'augmentation de nombre de correlateurs dans le récepteur Rake permet d'améliorer la performance des systèmes, mais augmente, malheureusement, la complexité de la conception à la réception. Afin d'y remédier, nous utilisons un récepteur sélectif S-Rake, qui tente de combiner les meilleurs trajets du signal reçu. En présence d'interférences d'accès multiple (IAM), nos résultats montrent que la performance du système se dégrade de manière significative, mais l'avantage de la coopération est encore modérément efficace. La performance dans ce cas est limitée en termes de diversité achevée parce que le canal entre la source et le relais devient moins favorable en présence d'IAM. Cependant, si une meilleure fiabilité est atteinte au récepteur du relais, la diversité peut être maintenue. C'est pourquoi nous proposons d'utiliser la technique de sélection d'antenne au relais afin d'améliorer la fiabilité du canal source-relais. Nous supposons que le nœud relais est équipé de plusieurs antennes et que le récepteur sélectionne la meilleure antenne qui correspond au meilleur sous-canal entre la source et le relais sur les sous-canaux disponibles. Cette proposition basée sur le principe de sélection d'antenne permet de maintenir une bonne performance en présence d'IAM. Ainsi, nous pouvons profiter de la diversité d'antennes multiples disponibles au relais toute en n'utilisant qu'une seul chaîne radiofréquence (RF), qui conduit à une réduction des coûts et de la complexité.

Mots-clés: *diversité coopérative, réseaux coopératifs, réseaux de capteurs, ULB, MIMO virtuel, sélection d'antennes, récepteur Rake.*

Contents

List of Figures **12**

List of Tables **13**

List of acronyms **19**

0.1 Context and Motivation 20

0.2 Thesis Contributions 22

0.3 Thesis Organization 23

1 Cooperative Network - Background **25**

1.1 Introduction 26

1.2 Signal Propagation Over Wireless Channel 26

1.2.1 Large-scale fading 27

1.2.2 Small-scale fading 27

1.3 Diversity techniques 28

1.3.1 Spectral diversity 28

1.3.2 Temporal diversity 29

1.3.3 Spatial diversity 29

1.4 Multiple-Input Multiple-Output (MIMO) system 29

1.5 Cooperative communications 31

1.5.1 Ad-hoc Networks 31

1.5.2 Relaying protocols 32

1.5.3 Virtual MIMO System (Cooperative Diversity) 35

1.6 Antenna/relay selection 38

1.7 Conclusion 39

2 Ultra Wideband Communications **41**

2.1 Introduction . . . 43

2.2 Definition of UWB signals . . . 43

2.3 Motivation for the use of ultra wideband (UWB) . . . 44

2.4 UWB Pulse Waveforms . . . 47

2.4.1 Gaussian Pulse . . . 47

2.4.2 Gaussian Monocycle Pulse . . . 48

2.4.3 Gaussian doublet Pulse . . . 49

2.5 Pulse Modulation . . . 50

2.5.1 Pulse Position Modulation (PPM) . . . 51

2.5.2 Binary Phase Shift Keying (BPSK) . . . 52

2.6 Multiple Access Techniques . . . 52

2.6.1 Time Hopping Multiple Access . . . 53

2.6.2 Direct Sequence Multiple Access . . . 54

2.7 UWB Channel Model . . . 55

2.7.1 General Overview of UWB channel models . . . 55

2.7.2 The IEEE 802.15.4a channel Models . . . 57

2.8 Conclusions . . . 61

3 Proposed System Model: Description and Methodology **63**

3.1 Introduction . . . 64

3.2 System Description . . . 64

3.3 Transmitter Model . . . 64

3.4 Channel Models . . . 67

3.4.1 Residential environments . . . 68

3.4.2 Indoor office environments . . . 68

3.5 Receiver Structure . . . 69

3.5.1 Rake Receiver . . . 71

3.5.2 Channel estimation . . . 73

3.5.3 Maximum Ratio Combining (MRC) . . . 73

3.6 Conclusions . . . 74

4 System Performance - TH-PPM **75**

4.1 Introduction 76

4.2 Cooperative TH-PPM Impulse Radio UWB system 76

4.3 Decision Variable Statistics 79

4.4 BER Performance Analysis 82

4.5 Simulation Results And Discussion 82

4.6 Conclusions 89

5 System Performance - DS-BPSK **91**

5.1 Introduction 92

5.2 Cooperative DS-BPSK IR-UWB system 92

5.3 Decision Variable Statistics 95

5.4 BER Performance Analysis 98

5.5 Simulation Results And Discussion 98

5.6 Conclusions 107

General Conclusions and Future Works **109**

Bibliography **113**

List of Figures

1.2.1 Path loss, shadowing and multipath fading versus distance. 27

1.4.1 Centralized MIMO System. 30

1.5.1 (a) Infrastructure exchange mode. (b) Ad-hoc exchange mode. 31

1.5.2 Principle of amplify-and-forward relaying protocol. 33

1.5.3 Principle of decode-and-forward relaying protocol. 33

1.5.4 Relaying architectures: (a) classical relay channel, (b) multiple-access channel with relaying, (c) parallel relay channel, (d) broadcast channel with relaying, (e) cluster-to-cluster relaying channel. 34

1.5.5 Virtual MIMO system using cooperative communication. 37

2.2.1 FCC emission limits mask for UWB indoor communications. 44

2.3.1 Coexistence of UWB with different narrowband communications (GPS: global positioning system, PCS: personal communications service, Bluetooth, 802.11b, cordless phones, microwave ovens, 802.11a HiperLan). 45

2.4.1 Gaussian pulse. (a) Time domain. (b) Normalized power spectral density. . . . 48

2.4.2 Gaussian monocycle pulse. (a) Time domain. (b) Normalized power spectral density. 49

2.4.3 Gaussian doublet pulse. (a) Time domain. (b) Normalized power spectral density. 50

2.5.1 Illustration of pulse modulation techniques. (a) PPM. (b) BPSK. T_p is the pulse duration, δ is the PPM pulse shift. 51

2.6.1 Pulse trains with TH sequences $\{2, 0, 3, ...\}$ for user 1 and $\{4, 2, 0, ...\}$ for user 2. T_f is the frame duration, T_c is the chip duration. 53

2.6.2 Time window of DS-UWB with PN sequences $\{1, 1, 1, -1, 1, -1, -1\}$. T_b is the bit duration, T_c is the chip duration. 55

2.7.1 IEEE 802.15.4a UWB channel model 59

3.2.1 Block diagram of multiple user UWB communication system. 65

3.3.1 General cooperative system model. 66

3.4.1 Power delay profile of the impulse responses for (a) CM1: IEEE 802.15.4a residential LOS and (b) CM2: IEEE 802.15.4a residential NLOS. 69

3.4.2 Power delay profile of the impulse responses for (a) CM3: IEEE 802.15.4a office LOS and (b) CM4: IEEE 802.15.4a office NLOS. 69

3.5.1 Block diagram of Rake Receiver. 72

4.5.1 BER performance of TH-PPM UWB non-cooperative and cooperative (with 1 and 2 relays) system with error-free detection at relay nodes for 5 P-Rake and 5 S-Rake under CM1 . (a) Without MAI. (b) In presence of MAI of one additional user. 84

4.5.2 The BER performance of TH-PPM UWB system with relay cooperation under CM2 with error-free detection at relay nodes. (a) Without MAI. (b) In presence of MAI of one additional user. 85

4.5.3 The BER performance of TH-PPM UWB system with relay cooperation under CM3 with error-free detection at relay nodes. (a) Without MAI. (b) In presence of MAI of one additional user. 85

4.5.4 The BER performance of TH-PPM UWB system with relay cooperation under CM4 with error-free detection at relay nodes. (a) Without MAI. (b) In presence of MAI of one additional user. 86

4.5.5 The BER performance of TH-PPM UWB system with relay cooperation under CM1 with error at relay nodes. (a) Without MAI. (b) In presence of MAI of one additional user. 87

4.5.6 The BER performance of TH-PPM UWB system with relay cooperation under CM2 with error at relay nodes. (a) Without MAI. (b) In presence of MAI of one additional user. 87

4.5.7 The BER performance of TH-PPM UWB system with relay cooperation under CM3 with error at relay nodes. (a) Without MAI. (b) In presence of MAI of one additional user. 88

4.5.8 The BER performance of TH-PPM UWB system with relay cooperation under CM4 with error at relay nodes. (a) Without MAI. (b) In presence of MAI of one additional user. 88

5.2.1 General cooperative system model. 93

5.5.1 BER performance of DS-BPSK UWB non-cooperative and cooperative (with 1 and 2 relays) system with error-free detection at relay nodes using 5 P-Rake receiver under CM1 . (a) Without MAI. (b) In presence of MAI of one additional user. 99

5.5.2 BER performance of DS-BPSK UWB non-cooperative and cooperative (with 1 and 2 relays) system with error-free detection at relay nodes using 5 P-Rake receiver under CM2 . (a) Without MAI. (b) In presence of MAI of one additional user. 100

5.5.3 BER performance of DS-BPSK UWB non-cooperative and cooperative (with 1 and 2 relays) system with error-free detection at relay nodes using 5 P-Rake receiver under CM3 . (a) Without MAI. (b) In presence of MAI of one additional user. 100

5.5.4 BER performance of DS-BPSK UWB non-cooperative and cooperative (with 1 and 2 relays) system with error-free detection at relay nodes using 5 P-Rake receiver under CM4 . (a) Without MAI. (b) In presence of MAI of one additional user. 101

5.5.5 BER performance of DS-BPSK UWB system with relay cooperation under CM1 with error at relay nodes. (a) Without MAI. (b) In presence of MAI of one additional user. 102

5.5.6 BER performance of DS-BPSK UWB system with relay cooperation under CM2 with error at relay nodes. (a) Without MAI. (b) In presence of MAI of one additional user 102

5.5.7 BER performance of DS-BPSK UWB system with relay cooperation under CM3 with error at relay nodes. (a) Without MAI. (b) In presence of MAI of one additional user 103

5.5.8 BER performance of DS-BPSK UWB system with relay cooperation under CM4 with error at relay nodes. (a) Without MAI. (b) In presence of MAI of one additional user 103

5.5.9 BER performance of DS-BPSK UWB system with relay cooperation under CM1 with error at relay nodes. (a) Without MAI. (b) In presence of MAI of one additional user. 105

5.5.10 BER performance of DS-BPSK UWB system with relay cooperation under CM2 with error at relay nodes. (a) Without MAI. (b) In presence of MAI of one additional user 105

5.5.11 BER performance of DS-BPSK UWB system with relay cooperation under CM3 with error at relay nodes. (a) Without MAI. (b) In presence of MAI of one additional user 106

5.5.12 BER performance of DS-BPSK UWB system with relay cooperation under CM4 with error at relay nodes. (a) Without MAI. (b) In presence of MAI of one additional user 106

5.6.1 Relay inter-vehicle transmission scheme. 111

List of Tables

3.4.1 Parameters for residential channel models CM1 and CM2. 70

3.4.2 Parameters for office channel models CM1 and CM2. 71

4.5.1 Difference in the average SNRs Between S-R or R-D and S-D links when the relay node is exactly located at the middle point between the source and the destination. 83

List of Acronyms

A-Rake	All-Rake
AF	Amplify-and-forward
ARQ	Automatic repeat request
AS	Antenna selection
AWGN	Additive white Gaussian noise
BPSK	Binary phase-shift keying
CDMA	Code division multiple-access
CF	Compress-and-forward
CSI	Channel state information
D	Destination
DA	Data-aided
DARPA	Defense advanced research projects agency
DF	Decode-and-forward
DoD	Department of defense
DS	Direct Sequence
DS-BPSK	Direct sequence-binary phase shift keying
DS-CDMA	Direct sequence code division multiple access
DSSS	Direct sequence spread spectrum
DS-UWB	direct sequence UWB system
EF	Estimate-and-forward
EGC	Equal-gain combining
FH-SS	Frequency hopping spread spectrum
EIRP	Equivalent isotropic radiated power

FC	Full-complexity
FCC	Federal Communications Commission
FD	Full diversity
FEC	Forward error correction
Gbps	Gigabits per second
GPS	Global positioning system
GSM	Global system for mobiles
HDAF	Hybrid decode-amplify-forward
IPI	Inter-path interference
IR	Impulse Radio
IR-UWB	Impulse radio ultra wideband
ISI	Inter-symbol interference
LOS	Line-of-sight
MANET	Mobile Ad-hoc network
MIMO	Multiple inputs multiple outputs
MPC	Multipath component
MRC	Maximum ratio combination
NLOS	Non-line-of-sight
OFDM	Orthogonal frequency-division multiplexing
OOK	On-off keying
OSD	Office of the secretary of defense
P-Rake	Partial-Rake
P-RAKE-MRC	Partial RAKE with MRC
PAM	Pulse amplitude modulation
PAN	Personal area network

PCS	Personal communications service
PDF	Probability density function
PN	Pseudo-noise
PPM	Pulse position modulation
PSD	Power spectral density
PSM	Pulse shape modulation
QoS	Quality of service
R	Relay
RF	Radio frequency
S	Source
S-Rake	Selective-Rake
SC	Successive channel
SIMO	Single input multiple outputs
SNR	Signal-to-noise ratio
SV	Saleh-Valenzuela
SW	Sliding window
TH	Time Hopping
TH-PPM	Time hopping-pulse position modulation
USB	Universal serial bus
UWB	Ultra wideband
WAN	Wide area network
WLAN	Wireless local area network
WPAN	Wireless personal area network
WSN	Wireless sensor network

General Introduction

Contents

0.1 Context and Motivation **20**

0.2 Thesis Contributions **22**

0.3 Thesis Organization **23**

0.1 Context and Motivation

During the last decades, we notice the trend in consumers technology towards wireless communication systems. Indeed, this technology offers the access capability to voice and data applications without limiting the liberty of movement. Wireless consumers and service providers do not stop to grow their demands for high data rates. The new researches in this field try to meet these demands with the new orientation of the industry towards low cost, low power consumption and multifunctional small devices. Therefore, designer and researchers face a compromise between these goals and the required quality of service (QoS). The wireless networks today exist on several levels: WANs (wide area networks) such as GSM (global system for mobiles), WLANs (wireless local area networks) with WIFI connections and WPANs (wireless personal area networks) with Bluetooth connectivity for example. These technologies connect computers, mobile phones and other devices without the disadvantages of wires. Nowadays, most people are always in touch with each others at anytime, almost any where through hand-held devices. Free of cable connections at home, one can surf the internet, share photos and movies across multiple devices, print wirelessly, play games and even stream TV stations.

The Bluetooth technology was dominant for many years in WPANs for short range transmission and peer-to-peer connection. Since the throughput of Bluetooth does not exceed 1Mbps [1], it could not compete with the high rate of the ultra wideband (UWB) technology. The high rate of UWB makes this technology promising for wireless networks across the worldwide especially for short rang high data rate transmission at up to 480Mbps [2].

Another alternatives of wireless network are Ad-hoc network, where the nodes of the network cooperate to relay and forward each others packets in a multi-hop fashion [3]. A mobile Ad-hoc network (MANET) can be used for facilitating the collection of data in a wireless sensor network (WSN). The WSN's can be found in a variety of modern applications including air pollution monitoring, surveillance, building control, factory automation, and in-vehicle sensing [4, 5]. In WSN, the nodes have to provide the ability for precise self-location and to operate under constraint on energy consumption since the recharge capability is impossible in most cases. Therefore, it is major challenge to minimize the battery charge consumption in order to extend the whole network lifetime. These requirements can be fulfilled very well by UWB transmission technology [6, 7].

For low rate applications, sensor networks are built on UWB technology which provides low cost design, low power consumption and the ability of precise localization. For high rate applications, UWB technology is proposed to replace transmission cables like the universal serial bus (USBs). This technology can therefore replace the wired connection between different informatic devices such as printers, scanners, webcams, monitors, etc. and more generally to multimedia devices such as digital cameras and camcorders, audio and video players as well as video projectors. UWB technology offers unique qualities such as the unlicensed re-utilization

of the allocated spectrum, it can underlay existing radio systems using signal with low power and quasi flat power spectral densities (PSD). In addition, UWB signals occupy wide bandwidth leading to fine time resolution which can be employed for localization applications as well as a high capacity of multiple access. All these advantages make this technology a very interesting choice for low and high rate communication in different applications.

Due to the wireless link nature and the arbitrarily movement of the users, fast fading, shadowing, and interference can cause the channel quality to fluctuate during transmission. The situation becomes dramatically complex when thinking of MANET where the nodes are self configurable and free to move arbitrarily with more functionality options. Indeed each mobile node in MANET works not only as a transceiver but also as a relay and must be able to route packets from other nodes towards a proper direction. This is in contrast of traditional cellular networks where a centralized network infrastructure is set up by installing base stations as access points, such as GSM. In such networks, the fixed base stations and the wired backbone are necessary to ensure the connection between two mobiles. In a MANET, such infrastructure does not exist and the information packets are transmitted between different nodes through multi-hop peer-to-peer connections [8]. Furthermore, the unpredictable mobility of the nodes leads to a dynamic change in the network topology. To realize the functions of Ad-hoc networks, the transmission between nodes must be optimized such as the surcharge reduction and routing information protocols in order to minimize the power consumption and extend the battery life. In fact, an exact knowledge of the position of each node is required and must be exchanged with their neighbors which means a large amount of routing information to be transmitted frequently. This leads to a degradation of the channel capacity and increase the power consumption. The optimization of such networks is facing many paradoxes: increasing the throughput versus the maintenance of the system robustness without increasing the transmission powers, the cost of devices, and the allocated frequency bands.

Many diversity techniques have been developed to fight the fading such as multiple antennas for the spatial diversity or coding for the time diversity. Multiple-antenna systems that provide high orders of spatial diversity and high capacity have been widely studied. These techniques are called MIMO for “multiple inputs multiple outputs”, MISO for “multiple inputs single output” and SIMO for “single input multiple outputs”. Note also that using a single antenna for transmission and reception is called SISO for “single input single output”. The inconvenience of the MIMO technology is the complexity associated. For example, for each antenna employment, it is necessary to use a radio frequency (RF) chain, which is heavy and expensive. In addition, the energy consumption is relatively high due to the complexity of the associated circuits. Given these constraints, MIMO is considered non-functional for some applications such as cellular networks and WSN. In the case of cellular networks, it is not possible to install multiple antennas with associated circuitry on a small mobile phone while maintaining its small size and affordable price. For WSN, where the nodes operate on batteries, energy autonomy is

a crucial requirement. As an alternative to the use of physically installed multiple antennas in MIMO systems, spatial diversity gain is fully achieved through the cooperative diversity [9–13]. In cooperative network, instead of installing multiple antennas on each node, network nodes can share their antennas to relay each others signal in such a way that they form a virtual antenna array (virtual MIMO system).

Our objective in this thesis is how to accumulate the merits of the two concepts, cooperative diversity and UWB technology, in order to satisfy most of the excessive requirements of modern wireless networks over short-range. To show the benefits of the proposed solution, we study an UWB system with cooperation schemes in multipath environment. We extend our research to a multiuser proposal, where we compare cooperative and non-cooperative UWB multiuser system performances.

0.2 Thesis Contributions

This thesis is a continuity of a long road of research started in our laboratory, with the collaboration of Concordia University and the (institut français des sciences et technologies des transports IFSTTAR), by the research of F. Shebli [14] who studied the routing protocols and the MAC layer of WSNs built on UWB technology. The objective of his thesis was to minimize the energy consumption of the WSNs with target localization application. Next, the cooperative diversity was studied by A. Eid [15] for asynchronous direct sequence code division multiple access (CDMA) over frequency selective slow fading environment; where the bit-error-rate performance of the system is studied for both cases of perfect and imperfect inter-user channel. Thereafter, in [16] my previous college, H. Ben Chikha, has studied a distributed turbo coding scheme dedicated to relay channels. He proposed a distributed turbo coded cooperative (DTCC) scheme, called parallel concatenated convolutional-based distributed coded cooperation. In this thesis, we introduce cooperative diversity to UWB transmission systems in order to accomplish a high data rate, reliable, and low cost communication. The main contributions of this thesis are summarized as follows:

- Analyze UWB system under different environments considering the IEEE 802.15.4a [17] channel model.
- Analyze the bit error rate performance of pulse position modulation (PPM) and binary phase shift keying (BPSK) modulation types.
- Apply the decode-and-forward (DF) cooperation protocol in UWB system to ensure the cooperative diversity.
- Implement the proposed cooperative UWB system with time hopping (TH) multiple access scheme using PPM modulation, and compare the performance of non-cooperative

with cooperative TH-PPM UWB system.

- Implement the proposed cooperative UWB system with direct sequence (DS) multiple access scheme using BPSK modulation, and examine the system performance of non-cooperative with cooperative DS-BPSK UWB system.

- Implement Rake receiver to exploit multipath diversity and analyze the decision variable statistics at the output of the receiver, which is decomposed into the desired signal, multipath interference, MAI, and Gaussian noise.

- Study the system performance of the proposed system in presence of multiple access interference (MAI), and investigate the impact of MAI on the overall cooperative performance.

- Use antenna selection at the relay receiver in order to improve the reliability of the source-relay link. This leads to performance improvement in the presence of MAI by taking advantage of available antennas at the relay node, while the cost and complexity are reduced due to the use of single RF chain.

0.3 Thesis Organization

The rest of this thesis is organized as following:

Chapter 1 represents the state of the art of cooperative diversity including the concepts and problems related to cooperative networks. First, we start with a brief description of signal propagation over wireless channel and different diversity techniques used in wireless communication to overcome channel fading. Next, we present amplify-and-forward (AF) and decode-and-forward (FD) relaying protocols and other cooperative protocols such as compress-and-forward (CF). Befor concluding this chapter, we introduce antenna/relay selection.

Chapter 2 introduce the fundamentals of UWB communication and the specifications of these systems. Several signal shapes are expressed in both time and frequency domains. This is followed by the introduction of pulse modulation techniques and multiple access techniques. This chapter demonstrates also the general UWB channel model used in this dissertation.

Chapter 3 describes our proposed cooperative UWB system model, including the transmitter, channel and receiver model and how to integrate UWB in the context of cooperative networks. The used receiver is the partial Rake receiver. This chapter presents also the channel estimation algorithms and the maximum ratio combining (MRC).

In **chapters 4 and 5**, we examine the BER performance of TH-PPM and DS-BPSK, respectively. Each chapter covers one proposed multiple access system. The reviews of each system

are presented first. Then, basic modulation/demodulation techniques and mathematical expressions are given for performance analysis. The analysis of the bit error rate (BER) performance show significant improvement due to the diversity gain provided by the relay nodes. However, the performance is limited when multiple access interference (MAI) is presented. So, we use antenna selection at the relay node to combat the MAI effect which improves the detection reliability at the relay node and make the cooperation more beneficial. Finally, we give a conclusion of this dissertation with a summary of the completed work and a list of suggested future research topics.

Finally, we conclude this dissertation by a brief summary of the work and suggestions for future research topics.

Chapter 1

Cooperative Network - Background

Contents

1.1 Introduction 26

1.2 Signal Propagation Over Wireless Channel 26

1.2.1 Large-scale fading 27

1.2.2 Small-scale fading 27

1.3 Diversity techniques 28

1.3.1 Spectral diversity 28

1.3.2 Temporal diversity 29

1.3.3 Spatial diversity 29

1.4 Multiple-Input Multiple-Output (MIMO) system 29

1.5 Cooperative communications 31

1.5.1 Ad-hoc Networks 31

1.5.2 Relaying protocols 32

1.5.3 Virtual MIMO System (Cooperative Diversity) 35

1.6 Antenna/relay selection 38

1.7 Conclusion 39

1.1 Introduction

The increasing demand for wireless applications with high quality of services has lead to considerable development in wireless networks. Multipath fading severely corrupts the link performance in wireless network. Nowadays, diversity techniques are the most practical and effective countermeasures to combat multipath effects. Spatial diversity requires implementing multiple antennas for transmission and reception (MIMO system). Theoretically, MIMO systems increase the capacity of wireless links compared to systems with single transmit or receive antenna (SISO system). Nevertheless, the practical implementation of separated antennas with the associated radio receivers is costly (e.g. materials, soft and hardware complexity, power consumption). An alternative method is to enable a network of single antenna devices to form a virtual antenna array by sharing their resources, and then to achieve the spatial diversity advantages of physical antenna arrays. In this chapter, we firstly present the independent phenomenon encountered in wireless channels and diversity techniques used to improve signal quality and/or channel capacity. Next, we present the main protocols used in cooperative networks and before concluding we introduce the principle of antenna/relay selection.

1.2 Signal Propagation Over Wireless Channel

The performance of any communication system is eventually affected by the medium which the message signal passes through, referred to as communication channel. The random and severe behavior of wireless propagation channels turns communication over such channels into a difficult task and puts fundamental limitations on the performance of wireless communication systems. Wireless channels may be distinguished by the propagation environment encountered. Many propagation environments have been identified, such as rural, mountainous, urban, suburban, indoor, underwater or orbital environments, which differ in various ways. There are a lot of mechanisms that influence the electromagnetic radio wave propagation generally attributed to the interaction between waves and material such as reflection, refraction, diffraction and scattering. The transmission path between the receiver and the transmitter can be altered from simple line-of-sight (LOS) to one that is drastically obstructed by obstacles encountered such as buildings, foliage and mountains. Even the speed of the mobile impacts how rapidly the signal level fades. The characteristics of the channel appear to change randomly with time. Due to the wireless channel limitations, radio propagation can be roughly described by three nearly independent phenomenon; path loss variation with distance, shadowing and multipath fading, see figure 1.2.1. The path loss is a deterministic effect which depends only on the distance between the transmitter and the receiver. It plays an important role on larger time scales since the distance between transmitter and receiver in most situations does not change significantly on smaller time scales. While shadowing and fading both have stochastic nature causes fluctuations and significant attenuation changes of the received signal strength within smaller

time scales. Shadowing occurs due to the varying terrain conditions in suburban areas and due to the obstacles such as buildings etc. The term fading in wireless communications refers to the interference caused by the reception of numerous reflected, diffracted, scattered copies of a given signal at an antenna. Fading leads to significant attenuation changes within smaller time scales [18–20]. In the communications literature, fading is roughly grouped into two categories: large-scale and small-scale fading.

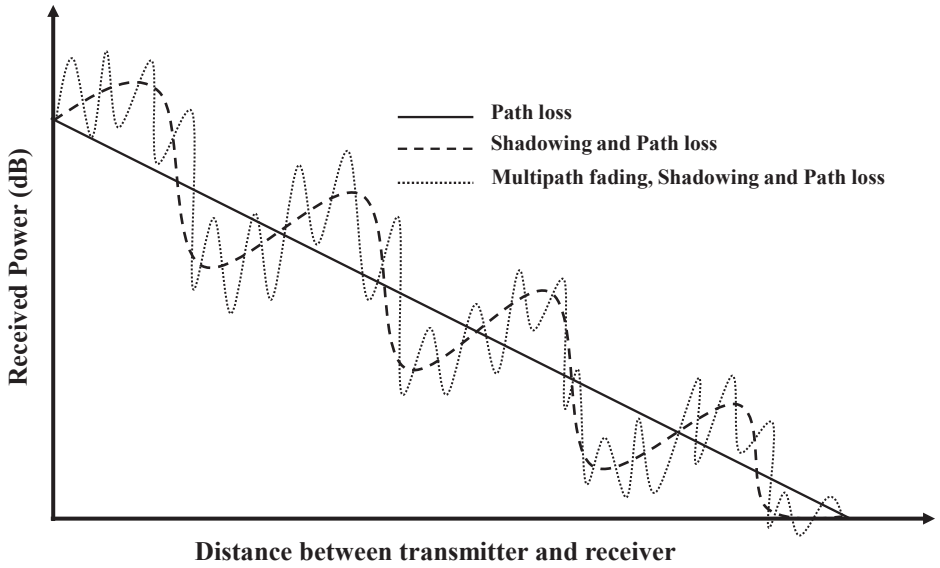


Figure 1.2.1: Path loss, shadowing and multipath fading versus distance.

1.2.1 Large-scale fading

Large-scale fading characterizes the attenuation of the average signal power or path loss as a function of distance and shadowing by large objects such as buildings and hills. This occurs as the receiver moves over large areas. The statistics of large-scale fading is typically frequency independent and normally described in terms of a mean-path loss and a log-normally distributed variation about the mean which is known as shadowing. Hence the term large-scale fading correspond to the combined effects of path-loss and shadowing loss.

1.2.2 Small-scale fading

Small-scale fading refers to the rapid fluctuations in signal amplitude and phase that occur as a result of the constructive and destructive interference of the multiple signal paths due to small changes in the spatial separation between a receiver and transmitter. Small-scale fading is

referred to as Rayleigh fading if the number of multiple paths at the receiver is large and there is no line of sight signal, hence the envelope of the received signal is modeled by a Rayleigh probability density function (PDF). However, if the line-of sight path is present as a dominant non-fading signal component, the small scale fading envelope is described by a Rician PDF.

During its propagation in space, electromagnetic signal undergoes many interactions with the environment. In addition, these signals take different paths before reaching their destination, so they do not travel the same distance and interact differently with the environment. Hence, these signals may arrive out of phase at the receiver and with different power levels. Multipath is the main cause of troubles in a wireless channel. When the delay differences between the multipath components are small compared to the inter-symbol interval, these components may be interfere constructively or destructively at the receiver depending on the carrier frequency and the delay differences. This phenomena lead to instantaneous and severe drop in the signal-to-noise ratio (SNR), which significantly degrades the performance.

The most practical and effective countermeasures nowadays to combat multipath effects are diversity techniques. Diversity provides a receiver with redundant signal information. It allows the receiver to average individual channel effects. In the following sections we give a brief background of the main diversity techniques.

1.3 Diversity techniques

Diversity is one of the most important methods used in combating the detrimental effects of channel fading. It is also a technique to fight against errors [21–24]. The idea behind diversity is to obtain two or more independent paths for the same transmitted signal to increase the chance of having fewer errors at the receiver. Indeed, if multiple copies of the original signal are sent through different paths, they will exhibit distinct channel properties. Diversity can effectively combat channel fading since the probability of all paths suffering from deep fading simultaneously is low and the duplication of the transmitted signal enhances SNR and improves signal robustness. The main common forms of diversity are frequency, time and space which well be presented in the following, respectively.

1.3.1 Spectral diversity

The signal is transmitted simultaneously over two or more frequency bands. This form of diversity is effective when the transmission bandwidth is large enough. The principle behind this technique is that bands separated by more than the coherence bandwidth of the channel will be uncorrelated. The coherence bandwidth of a wireless channel is the range of frequencies that are allowed to pass through the channel without distortion and the channel can be considered flat fading. The separated bands therefore will experience different fades giving rise to a set of subbands with different fading rates. Examples of systems employing frequency diversity are

frequency hopping spread spectrum (FH-SS) and orthogonal frequency-division multiplexing (OFDM) communication systems.

1.3.2 Temporal diversity

The signal is transmitted multiple times over several time slots. Signals that are received at different times are uncorrelated, since the wireless propagation channel is time variant. The time slots must exceed the coherence time of the channel which is the time duration over which the channel impulse response is considered invariant. Therefore, distinct time slots well experience independent channel fading. However, this diversity technique introduces a significant delay in the system. Temporal diversity can be employed using techniques such as interleaving, forward error correction (FEC) code, or automatic repeat request (ARQ) protocols.

1.3.3 Spatial diversity

The signal transmission is done using multiple transmitting and/or receiving antennas. The principal requirement is the separation among adjacent antennas which should be large enough (at least 10 carrier wavelength) to ensure that signals from different antennas undergo independent fading. This diversity technique is not, therefore, suitable for application involving **small devices such as handsets and sensor nodes**. In addition to the physical hardware requirement and complex software integration versus a single antenna system. Spatial diversity can be achieved through multiple-input multiple-output (MIMO) techniques as we well show in section 1.4.

Diversity is not only achieved by the previously presented techniques, other mechanisms exist such as angle-of-arrival diversity, polarization diversity, and pattern diversity [25–27].

1.4 Multiple-Input Multiple-Output (MIMO) system

Spatial diversity is traditionally implemented by the use of multiple antennas for transmission and/or reception, referred to as MIMO technique in contrast with a SISO (single-input single-output) system that uses one transmit antenna and one receive antenna. In the literature, there are other models of simplified MIMO systems that exploit spatial diversity. The use of a single transmit antenna and multiple receive antennas is known as single-input multiple-output (SIMO) system, whereas the reverse case of using multiple transmit antennas and a single receive antenna is called multiple-input single-output (MISO) system [28, 29].

For richly scattered wireless environments, MIMO systems (i.e. separation among adjacent antennas) allow the receiver to see independent versions of the transmitted information by providing independent spatial paths between each pair antennas as illustrated in Fig. 1.4.1. MIMO systems use space-time processing techniques to provide reliable and high data communication and it is necessary that fading signals at different antennas are uncorrelated or slightly correlated

in order to achieve the maximum diversity. These diversity techniques have revolutionized wireless communications over the past decade since it serves to improve reliability (bit error rate) and throughput (bit/sec) in these systems.

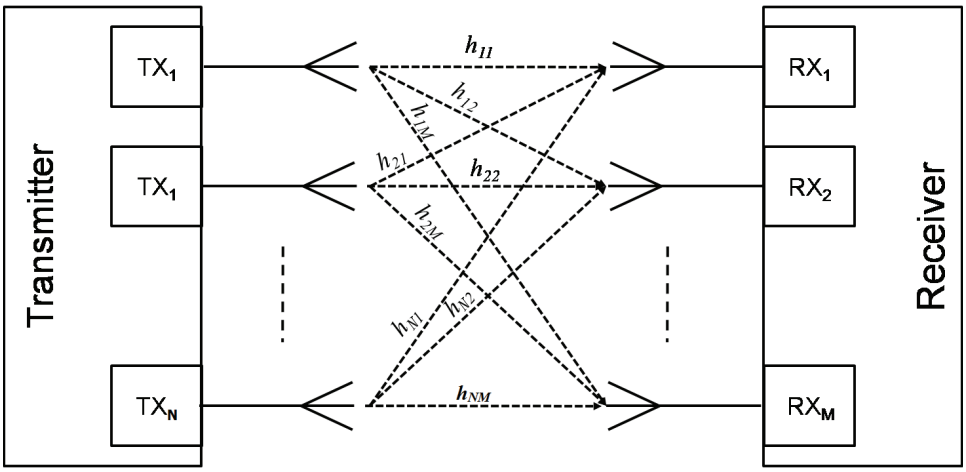


Figure 1.4.1: Centralized MIMO System.

Shannon theory measures the channel capacity in bits per second per Hertz which is the maximum amount of information that could be transmitted through a channel and received with negligible error [30]. Given a SISO link with input signal S corrupted by an additive white Gaussian noise (AWGN) and the occupied bandwidth B in hertz, the capacity can be written as:

$$C_{SISO} = B\log_2(1+\rho) \tag{1.4.1}$$

where ρ is the average SNR. This relationship indicates that for a linear increase of the channel capacity an exponential increase of the signal-to-noise ratio SNR is required.

We now consider a full MIMO link as in Fig. 1.4.1 with respectively N transmit an M receive antennas. The channel matrix H is given by

$$H = \begin{bmatrix} h_{11} & h_{12} & \cdots & h_{1M} \\ h_{21} & h_{22} & \cdots & h_{2M} \\ \vdots & \vdots & & \vdots \\ h_{N1} & h_{N2} & \cdots & h_{NM} \end{bmatrix} \tag{1.4.2}$$

where $h_{i,j}$ are the channel coefficients between the ith transmit antenna and the jth receive antenna. The entries of H follow the Rayleigh distribution. It was shown in [31–33] that the capacity of such a MIMO system is done by:

$$C_{MIMO} = B\log_2\left[det\left(\mathbf{I}_M + \frac{\rho}{N}\mathbf{H}\mathbf{H}^*\right)\right] \tag{1.4.3}$$

where ρ is the average SNR at any receiving antenna, $\mathbf{I}_M$ is a unitary $M \times M$ matrix. In fact, for a large number $M = N$ of antennas the average capacity increases linearly with M:

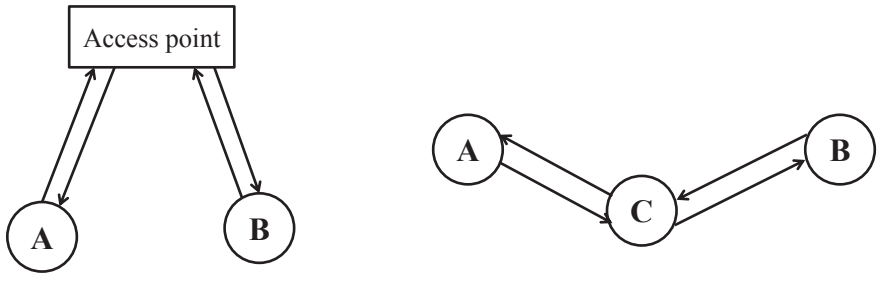
$$C_{MIMO} = M \times B \log_2 (1 + \rho) \tag{1.4.4}$$

In general, the use of M antennas at both sides of a given wireless communication system has the potential to scale linearly by M the fundamental relationship of Shannon capacity [34]. However, **the major drawbacks of MIMO systems is the increased complexity and the multiple radio-frequency (RF) chains** associated with multiple antennas which are costly in terms of size, power, and hardware.

1.5 Cooperative communications

Next generation of wireless communication will be based on complex interaction transmission that goes beyond the classical point-to-point or point-to-multipoint transmission. The involved nodes in such network well cooperate with one another to share their limited resources and antennas. By relaying each other signals, cooperating nodes will be able to improve their own transmission and that of the global network. Cooperative communications have the potential to increase spectral efficiency and to reduce cost, outage probability and power consumption. Co-operation is also extended to multi-hop relaying topology, which is targeted to increase network coverage. Similar to physical MIMO system, cooperative communication provide spatial diversity by creating multiple replicas of the signal of interest. The spatially distributed cooperating nodes form a virtual antenna array that emulates the operation of a MIMO system.

1.5.1 Ad-hoc Networks



Infrastructure mode exchange

Ad-hoc mode exchange

Figure 1.5.1: (a) Infrastructure exchange mode. (b) Ad-hoc exchange mode.

By definition, an ad-hoc network is a decentralized wireless network that does not depend on a pre-existing infrastructure or centralized administration to route data exchange between nodes. Ad-hoc networks consist of terminals that move randomly and are capable to communicate directly with each other's. To communicate between non-adjacent nodes, it is necessary to establish a multi-hop connection through the intermediate nodes. For this, it is important that the nodes are located relative to each other, and are able to establish routes between them: it is the role of the routing protocols. Thus, the operation of an ad-hoc network significantly differs from the traditional wireless networks which have pre-installed infrastructure like base stations or routers required to connect the different nodes. Ad-hoc networks organize themselves and each node can play different roles. Figure 1.5.1 illustrate the difference between infrastructure and ad-hoc exchange modes. the An ad-hoc network can consist of different elements that use different short-range and long-range communication like mobile phones, computers, handheld devices, wireless sensors and many other devices. These terminals are usually single antenna elements and work under temporary or permanent energy constraints. Therefore, it is major challenge for ad-hoc terminals to minimize the power consumption in order to extend the whole network lifetime.

1.5.2 Relaying protocols

The key idea behind cooperative communications is to allow nodes to cooperate with each other to provide spatial diversity gain at the destination. In this case, at any given time, any node can be a source, relay, or destination. The function of the relay node is to assist in the transmission of the source signal to the destination node. To ensure diversity gains, this relay is chosen in such a way that its link to the destination is independent from that of the source. The way that the relay operates the source's signals is called relaying protocol or processing mode. Typically, the relaying protocols fall into one of the following three categories : amplify-and-forward (AF) [12,35], decode-and-forward (DF) [11,36], and compress-and-forward (CF) [37]. Besides these main relaying protocols, other techniques such as hybrid decode-amplify-forward (HDAF) which exploits the advantage of both DF and AF modes, estimate-and-forward (EF), and coded cooperation are extensively reported in the literature [38].

In the AF relaying mode, the relay terminals amplify the received signal from the source terminal and then transmits the resulting signal to the destination as shown in figure 1.5.2. No demodulation or decoding of the received signal is performed in this protocol. This results in reduced hardware complexity of relay terminals compared to another relaying protocols. However, the received signal at the relay is corrupted by noise and the amplifying process well increase the noise level as well as the desired signal with respect to power constraint. In addition, when the instantaneous Channel State Information (CSI) is not available at the receiver, then the analysis, and fulfillment of the relay power constraints is significantly complex [39]. Although

the noise is amplified by the relay, the cooperation is made at the destination by combining two independently faded signals resulting from source and relay. Hence, the second order diversity is achieved which is the best possible result of this protocol [12, 40].

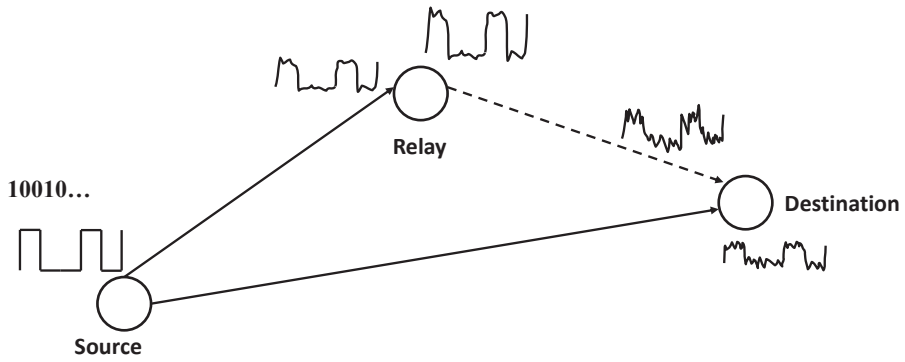


Figure 1.5.2: Principle of amplify-and-forward relaying protocol.

In DF mode, the relay decodes the source's message and re-encodes an estimate of this message before forwarding it to the destination. Figure 1.5.3 illustrate the principle of this protocol. Due to the error propagation, the potentially wrongly decoded message at the relay can significantly degrade the system performance. Obviously, DF protocol requires more signal processing than AF, because the signal must be decoded and re-encoded before being retransmitted by the relay node. However, if the signals are correctly decoded at the relay, the performance is better than the AF protocol, because the noise is eliminated. In addition, for DF, the relay power constraints can be easily satisfied and DF method can be extended to combine coding techniques and might be easier to incorporate into network protocols [41–44].

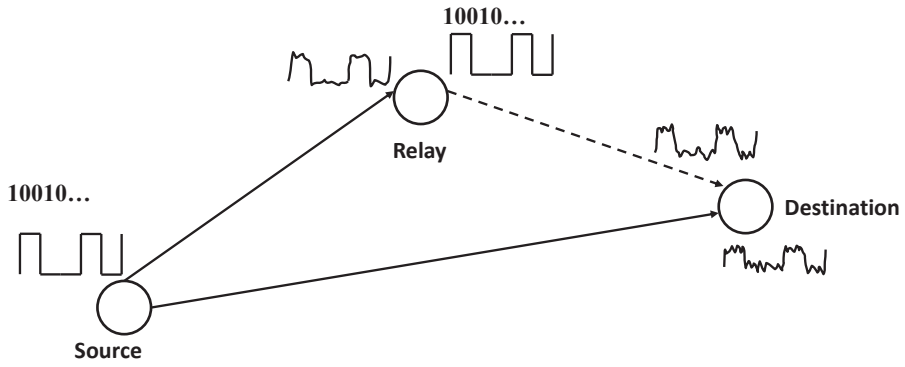


Figure 1.5.3: Principle of decode-and-forward relaying protocol.

The principle of CF protocol is that the relay forwards a quantized and compressed version of the received signal to the destination, so that the latter can combine its own direct observation

with that of the relay subject to the source's signal. The compressing can be done using either the standard source coding or the Wyner-Ziv coding (WZC) technique [45].

Figure 1.5.4 shows various relaying architectures that related to the used channel models as explained in [12]. The classical relay architecture is shown in Figure 1.5.4 (a), which is also called the (three body problem). As described previously, the source broadcasts the signal to the relay and destination simultaneously, and then the relay retransmits the information to the destination. In figure 1.5.4 (a), the architecture reduces to direct transmission when the relay is removed, and cascade multihop communication when the destination is unable to hear (or ignores) the source transmission. When two source nodes transmit simultaneously and cooperate to relay each other signal to the destination, the configuration is called a classical multiple-access channel with relaying as presented in figure 1.5.4 (b). The parallel relay channel without direct transmission is presented in figure 1.5.4 (c). The relay and destination can cooperate as shown in Figure 1.5.4 (d), which is known as broadcast scheme. Finally, the cluster-to-cluster relaying architecture as shown in Figure 1.5.4 (e), where the source cluster nodes broadcast towards destination cluster nodes in multiple-access mode.

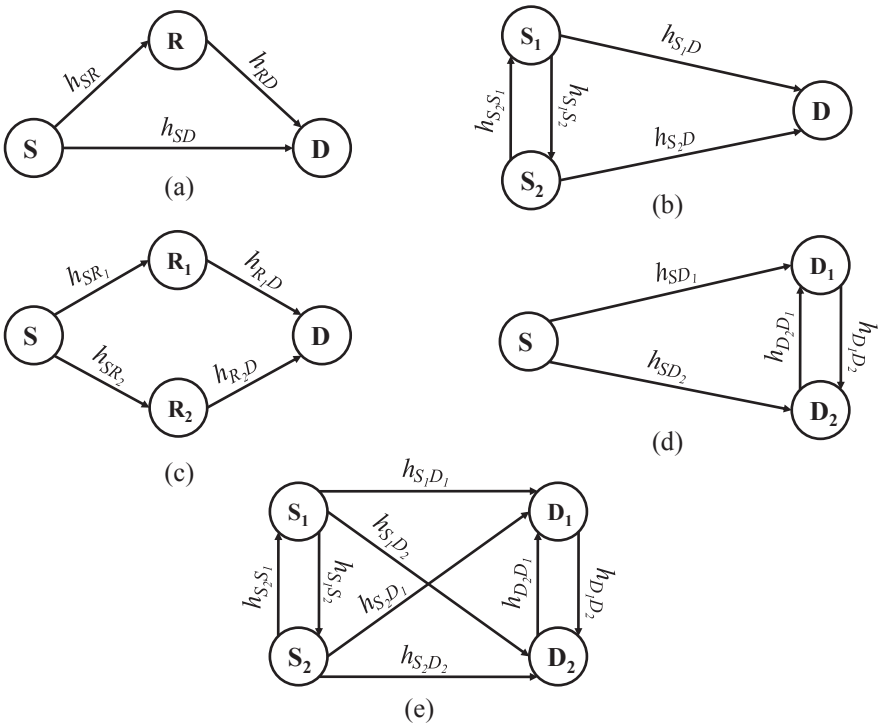


Figure 1.5.4: Relaying architectures: (a) classical relay channel, (b) multiple-access channel with relaying, (c) parallel relay channel, (d) broadcast channel with relaying, (e) cluster-to-cluster relaying channel.

The benefits of user cooperation were first demonstrated for transmission in narrow-band systems. Many of the initial works performed in this area have focused on AWGN channels, and examined the performance in terms of the well-known Shannon capacity [37]. Later, sendonaris

et al. have shown the advantages of cooperation for two active users using conventional code division multiple-access (CDMA) in terms of throughput, cell coverage and resistivity to channel variations [9, 10]. The authors in [15] employ DF protocol and investigate the error probability performance of cooperative diversity for asynchronous direct sequence code division multiple access (DS-CDMA) system in frequency selective slow fading environment. The performance of user cooperation in terms of outage probability has been studied in [12] for delay-limited and non-ergodic environments.

1.5.3 Virtual MIMO System (Cooperative Diversity)

MIMO system requires implementing multiple transmit and/or receive antennas. For independent fading influence, the separation between adjacent antennas must be larger than half of the carrier wavelength. This spacing is not always available especially in portable consumer devices. In addition, multiple antennas mean multiple RF chains, i.e. one RF for each antenna employment, which is cumbersome and expensive. Besides, the energy consumption is relatively high due to the complexity of the circuits and computations for signal processing. Power consumption is a critical restrictive that dissipates the battery lifetime of battery-powered devices. These constraints make MIMO diversity sensitive to cost and size arguments especially in small and low cost terminals. Therefore, MIMO is considered non-practical for some applications such as cellular networks and sensor networks. In the case of cellular networks, it is not possible to install multiple antennas with associated circuits on a small mobile phone while maintaining its small size and affordable price. Whereas, for wireless sensor networks where nodes operate on batteries, energy autonomy is a crucial requirement.

The concept of cooperative communications, known also as virtual MIMO system, has more recently emerged as a solution to exploit the potential MIMO gains on a distributed scale. This technology relies on concepts that appeared in 1968-1971 by Van Der Meulen–and by Cover and El Gamal in 1979 [37, 46]. Over the last decade, researches in cooperative communication has received tremendous interest motivated by Laneman and Wornell [12, 36, 47], Sendonaris et al [9, 10], Hunter and Nosratinia [48], Zhao and Valenti [41], Nabar and Bolcskei [11, 13], and Eid et al [15]. These researches show that cooperative diversity is an attractive way to increase throughput, reduce energy requirement, and provide resistance to channel fading in wireless networks.

In cooperative communication environment, a collection of mobile nodes can cooperate to relay signals of each other; in such a way that they form a virtual antenna array and thus exploit spatial diversity in wireless fading channels. Using cooperation, it is possible to exploit the spatial diversity of traditional MIMO techniques without necessarily each node has multiple antennas. The destination therefore receives multiple versions of the source message coming

from the source and one or more relays. As a result, a combination is possible to obtain a more reliable estimate of the transmitted message.

Cooperative techniques take advantage of the broadcast nature of wireless signals by observing that a source signal intended for a particular destination can be "overheard" at neighboring nodes. These nodes, called relays or partners, give assistance to the source by processing its signals they overhear and re-transmit towards the destination. The destination combines the signals coming from the source and the relays, enabling diversity gain resulting in higher transmission rates and robustness against channel variations due to fading [16, 49].

Because of their significant advantages, cooperative communications have recently emerged as a strong candidate for the underlying technologies of most future wireless applications, including 4G cellular networks, wireless sensor networks (IEEE 802.15.4), and IEEE 802.16j WiMAX networks. The main advantages of cooperative communication are:

- High flexibility of network configuration with the possibility to change the number of cooperating nodes according to the desired performance;
- Relaying strategy can be adapted to different scenarios;
- Higher spatial diversity: resistance to both small scale and shadow fading;
- Higher throughput/lower delay: higher achievable data rates, fewer retransmissions, and lower transmission delay;
- Network coverage extension which becomes larger due to neighboring relay nodes;
- The transmission power can be better controlled leading to interference reduction of multiple access environment. In addition, power adaptation capability allows achieving maximum capacity.
- Adaptability to network conditions: opportunistic use and redistribution of network energy and bandwidth;

The cooperative communication system model consists of three terminals: a source, a destination, and several relays distributed throughout the network. The source and relay cooperate with each other to provide spatial diversity at the destination, this cooperation may be reciprocal, they can exchange roles, or each node could behave as source and relay simultaneously by using separate channels. Figure 1.5.5 shows an example of virtual MIMO system. This system consists of a source node, N relay and a destination node. The channel fading coefficients are designated by h_{SD}, h_{SR_n} and h_{R_nD}, $n = 1, 2, \ldots, N$.

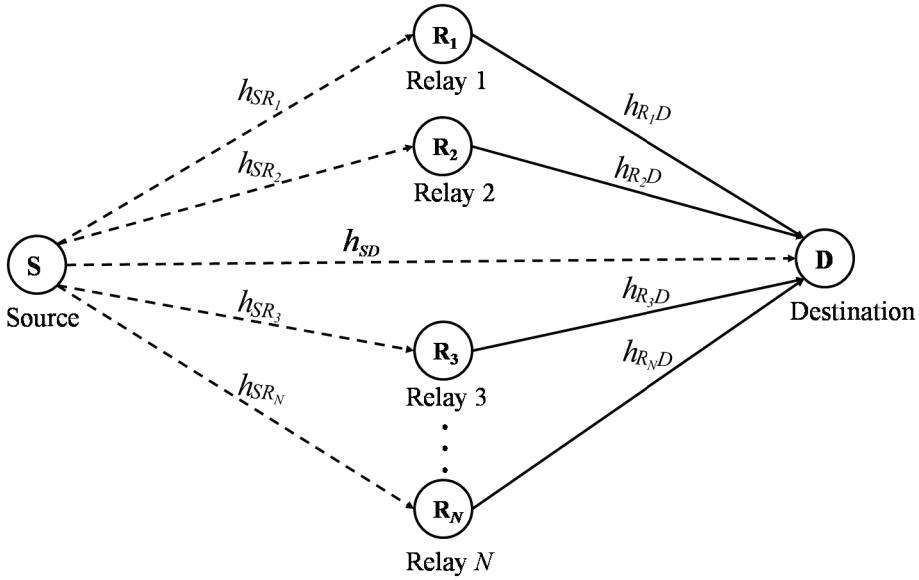


Figure 1.5.5: Virtual MIMO system using cooperative communication.

Despite all those benefits of cooperative communication, there are also challenges for implementing this technology [50, 51], those challenges include:

- Increased overhead: Cooperative system uses multiple links to transmit data where each link requires access control, synchronization, channel estimation, scheduling, additional security, etc. All these requirements certainly induce an increased overhead in comparison with traditional point-to-point communication systems.
- Increased relay traffic and interference: Sending data to destination via several relays will certainly cause interference to other users. Furthermore, additional resources in the form of frequency channels, time slots or orthogonal codes are required for relaying traffic.
- Increased end-to-end latency: Cooperative communications typically involve extra delay at relay nodes including the reception and decoding of a data packet before it is retransmitted by relays. The extra latency introduced by relaying may become detrimental with regard to delay-sensitive services, such as voice and increasingly popular multimedia services.
- Overall performance sensitivity to relay detection reliability: In cooperative networks, the performance of the end-to-end connection depends significantly on the detection reliability of the relay nodes. In the ideal situation where the detection reliability at the relay nodes is perfect, the diversity of the system is maintained as the relay nodes is collocated as a transmitter source node [11–13, 15]. However, the diversity degrades with imperfect detection. The degree of this degradation depends widely on the level of detection

reliability at the relay nodes. In fact, diversity begins to degrade when the source-relay link is worse in terms of detection reliability than that of the source-destination and / or relay-destination. To improve the detection reliability at the relay nodes, it is better to use DF strategy. Most of the work devoted to the study of this strategy assumed error-free detection at the relay nodes using error control mechanism and ARQ for data transmission.

1.6 Antenna/relay selection

The limitation on the implementation of multiple antennas is the cost and complexity of the associated RF chains. The increase in system hardware and signal processing complexity has inhibited the widespread adoption of MIMO systems. Fortunately, a low-cost alternative for MIMO systems is the utilization of antenna selection approaches with reduced-complexity and without significant performance degradation compared to the full-complexity (FC) MIMO system [52, 53]. This approach alleviates system hardware complexity by using fewer RF chains than the actual number of antenna elements. Antenna selection has been considered before for centralized MIMO systems. This strategy has shown impressive diversity and coding gains [54–58]. The idea is to use only a subset of the available antennas. The consequence of this is that, while leveraging the benefits of available antennas, the number of RF chains is reduced to the number of selected antennas, which leads to reduced cost and complexity.

As we well show in chapters 4 and 5, the performance of cooperative communication is limited in terms of attainable diversity when the source-relay link is bad and/or when MAI is present. This degradation is attributed to the errors made at the relay nodes. Hence, if better reliability is achieved at the relay nodes, the diversity may improve, or may even maintained. In light of this, we propose to employ antenna selection at the relay receiver in order to improve the reliability of the source-relay link. We assume that the relay node is equipped with multiple antennas the receiver selects the best antenna which corresponds to the best S-R sub-channel with the highest SNR (out of the available sub-channels). A natural extension of antenna selection is relay selection, whereby the relay that enjoys the best reliability is selected. In the latter case, each relay node is assumed to be equipped with one antenna and one RF chain, while in the former case, one relay is supposed equipped with multiple antennas and thus only one RF chain is required. Furthermore, to accomplish relay selection, the source will have to know the reliability of the available nodes through some feedback to decide on what relay to use for relaying. It is also possible to select multiple relays for cooperation.

It is remarkable that cooperative diversity can increase the diversity gain at the cost of losing the wireless resource such as frequency, time and power resources for the relaying phase. Therefore, it is important to note that there is a trade-off between diversity gain and spectrum

resource in cooperative diversity. A large number of publications have been made in the area of cooperative communications, studying variety of topics, but little have studied the cooperative scheme with UWB signal. UWB is one of the most competing technologies for short-range future wireless communication. It uses very short pulses of duration of fraction of nanosecond to convey information, thus the spectrum of the emitted signals may spread over several GHz. UWB technology is a license-free frequency radio that can provide high data rate at low cost with low power consumption.

1.7 Conclusion

We have presented in this chapter the main characteristics of wireless channel and the known diversity techniques that can be used to improve transmission quality and channel capacity. We have shown our interest in cooperative diversity as well as in antenna/relay selection and presented a review of the relevant work existing in the literature. Thus, for the concept of a relay cooperation, we have mainly presented the DF, AF and CF relaying protocols need to preserve diversity by employing appropriate channel coding systems. In the next chapter, we give a brief introduction of UWB communication, the UWB channel model and different transmission basics for UWB systems.

Chapter 2

Ultra Wideband Communications

Contents

2.1 Introduction 43

2.2 Definition of UWB signals 43

2.3 Motivation for the use of ultra wideband (UWB) 44

2.4 UWB Pulse Waveforms 47

2.4.1 Gaussian Pulse 47

2.4.2 Gaussian Monocycle Pulse 48

2.4.3 Gaussian doublet Pulse 49

2.5 Pulse Modulation 50

2.5.1 Pulse Position Modulation (PPM) 51

2.5.2 Binary Phase Shift Keying (BPSK) 52

2.6 Multiple Access Techniques 52

2.6.1 Time Hopping Multiple Access 53

2.6.2 Direct Sequence Multiple Access 54

2.7 UWB Channel Model 55

2.7.1 General Overview of UWB channel models 55

2.7.2 The IEEE 802.15.4a channel Models 57

2.8 Conclusions 61

2.1 Introduction

The acronym UWB groups a number of synonymous terms such as: impulse, carrier-free, base-band, time domain, nonsinusoidal, orthogonal function and large-relative-bandwidth radio/radar signals [59]. Although the foundations of this technology are known since the sixties of the last century, the term UWB was introduced for the first time in 1990 by the department of defense (DoD) in the United States. UWB signals have been mainly used for radar applications and not for objectives of radio communications [60].

UWB is not a new concept in wireless network. The first researches on this technology have been done from the 1960's to the 1990's and were restricted to military applications by the US army under classified programs. By late 1960's until approximately 1989, UWB theory, techniques and many hardware approaches had experienced well at the Sperry Research Center (Sudbury, MA), then part of the Sperry Rand Corporation [61]. Recent progress in microprocessing and fast switching in semiconductor technology has enabled the commercial utilization of UWB technology. Despite the absence of any regulation allowing the use of UWB technology, some laboratories are turning to UWB and strengthened their basic research and development in communications and positioning systems. However, this interest remains somewhat limited and the scientific community has little interest in this subject until the authorization promulgated by the Federal Communications Commission (FCC) in February 2002. This regulations permits the use of UWB signals for wireless communication in the frequency band [3.1 GHz-10.6 GHz] [62].

In this chapter, we illuminate the fundamentals of UWB communications and their regulations. The main signal shapes used as UWB waveform are expressed in both time and frequency domains. This is followed by the introduction of pulse modulation, multiple access techniques, and also the UWB channel model.

2.2 Definition of UWB signals

UWB technology has owned a prior interest in the research during the last decades after recognizing its potential advantages. This research topic has been reinforced since the FCC has published its report in February 2002 [62]. According to this report, the FCC authorized the unlicensed use of UWB for communications from 3.1 GHz to 10.6 GHz and for imaging below 960 MHz of the wireless frequency spectrum under specified power limits. The FCC adopts the UWB definition established by the office of the secretary of defense (OSD) and defense advanced research projects agency (DARPA) [60] but with modification, which implies that an UWB signal is a signal whose the fractional bandwidth is greater than 0.25; i.e. UWB signal have a fractional bandwidth of at least 20% of the central frequency or occupying at least 500 MHz of spectrum. The fractional bandwidth B is defined as

$$B_{\triangle} = \frac{2(f_H - f_L)}{f_H + f_L} \tag{2.2.1}$$

where f_H and f_L is the upper and lower frequencies of the -10 dB below the peak emission point, respectively. UWB technique does not use sinusoidal carriers, but instead it generates very short pulses of duration of fraction of nanosecond to convey information, resulting in an ultra wideband signal. Therefore, it is referred to as carrierless short pulses or impulse radio (IR). To avoid interference with existing narrow-band wireless systems, the maximum emission power for UWB transmission is specified by the FCC. For indoor communication the equivalent isotropic radiated power (EIRP) density is limited to -41.3 dBm/MHz, which complies with the long standing Part 15 general emission limits to successfully control radio interference [62]. Respecting the FCC power constraints, UWB power spectrum density (PSD) is very low and close to the noise floor; therefore the interference to any other existing technology like 802.11a and 3G mobile communication can be ignored. Figure 2.2.1 shows the spectrum mask for UWB indoor communication and maximum emission levels set by the FCC.

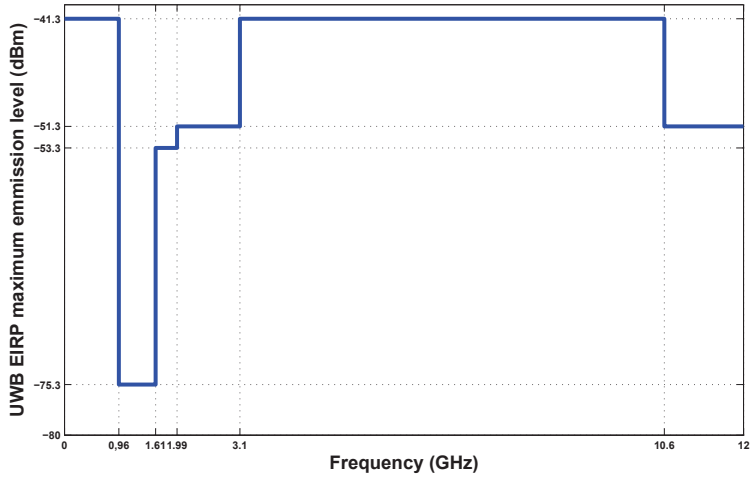


Figure 2.2.1: FCC emission limits mask for UWB indoor communications.

2.3 Motivation for the use of ultra wideband (UWB)

Even though, UWB concept has been existent for over forty years, this technology is an emerging research topic in the wireless communications field for a variety of reasons. Nowadays, a fast expanding of indoor networking market is promoted by the variety and widespreadly of

entertainment portable devices accompanied with the wide growth in consumer applications. This expansion have created a need for reliable short-range high-throughput data links (more than 100 Mbits/s over several centimetres to about ten meters) [63]. In addition to the crowded spectrum which is sliced and licensed by rigid authorities, power saving and cost have become increasingly important factors for portability, economic, and marketing considerations. The UWB technology is a promising physical layer offering potential for addressing all of these issues. This makes this "new" transmission technique a likely candidate for network applications like WSN (wireless sensor network), WLAN (wireless local area network), WPAN (wireless personal area network) or WBAN (wireless body area network).

Because of the nature of the extremely short pulse duration used in UWB communications, they offer several potentially attractive advantages over narrowband communications:

- **Ability to share the licensed spectrum**

UWB signals have a low PSD constraints according to the FCC of –41.3 dBm/MHz, which equal to 75 nanowatts/MHz. This power constraint allows UWB systems to reside below the noise floor of a typical narrowband receiver and enables UWB signals to coexist with current radio services with minimal or no interference. Figure 2.3.1 shows the spectrum allocation and coexistance of UWB with different narrowband communication systems.

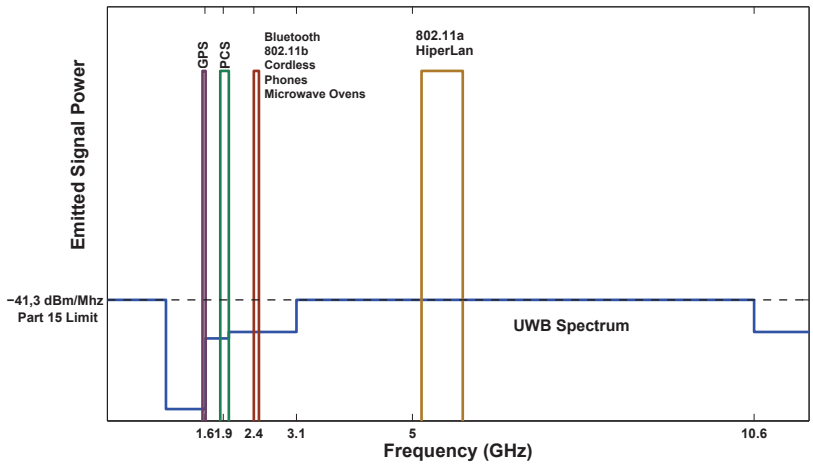


Figure 2.3.1: Coexistence of UWB with different narrowband communications (GPS: global positioning system, PCS: personal communications service, Bluetooth, 802.11b, cordless phones, microwave ovens, 802.11a HiperLan).

- **Large channel capacity**

Channel capacity is an important issue for communication systems which is defined as the maximum amount of data that can be transmitted per second over the communication channel and is given by Hartley-Shannon's theorem:

$$C = B.log_2(1 + SNR) \tag{2.3.1}$$

where C is the channel capacity, B is the channel bandwidth. This formula indicates that increasing the channel capacity requires linear increase of the bandwidth and/or exponential increase of the output power. For narrow band system, once the bandwidth of the system is fully utilized, any further increase in capacity comes at an exponential increase in the required SNR. Whereas, for UWB systems, since they spam several gigahertz of the spectrum, they enable higher channel capacity and thus UWB technology support high data rates of one gigabits per second (Gbps). However, due to the FCC's power limitation on UWB transmissions, such a high data rate is available only for short ranges, up to 10 meters [64].

- **High throughput even at low SNR**

It is also obvious from 2.3.1 that the channel capacity scale logarithmically with the SNR. Thanks to their large bandwidth, UWB communications systems support high data rates even working in harsh communication channels with low SNRs.

- **Low probability of intercept and detection**

UWB operates within the electronic noise with low average transmission power, as discussed previously. In order to be heard, the eavesdropper has to be very close to the transmitter (about 1 meter). Therefore UWB communication systems are extremely difficult to intercept. In addition, the coded time modulation of extremely short pulses adds more security to UWB transmission, because detecting picosecond pulses without perfect synchronization is next to impossible. This makes UWB technology particularly useful for highly secure communication with low probability of intercept and detection.

- **Immunity to multipath fading**

A natural outcome of using very short duration pulses is multipath immunity. Because the UWB pulse duration is shorter than a nanosecond, the reflected pulse has an extremely low potential to collide with the first arriving pulse and cause signal degradation. However, UWB communications is not totally immune to multipath distortion. In some environments such as indoor channels where a large number of objects and scatterers are closely spaced, low-powered UWB signals can become significantly distorted [64].

- **Resistance to jamming**

UWB communication systems spam several gigahertz of the frequency spectrum and offer high processing gain (PG) which is a measure of a radio system's resistance to jamming and is given by the ratio of the RF bandwidth to the information bandwidth of a signal. The high processing gain of UWB communications results in high frequency diversity making UWB signals strongly resistant to intentional and unintentional jamming. This is explained by the fact that no jammer can jam every frequency in the UWB spectrum at once.

- **Simple transceiver architecture**

Unlike narrowband systems, UWB transmission is carrierless, meaning that data is not modulated on a continuous waveform. For this raison, the design of a UWB system requires significantly simpler radio frequency (RF) electronics. This simplicity makes UWB ideal for low cost production.

2.4 UWB Pulse Waveforms

The core of any UWB system is the pulse generator, which is used for both transmitter and receiver. UWB transmitters convert data bits directly to extremely short pulses, typically from a few tens of picoseconds to a few nanoseconds, while receivers must generate a template pulse that matches the incoming waveform in order to perform the correlation and extract message data bits. Since UWB systems use the baseband conception, the choice of pulse shapes will affect the transceiver design as well as the bit error performance. Gaussian waveforms are a family of functions deriving from a Gaussian pulse and are used in the literature for UWB communications. An important aspect of the Gaussian waveforms is their wideband spectrum which can fit the FCC mask by employing pulse shaping filter design and waveform optimization techniques [65]. In addition, they are smooth, well behaved functions and can be directly generated in electronics making them easier to implement.

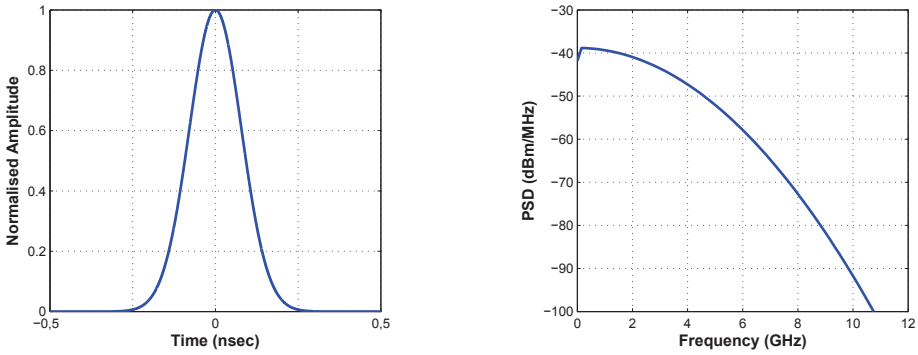
2.4.1 Gaussian Pulse

A Gaussian pulse, as shown in Figure 2.4.1 (a), is defined as

$$p(t) = A \exp\left(\frac{-t^2}{\tau_m^2}\right) \tag{2.4.1}$$

where A is an amplitude scaling factor and τ_m is a time scaling factor, which determines the width of the pulse. In the frequency domain, the Gaussian pulse is also a Gaussian shape given by:

$$P(f) = A\tau_m\sqrt{\pi}\exp\left(-(\pi\tau_m f)^2\right) \tag{2.4.2}$$



(a) (b)

Figure 2.4.1: Gaussian pulse. (a) Time domain. (b) Normalized power spectral density.

The Gaussian pulse is inappropriate since it puts considerable quantity of energy near DC as shown in Figure 2.4.1 (b). If a band-pass filter is used to eliminate DC and low frequency components, the pulse is distorted and extended in time, which is undesirable for UWB systems. The raison is related to the high number of signal paths arriving at the receiver due to the frequency selective nature of the UWB channel and the large signal bandwidth. Band-pass pulse filtering results in considerable pulse broadening in time domain and inter-path interference (IPI), which consequently corrupt the performance of the system. It is therefore more appropriate to push the signal spectrum away from DC by using higher-order derivatives of the Gaussian pulse and puts it within the required range [66].

2.4.2 Gaussian Monocycle Pulse

The Gaussian monocycle is the first derivative of the Gaussian pulse and is given by

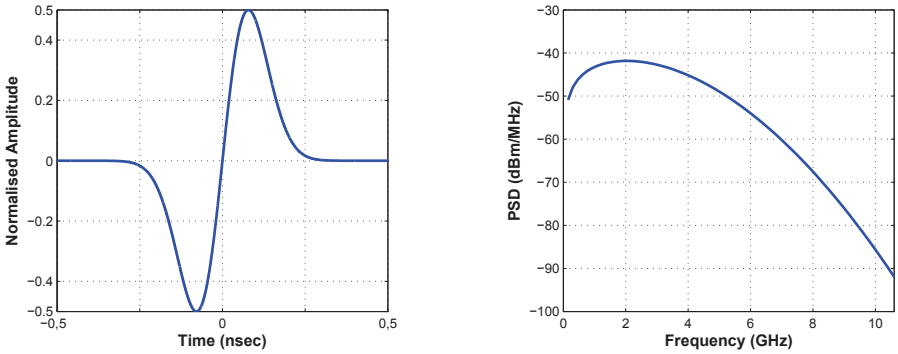
$$p(t) = \frac{2At}{\tau_m^2}\exp\left(\frac{-t^2}{\tau_m^2}\right) \tag{2.4.3}$$

In the frequency domain, it has the following form

$$P(f) = A\tau_m\sqrt{\pi}(j2\pi f)\exp\left(-(\pi\tau_m f)^2\right) \tag{2.4.4}$$

Figures 2.4.2.a and 2.4.2.b show the time representation and the normalized PSD of this pulse. Actually, as the order of Gaussian pulse derivation increases, the number of zero crossings in the time domain also increases. More zero crossings in the same pulse width make high-order

derivatives pulses close to sinusoids higher frequency carrier modulated by Gaussian envelope. For these observations lead, higher-order derivatives of the Gaussian pulse are considered as candidates for UWB transmission.



(a) (b)

Figure 2.4.2: Gaussian monocycle pulse. (a) Time domain. (b) Normalized power spectral density.

2.4.3 Gaussian doublet Pulse

The second derivative of a Gaussian pulse is called a Gaussian doublet. The time domain representation of this pulse is given by

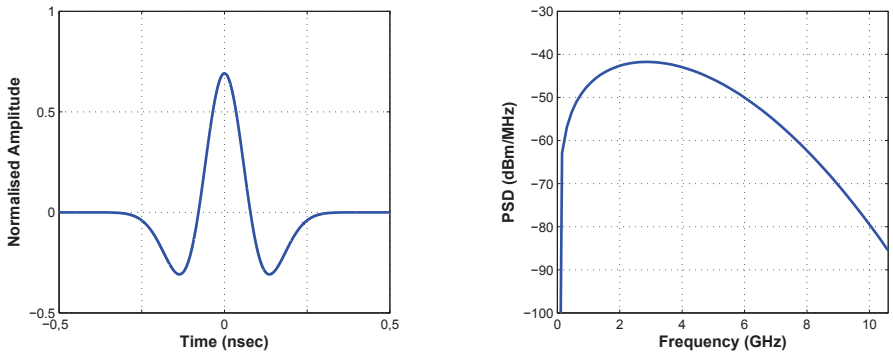
$$p(t) = \frac{2A}{\tau_m^2}\left(1 - \frac{2t^2}{\tau_m^2}\right)\exp\left(\frac{-t^2}{\tau_m^2}\right) \tag{2.4.5}$$

The frequency spectrum of the Gaussian doublet

$$P(f) = A\tau_m\sqrt{\pi}(j2\pi f)^2\exp\left(-(\pi\tau_m f)^2\right) \tag{2.4.6}$$

The time and frequency domains of an example Gaussian doublet shown in Figure 2.4.3

It must be pointed out that many more different pulse shapes may be used for UWB applications [67]- [68]. The choice of pulse shape is usually driven by the system design and application requirements and it is critical to the FCC mask and power emission limits. Gaussian pulse shapes are chosen because they are relatively easy to generate. An important factor to the use of the Gaussian waveform is the general effect of differentiating due to antennas at transmitters and



(a) (b)

Figure 2.4.3: Gaussian doublet pulse. (a) Time domain. (b) Normalized power spectral density.

receivers. Therefore, if the pulse used at the input of the transmitter antenna is of zero order, the output signal in the channel will be the first derivative of the input signal. Similar differentiation process will also take place in the receiving antenna. Therefore, a Gaussian doublet is always considered as the received pulse shape if a Gaussian pulse is used at the input of the transmitter antenna.

2.5 Pulse Modulation

An UWB pulse by itself contains no data; therefore a long sequence of pulses termed a pulse train with data modulation is used for communication. A number of techniques can be used with UWB systems to encode information, including amplitude, time and phase modulations. The potential modulation schemes include both orthogonal and antipodal schemes. The most popular modulation schemes developed for UWB are pulse amplitude modulation (PAM), pulse position modulation (PPM), on-off keying (OOK), binary phase-shift keying (BPSK), and pulse shape modulation (PSM); see [69], [70] and references therein. PPM and BPSK are the best candidates for UWB due to their interference robustness and power efficiency. Therefore, we have chosen to investigate the performance of PPM and BPSK modulation schemes in our researches.

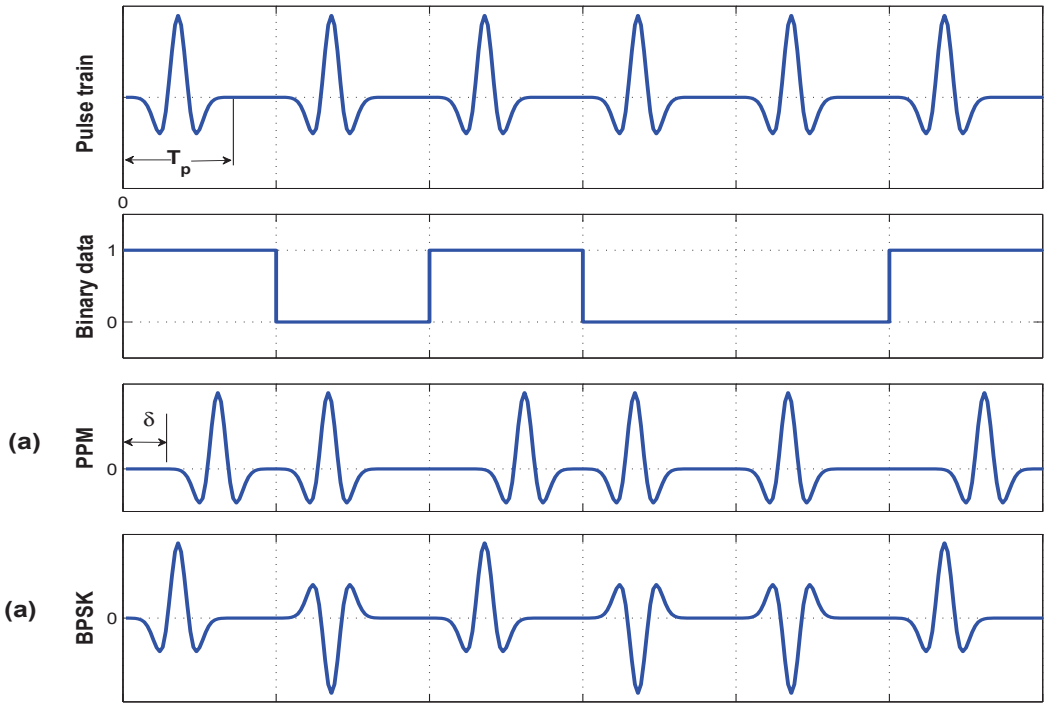


Figure 2.5.1: Illustration of pulse modulation techniques. (a) PPM. (b) BPSK. T_p is the pulse duration, δ is the PPM pulse shift.

2.5.1 Pulse Position Modulation (PPM)

The principle of pulse position modulation is to encode information into two or more positions in time, with references to the nominal pulse position. For example, in a binary system, as shown in Figure 2.5.1 (a), pulse representing a bit 0 is transmitted at the nominal position, and a pulse representing a bit 1 is transmitted after the nominal position. This is achieved by time shifting, which is typically a fraction of a nanosecond and less than the time duration between nominal positions to avoid interference between impulses. In PPM, all pulses (both "0"s and "1"s) are of the same amplitude. The receiver distinguishes between the binary bits by the time of arrivals of the pulses, or the time lag between pulses. Since the transmitted information is contained in the time lag, higher timing accuracy is required for the system when employing PPM modulation. Nevertheless, this modulation has its advantages on implementation simplicity and good ability against attenuation effects when compared to other modulation schemes [71]. PPM modulation will also smooth the spectrum of the signal, thus making the system less likely to interfere with conventional radio systems [72].

The PPM signal in UWB system can be represented as follows

$$s_{PPM}(t) = \sum_{m=0}^{M-1} p(t - mT_f - b_m\delta) \tag{2.5.1}$$

where M is the number of transmit symbols, $b_m \in \{0, 1\}$ is the information mth bit, $p(t)$ is the

UWB impulse, δ represents the PPM time shift, T_f is the pulse repetition period.

2.5.2 Binary Phase Shift Keying (BPSK)

This modulation is also called biphase or antipodal modulation and concentrates on changing the polarity of the transmitted impulses according to the incoming data as can be shown in the figure 2.5.1 (b). The impulse has positive polarity to encode a 1 and negative polarity to encode a 0. In this case, only one bit per impulse can be encoded because there are only two polarities available to choose from. The advantages of using BPSK is its power efficiency and reduced jitter requirements [73].

The UWB BPSK signal can be expressed as

$$s_{BPSK}(t) = \sum_{m=0}^{M-1} (2b_m - 1)p(t - mT_f) \tag{2.5.2}$$

where

$$b_m = \begin{cases} -1 & \text{if information bit is 0} \\ 1 & \text{if information bit is 1} \end{cases} \tag{2.5.3}$$

is the polarity of the modulated pulse, M is the number of transmit symbols, $p(t)$ is the UWB impulse, T_f is the pulse repetition period. The BPSK modulation has better performance than other modulation techniques since the difference impulse level is twice the impulse amplitude. This advantage makes the BPSK signal less susceptible to distortion. Another advantage of BPSK is that the change in polarity of pulses produces a zero mean and can thus remove the discrete spectral lines in the PSD. However, the physical implementation of the transmitter using this modulation scheme requires two pulse generators for positive and negative pulses which results in more complexity.

2.6 Multiple Access Techniques

The future of UWB technology engages the operation of a large number of devices and many collocated noncordinated networks. In such environment, multiple users must be able to share the UWB spectrum simultaneously. Systems designers can utilize multiple access methods to accommodate these multiple users. In UWB system the multiple access capability can be achieved by applying a randomizing technique to the pulse train before transmission. This makes the spectrum of UWB transmission more noise-like and provides immunity to multipath interference [69]. Time hopping (TH) and direct sequence (DS) multiple access techniques are two commonly used methods in traditional wireless communication. A TH technique apply a

time offset determined by user-specific TH sequence to the position of the transmitted UWB pulses, while the DS method uses a pseudo-noise (PN) code to produce a random sequence of antipodal pulses. Although TH and DS techniques are known as spreading spectrum techniques in narrow-band system, neither of them leads to further spectrum spreading in UWB communication.

2.6.1 Time Hopping Multiple Access

When applying TH multiple access technique, the transmission instance of the UWB pulses is changed according to a TH sequence. The basic of TH is to divide the frame interval T_f into multiple smaller segments called time slots "chips" and only one of these slots carries the user's transmitted pulse. The TH sequence is a unique code assigned to each user and serve to specify which slot in each frame is used for transmission; hence the multiple accesses are accomplished by allocating different time slots for different users. For a large time frame, the use of a PN code to determine the transmission time randomizes the pulse train in both time and frequency domains. This makes the spectrum of the UWB transmission become much more noise-like [69].

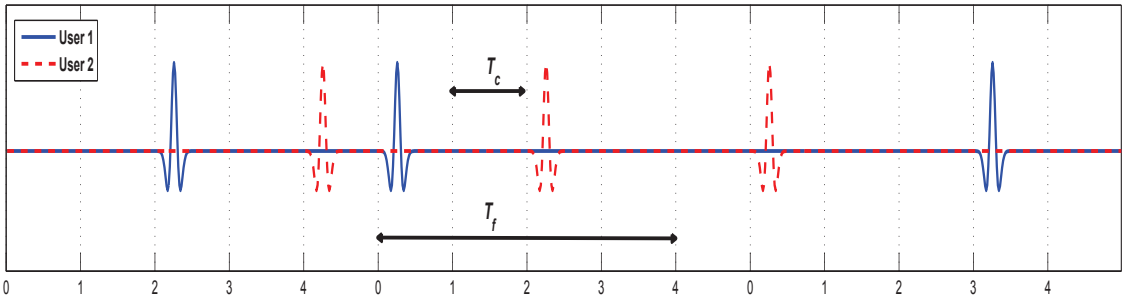


Figure 2.6.1: Pulse trains with TH sequences $\{2, 0, 3, ...\}$ for user 1 and $\{4, 2, 0, ...\}$ for user 2. T_f is the frame duration, T_c is the chip duration.

In a TH-based system, the signaling interval T_s contains N_f frames each of duration T_f. Each frame is composed of N_h time slots with chip duration T_c such that $N_h T_c \leq T_f$. Each frame can hold up to N_h users which can access the transmission medium sequentially using TH sequences. The TH sequence is denoted by $\{C_k\}$, $0 \leq C_k \leq N_h - 1$. It provides an additional time shift of $C_k T_c$ seconds to the kth transmitted pulse. The pulse train incorporating TH sequence becomes

$$s_{TH}(t) = \sum_{k=-\infty}^{\infty} p(t - kT_f - C_k T_c) \tag{2.6.1}$$

Figure 2.6.1 show pulse trains of two users without modulation with TH multiple access technique where $N_h = 5$ and the TH sequences are $C_k^1 = \{2, 0, 3, \ldots\}$ for user 1 and $C_k^2 = \{4, 2, 0, \ldots\}$

for user 2. The frame duration typically ranges from a hundred to a thousand time the pulse width. The data rate of the transmission can be modified by changing the number of pulses representing a single data bit [69, 74].

$$R = \frac{1}{T_s} = \frac{1}{N_f T_f} \tag{2.6.2}$$

where R_s is the data rate in [bit/Hz], T_s is the signaling interval used to transmit one data bit, N_f is the number of pulses per data bit, T_f is the TH frame. In 2.6.2, higher processing gain can be obtained by increasing the number of pulses per data bit while maintaining the same frame duration. The penalty is the reduced data rate.

2.6.2 Direct Sequence Multiple Access

Direct sequence spread spectrum (DSSS) is a well-known multiple access technique in wireless communications [75]. It has been widely used in conventional communication to spread the energy of the signal over a large bandwidth. Thus, the energy per unit frequency is reduced and the interference is decreased. This enables multiple users to share the same spectrum bandwidth simultaneously without interfering with one another. It is exactly this situation that is of interest to UWB system designers. A direct sequence UWB system (DS-UWB) is almost identical to the ordinary DSSS system except that the bandwidth spreading effects are realized by pulse shaping. By assigning each user a unique PN sequence, the DS-UWB system generates a train of high-duty-cycle pulses (analogous to chips) whose polarities follow the PN code. A data bit is then used to modulate this train of UWB pulses. The chipping code forms a redundant pulse pattern for each bit that is transmitted. The processing gain is defined by the number of pulses/chips per bit. It is a key parameter for DS-UWB systems which provides signal's resistance to interference. If an interference or jammer resides in the same band, it will be spread out by a factor equivalent to the processing gain during the despreading process at the receiver.

In a DS-UWB system, the pulse train embodying the PN code is given by

$$s_{DS}(t) = \sum_{k=-\infty}^{\infty} \sum_{n_c=0}^{N_c-1} C(n_c) p(t - kT_b - n_c T_c) \tag{2.6.3}$$

where N_c is the processing gain denoting the number of chip per bit. $T_b = N_c T_c$, where T_c is the chip duration and T_b is the bit duration. $\{C(n_c)\}_{n_c=0}^{N_c-1}$ is the PN spreading sequence. In the case of DS-UWB system, the pulse waveform takes the role of the chip i.e. each chip is presented by one pulse. Even though, to avoid pulses overlapping and reduce the effect of intersymbol and intrasymbol interference the chip duration is usually chosen greater than the pulse width ($T_c > T_p$). Figure 2.6.2 shows the pulse train of coded data signal with a PN sequence $C(n_c) = \{1, 1, 1, -1, 1, -1, -1\}$ where $N_c = 7$.

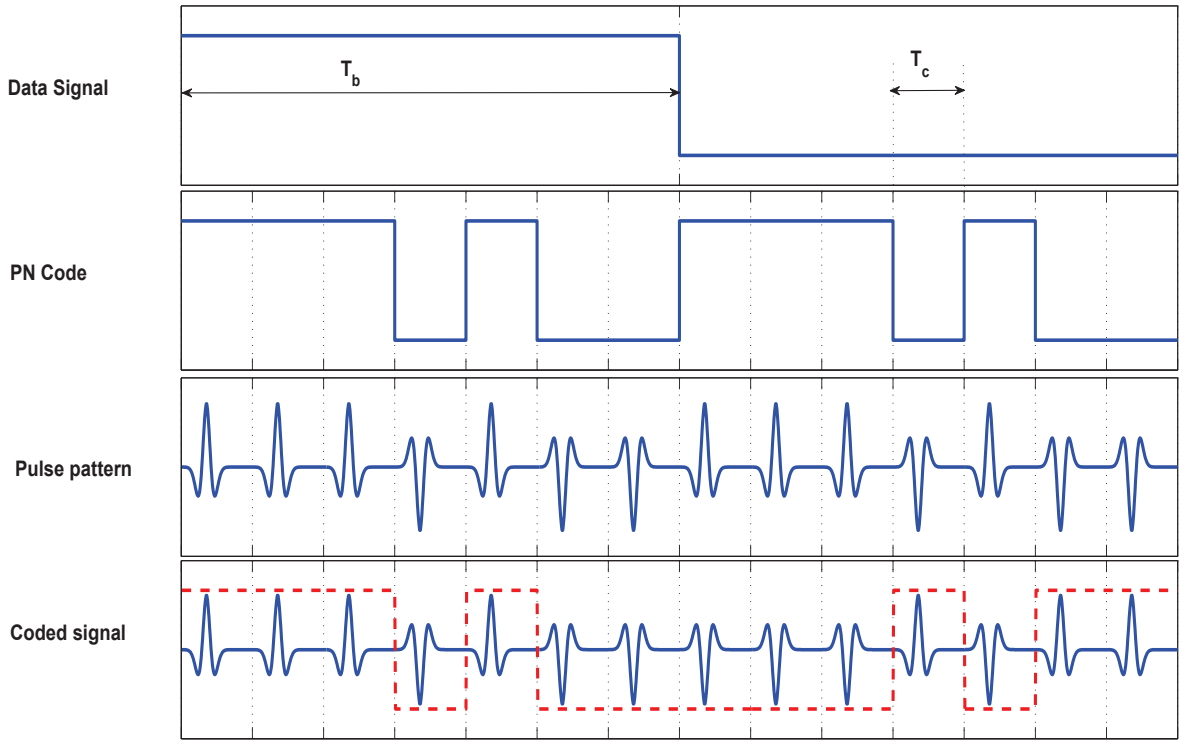


Figure 2.6.2: Time window of DS-UWB with PN sequences $\{1, 1, 1, -1, 1, -1, -1\}$. T_b is the bit duration, T_c is the chip duration.

2.7 UWB Channel Model

As with any other communications system, the theoretical and practical performance limits of any system depends directly on the channel it is operating. In order to build UWB systems that achieve all the prospective, a detailed understanding of the channel and its interaction with the system is required.

2.7.1 General Overview of UWB channel models

Although channel models for narrow-band have been well demonstrated in the literature, they cannot be generalized directly to UWB channels. The propagation of a signal in wireless channel generates multiple replicas at the receiver; this phenomenon is known as multipath propagation. Channel modeling usually characterizes the different multipath components (MPCs) by different delays and attenuations. For a narrowband signal with a bandwidth less than the coherence bandwidth of the propagation channel, the impulse response of the channel can be

represented as the sum of the contributions of the different MPCs. When the system bandwidth is so small that the delays of the individual MPCs do not impact the system performance, the channel model is thus flat Rayleigh-fading. Otherwise, if a large number of MPCs are observed at the receiver, the central limit theorem is commonly used to model the complex amplitudes of the different received paths as Rayleigh distributed. Thus, Rayleigh-fading is widely used for channel models in many narrowband systems [76]. The impulse response of the Rayleigh-fading channel can be written as

$$h(t) = \sum_{i=1}^{N_p} a_i e^{(j\varphi_i)} \delta(t - \tau_i) \tag{2.7.1}$$

where $\delta(.)$ is the Dirac delta function, N_p is the number of resolvable MPCs, a_i is the i path amplitude whose phaseφ_i is uniformly distributed random variable in the range $[0, 2\pi]$ and τ_i is the i path delay.

Furthermore, with the continuous growth of wireless communications; new systems with larger bandwidth have emerged as the second- and third-generation cellular systems. The performance of such systems is highly affected by the different delays of the MPCs. The channel for such system is modeled by the power delay profile which describes how much power arrives within certain delay intervals. The delay interval (also called time resolution or delay bin) is comparable to the inverse of the system bandwidth. The amplitude statistics of the MPCs that fall within each delay interval is Rayleigh or Rice. However, those considerations are termed for system with bandwidth of up to 20 MHz [76].

Compared to the aforementioned narrow-band and large-band channels, UWB channels behave differently since it cover a bandwidth of almost 10 GHz. This gives rise to new effects considering the following points [69, 77, 78]:

- Due to the fine delay resolution considered for UWB systems, it often happens that only a few physical components contribute to one resolvable MPC. The amplitude statistics of such a resolvable MPC is therefore not complex Gaussian anymore.

- For the same reason, there is a considerable probability that resolvable delay intervals of no energy can exist during which no significant amount of energy is arriving at the receiver.

- Due to the frequency-selective nature of UWB signal propagation including reflection, diffraction and scattering on objects in the environment, each MPC shows distortions by itself.

- In a UWB system, the delays τ_i of the MPCs can change noticeably on a much shorter timescale (e.g. due to relative movements of transmitter and receiver by a wavelength).

Thus, a lot of work has been dedicated to modeling UWB channels in recent years, as the interest for UWB becomes one of the hottest topic in communication research. The objective is to develop channel models for UWB system that are able to capture these important characteristics of UWB channels in order to make them as realistic as possible [76, 79–82]. The channel measurements in UWB systems showed that the MPCs tend to occur in clusters rather than in a continuum, as is common for narrow-band channels. This is due to the very fine resolution of UWB waveforms allowing different objects in the environment to contribute different clusters of MPCs. The measurements of UWB propagation channels were performed only in the late 1990s, and the first published papers on statistical UWB channel models appeared in 2001 [80]. Since then, UWB propagation research has met more attention, particularly, the standardization activities of IEEE 802.15.3a and 802.15.4a working groups. The IEEE 802.15.3a models show some drawbacks as they neglect several effects and do not cover many of the ranges and environments that were considered in the IEEE 802.15.4a models. In fact, the IEEE 802.15.3a models were recently withdrawn as unanimous decision was not reached [83]. This why we have chosen to adopt the IEEE 802.15.4a models in this study.

2.7.2 The IEEE 802.15.4a channel Models

In its final report [17], The IEEE 802.15.4a channel modeling subgroup provides models for different frequency ranges and environments. The resulting models for the 2-10 GHz range are a modified Saleh-Valenzuela (SV) model, with channel parameters defined for indoor residential, indoor office, industrial, outdoor, and open outdoor environments. For each of those environments, LOS and Non-line-of-sight (NLOS) properties are distinguished, with the exception of open outdoor environments, where only NLOS situations are modeled. According to [17], the key features of the proposed model are:

- model treats only channel, while antenna effects are to be modeled separately
- d^{-n} law for the pathloss
- frequency dependence of the pathloss
- modified SV model:
  - the paths arrive in clusters within each there are multiple consequent arrivals of MPCs called rays
  - mixed Poisson distribution for ray arrival times
  - possible delay dependence of cluster decay times
  - some NLOS environments have first increase, then decrease of power delay profile

- Nakagami-distribution of small-scale fading, with different m-factors for different components
- block fading: channel stays constant over data burst duration

Pathloss

The pathloss is assumed to depend on distance and frequency which can be written as a product of the terms

$$PL(f,d) = PL(f)PL(d) \tag{2.7.2}$$

The distance dependance of the path gain in dB decays following

$$PL(d) = PL_0 + 10n\log_{10}\left(\frac{d}{d_0}\right) \tag{2.7.3}$$

where the reference distance d_0 set to 1 m, PL_0 is the path gain at the reference distance, n is the propagation exponent. The propagation exponent depends on the environment, and on whether a line-of-sight (LOS) connection exists between the transmitter and receiver or not [17].

The frequency dependency of the pathloss is given as [84, 85]

$$\sqrt{PL(f)} \propto f^{-\kappa} \tag{2.7.4}$$

where the coefficient κ can be positive or negative, depending on the environment and whether the antenna effects are considered or not. Throughout this study, the antenna effect as well as the frequency dependency of the pathloss have been ignored.

Shadowing or large-scale fading

Similar to the narrow-band fading, this process is defined as the variation of the local mean around the pathloss. Shadowing is not included in the IEEE 802.15.4a models for reasons related to the specific simulation requirements.

Power delay profile

As mentioned before, the most distinctive characteristics of UWB channel are its rich multipath profile and non-Rayleigh fading amplitude. In UWB propagation environment, different parts of the same object can broadcast several MPCs, all of which would be part of one cluster. Therefore, the MPCs tend to arrive at the receiver in clusters; within each there is a random

number rays. The modified SV model was adopted by the IEEE 802.15.4a modeling subgroup as a reference UWB channel model. The discrete representation of the impulse response in complex baseband according to SV model is given in general as [86]

$$h_{discr}(t) = \sum_{l=0}^{L} \sum_{k=0}^{K} \alpha_{k,l} \exp(j\phi_{k,l}) \delta(t - T_l - \tau_{k,l}) \tag{2.7.5}$$

where $\alpha_{k,l}$ is the tap weight of the kth component in the lth cluster, T_l is the arrival time of the lth cluster and $\phi_{k,l}$ is the delay of the kth component relative to the lth cluster arrival time T_l. The phases$\phi_{k,l}$ are uniformly distributed random variables in the range $[0, 2\pi]$. K is the number of MPCs within each cluster, and L is the number of clusters. Figure 2.7.1 shows the IEEE 802.15.4a model with its different parameters that well be discussed in what follow.

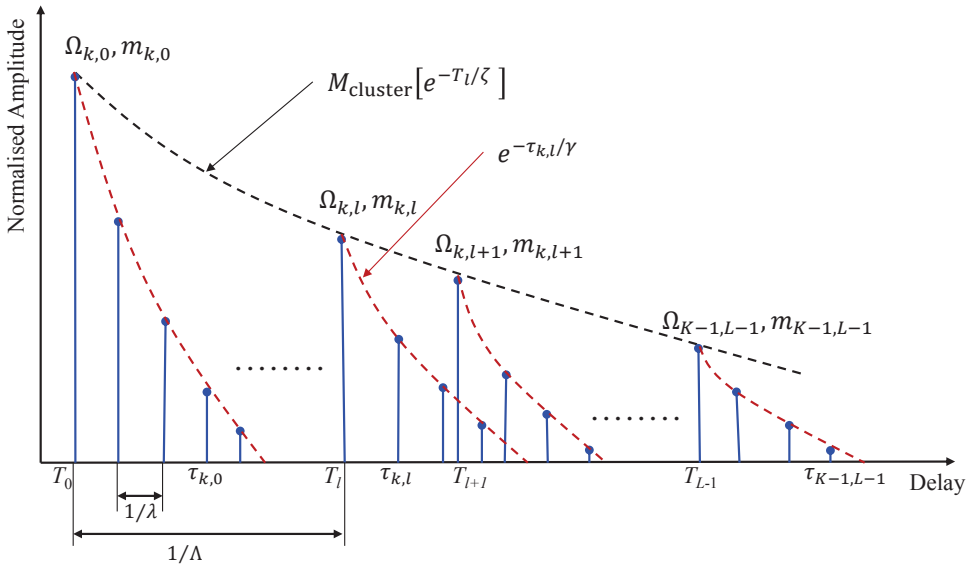


Figure 2.7.1: IEEE 802.15.4a UWB channel model

A. Cluster distribution

The number of clusters L is an important parameter of the model. It depends on both the measurement bandwidth, and the considered environments and is assumed to be Poisson-distributed as:

$$pdf_l(L) = \frac{(\bar{L})^L \exp(-\bar{L})}{L!} \tag{2.7.6}$$

so that the mean $\bar{L}$ completely characterizes the distribution.

The distributions of the cluster interarrival times are given by a Poisson processes

$$p(T_l|T_{l-1}) = \Lambda_l \exp\left[-\Lambda_l \left(T_l - T_{l-1}\right)\right], l > 0 \tag{2.7.7}$$

where Λ_l is the cluster arrival rate assumed to be independent of l.

B. Ray interarrival times

In order to give an appropriate matching to the ray interarrival times, the IEEE 802.15.4a subgroup propose to use a mixture of two Poisson processes for the modified SV model with respect to the single Poisson process used in the original SV model. The distribution of the ray interarrival times is thus given as follows [17]

$$\begin{aligned} p(\tau_{k,l}|\tau_{(k-1),l}) = {} & \beta\lambda_1 \exp\left[-\lambda_1(\tau_{k,l} - \tau_{(k-1),l})\right] \\ & + (\beta - 1)\lambda_2 \exp\left[-\lambda_2(\tau_{k,l} - \tau_{(k-1),l})\right], k > 0 \end{aligned} \tag{2.7.8}$$

where β is the mixture probability, while λ_1 and λ_2 are the ray arrival rates.

C. Cluster powers and cluster shapes

The power delay profile (mean power of the different paths) is exponential within each cluster

$$E\left\{|\alpha_{k,l}|^2\right\} = \Omega_l \frac{1}{\gamma_l\left[(1-\beta)\lambda_1 + \beta\lambda_2 + 1\right]} \exp\left(\frac{-\tau_{k,l}}{\gamma_l}\right) \tag{2.7.9}$$

where Ω_l is the integrated energy of the lth cluster, and γ_l is the intra-cluster decay time constant. The mean over the cluster shadowing follows in general an exponential decay

$$10\log(\Omega_l) = 10\log\left(\exp\left(\frac{-T_l}{\zeta}\right)\right) + M_{cluster} \tag{2.7.10}$$

where $M_{cluster}$ is a Gaussian distributed random variable with standard deviation $\sigma_{cluster}$ around it, ζ is the cluster decay factor.

The cluster decay rates depend linearly on the arrival time of the cluster [17],

$$\gamma_l \propto k_\gamma T_l + \gamma_0 \tag{2.7.11}$$

where k_γ describes the increase of the decay constant with delay.

Small-scale fading

The small-scale amplitude distribution is Nakagami

$$pdf(x) = \frac{2}{\Gamma(m)} \left(\frac{m}{\Omega}\right)^m x^{2m-1} \exp\left(-\frac{m}{\Omega}x^2\right) \tag{2.7.12}$$

Where $m \geq 1/2$ is the Nakagami m-factor, $\Gamma(m)$ is the gamma function, and Ω is the mean-square value of the amplitude.

The m-factor is modeled as a lognormally distributed random variable, whose logarithm has a mean μ_m and standard deviation σ_m. Both of these can have a delay dependence

$$\mu_m(\tau) = m_0 + k_m\tau \tag{2.7.13}$$

$$\sigma_m(\tau) = \hat{m}_0 + \hat{k}_m\tau \tag{2.7.14}$$

With the exception of the first component of each cluster, for which the m-factor is modeled differently. It is assumed to be deterministic and independent of delay

$$m = \tilde{m}_0 \tag{2.7.15}$$

More descriptions of the IEEE 802.15.4a UWB channel models with their detailed parameters can be found in [17].

2.8 Conclusions

In this chapter, the basic properties of UWB signals were outlined, starting with the definition given by the FCC, as well as the limits of the power output and spectrum of UWB pulses. Several signal shapes namely – rectangular pulses, Gaussian pulses, Gaussian monocycle pulses and Gaussian doublet pulses – were presented. The frequency spectrum and signal expression of each pulse were derived and explained. Thereafter, pulse modulation methods and multiple access techniques for UWB radios were presented. Then, we gave a state of art of UWB channel measurement and modeling and discussed some characteristics of UWB propagation channels, such as the number of multipath components, multipath amplitude fading distribution and multipath intensity profiles. In the following chapter we present the system model for cooperative diversity that uses UWB communication.

Chapter 3

Proposed System Model: Description and Methodology

Contents

3.1 Introduction 64

3.2 System Description 64

3.3 Transmitter Model 64

3.4 Channel Models 67

3.4.1 Residential environments 68

3.4.2 Indoor office environments 68

3.5 Receiver Structure 69

3.5.1 Rake Receiver 71

3.5.2 Channel estimation 73

3.5.3 Maximum Ratio Combining (MRC) 73

3.6 Conclusions 74

3.1 Introduction

In this chapter, we summarize the key ingredients of a simple system model for examining cooperative diversity in different UWB channel environments. UWB transceiver well be developed considering multiple user transmission. The power constraint and the extremely fading properties of the UWB channel are great motivations to use Rake receiver. Since UWB signals have very wide bandwidth, then the number of resolvable MPCs is usually very large. A Rake receiver exploits the diversity by capturing the energy dispersed over many multipath components of the UWB channel and increase the collected power at the receiver side. With perfect knowledge of CSI and in the presence of AWGN, the Rake receiver with maximum ratio combining (MRC) maximizes the output SNR and thus it can improve the receiver performance.

3.2 System Description

The block diagram of the generalized UWB transceiver system is illustrated in figure 3.2.1. In this system model, multiple users transmit their UWB signals simultaneously applying multiple access technique to avoid catastrophic collisions. Information data can be an exchange of data among nodes in WSN or from any application in WPAN, such as a personal digital device or a digital stream from a DVD player, an e-mail, or a web browser. User's data are used to modulate the UWB pulse train at the output of the pulse generator. The UWB channel fading is modeled according to the IEEE 802.15.4a standard. Due to the multiuser transmission, the received signal at the destination is corrupted by interference plus noise. Since UWB transmission is power limited, we use Rake receiver in order to collect power from multipath propagation. Another required equipments like precise timing circuits and optional amplifier circuits, are not shown in figure 3.2.1 for simplicity reasons.

The network nodes consists of synchronous radio terminals each equipped with a single antenna and they are operating in half-duplex mode; i.e. at any time, a node can either transmit or receive, but not both. This constraint is justified by the typically large difference between the incoming and outgoing signal power levels. Note that, for antenna selection scenario, the relay node are assumed to be equipped with multiple antennas as we will see in chapter 4 and 5.

3.3 Transmitter Model

In the presented system model, K simultaneous users transmit impulsive signals through UWB channel. Different coding techniques such as interleaving, channel coding and error correction codes can be applied to the binary data in order to provide flexible and robust performance. After that, the binary data is mapped from bits to symbols. These symbols are then modulated

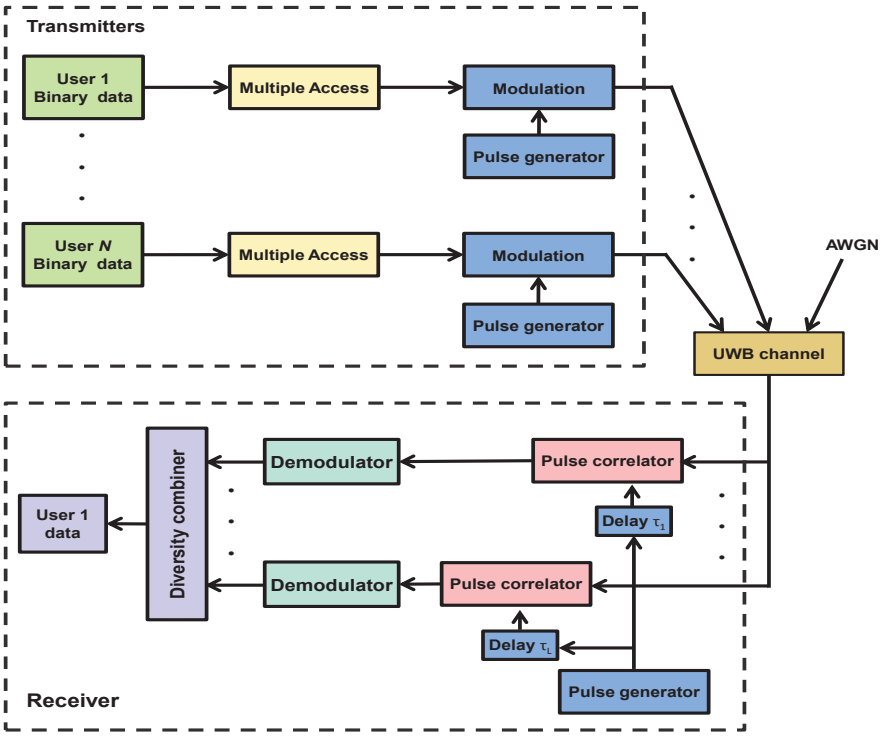


Figure 3.2.1: Block diagram of multiple user UWB communication system.

into analog UWB pulse shapes and transmitted through antenna. Basically, each user generates a pulse train modulated by the data stream. In this case, multiuser transmissions can be achieved by pulse modulation and multiple access techniques. In general, the transmitted signal of user k can be expressed as

$$s_k(t) = \sqrt{\frac{E_k}{N_f}} \sum_{m=0}^{M} \sum_{n=0}^{N_f-1} F(n,k)\, p(t - t_k - mT_s - nT_f - G(n,k)) \tag{3.3.1}$$

where E_k is the energy per symbol; m is the symbol index in a frame of length M symbols, the N_f is the number of pulse per symbol; T_s is the symbol duration; $p(t)$ is the pulse shape; t is the first user transmission time delay; t_k is the transmission time delay of the user k relative to the first user transmission delay with $t_1 = 0$. The functions $F(n,k)$ and $G(n,k)$ are used here to generalize the access method and the type of modulation. These functions well be derived in what follow.

For simplicity, we will focus, in our analysis, on the communication model depicted in figure 3.3.1, with one source, one destination, and one or more relays denoted by S, D, and R respectively. This model can be easily upgraded to different cooperative schemes. As we will see, the number of involved relays is effectual factor in the total performance.

The relay assists the S-D transmission using DF protocol in order to provide diversity gain and thus improve the detection reliability at the destination. We have chosen to apply DF cooperation strategy at the relay node for power considerations. The communication scenario

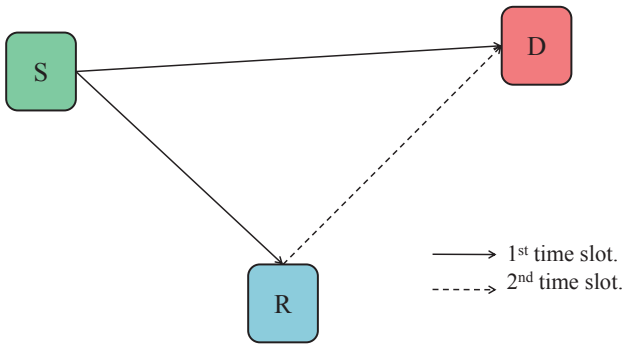


Figure 3.3.1: General cooperative system model.

takes place in two phases. In the first phase, S broadcasts signal toward R and D. Then, R and D receive faded noisy versions of the source signal. In the second phase, S remains silent, while R re-encodes and retransmits an estimated version of the received signal to D. Subsequently D combines the received signals during the two phases. The transmission interval divides into two time-slots of equal duration.

The transmitted energy is chosen to be equally distributed among the two halves of the cooperation phases. More specifically, UWB signals must be in the power-limited regime. Therefore, the transmitted energy from source and relays must be scaled in order to respect the UWB emission mask. It is at most equal to −41.3 dBm/MHz which is the maximum emission power limit for UWB transmission as specified by the FCC.

Pulse shape: Since a typical UWB system is carrierless, the choice of the pulse shape is an important factor for design consideration and should be convenient for physical implementation and for mathematical modeling. Thus the second derivative of the Gaussian pulse, known as Gaussian doublet, is typically considered in the literature for UWB systems [87, 88]. It is assumed to include the differential effects of the transmitter and receiver antennas. The discrete time representation of the Gaussian doublet pulse is given by 2.4.5.

Modulation types: under the imposed regulations, UWB transmit power will be limited, and this affects the selection of the modulation in the transmitter as well as the receiver sides. First, the modulation technique needs to be power efficient, which means it must grant best error performance for a given energy per bit. Second, the modulation scheme affects the structure of the PSD and thus has the potential to impose further limitations on the total transmitted power. Therefore, we chose to use PPM and BPSK modulations since they present the best spectral efficiency with a smooth PSD compared to the other modulation techniques as discussed in the past chapter.

Multiple access: After modulation, multiple-access is introduced. We apply DS and TH multiple access methods in both cooperative phases to attain orthogonality among different sources and relays. We study the performance of the proposed three nodes scheme in presence of multiple accesses in order to facilitate the generalization. MAI occurs even of applying multiple

access techniques due to multipath propagation, asynchronous transmission, and the imperfect correlation of multiple access codes. Thus, the perfect orthogonal transmission cannot be achieved in practice [89].

At the receiver, the signals of all K users with multipath propagation are summed, such that the total received signal is given by

$$r(t) = \sum_{k=1}^{K} s_k(t) * h_k(t) + n(t) \tag{3.3.2}$$

where $*$ denotes the convolution operation, $h_k(t)$ is the discrete channel model between user k and the receiver and $n(t)$ is AWGN with two-sided power spectral density $\frac{N_0}{2}$ watts/Hz .

In the considered communication scheme, the received signals at the destination and the relay during the first time slot are given in 3.3.3 and 3.3.4, respectively. In the second time slot, the relay first decodes the source signal, re-encodes and then transmits the source estimated data to the destination. The received signal at destination in the second time slot is given in 3.3.5.

$$r_{d_1}(t) = s_s(t) * h_{sd}(t) + \sum_{k=1,k\neq s}^{K} s_k(t) * h_{kd}(t) + n_{d_1}(t) \tag{3.3.3}$$

$$r_r(t) = s_s(t) * h_{sr}(t) + \sum_{k=1,k\neq s}^{K} s_k(t) * h_{kr}(t) + n_r(t) \tag{3.3.4}$$

$$r_{d_2}(t) = s_r(t) * h_{rd}(t) + \sum_{k=1,k\neq r}^{K} s_k(t) * h_{kd}(t) + n_{d_2}(t) \tag{3.3.5}$$

where $s_s(t)$ and $s_r(t)$ are the source signal broadcasted in the first time slot and the relay signal which is the retransmission of the source signal after decoding, estimation and re-encoding, respectively; $h_{ab}(t)$ is the channel coefficients between node a and node b; $n_{ind}(t)$ is AWGN with zero mean and variance $\frac{N_0}{2}$. In 3.3.3–3.3.5, the first, second and third terms are respectively, the received signal, the MAI and the complex AWGN.

3.4 Channel Models

Different types of UWB channels, that meet measurement results, are defined by the IEEE 802.15.4a subgroup for UWB wireless communication within the $3.1 - 10.6$ GHz range . In this study, we investigate the utility of cooperative diversity for UWB communication considering the IEEE 802.15.4a channel models for residential and office indoor environments. These models are based on measurements and simulations done by the authors of [90–92] (other environments such as outdoor, industrial and farms are also modeled). These models have been developed by the authors of [93] during their work for the IEEE 802.15.4a subgroup, and was

accepted by that body as the official model for comparing different system proposals for standardization. The channel modeling for residential and office indoor environments differentiates between LOS and NLOS scenarios resulting in four types of UWB channels defined by [17] to meet measurement results, namely CM1, CM2, CM3 and CM4.

3.4.1 Residential environments

The model was extracted based on measurements that cover a range from $7-20$ m, up to 10 GHz. The LOS case referred to CM1 and the NLOS referred to CM2. These environments are critical for "home networking," linking different appliances, as well as safety (fire, smoke) sensors over a relatively small area. The building structures of residential environments are characterized by small units, with indoor walls of reasonable thickness [17, 93]. Figure 3.4.1 shows the power delay profile of the impulse responses of these channel types and table 3.4.1 presents the list of their parameters. The following list give the description of parameters used in table 3.4.1and 3.4.2

PL_0 : pathloss at 1m distance

n : pathloss exponent

κ : frequency dependence of the pathloss

$\bar{L}$: mean number of clusters

Λ_l : inter-cluster arrival rate

λ_1,λ_1,β : ray arrival rates (mixed Poisson model parameters)

ζ : inter-cluster decay constant

k_γ, γ_0 : intra-cluster decay time constant parameters

$\sigma_{cluster}$: cluster shadowing variance

m_0: Nakagami m factor mean

$\hat{m}_0$: Nakagami m factor variance

3.4.2 Indoor office environments

The model was extracted based on measurements that cover a range from $3-28$ m, within the $2-8$ GHz frequency range. The LOS case referred to CM3 and the NLOS referred to CM3. Some of the office rooms are comparable in size to residential, but other rooms (especially cubicle areas, laboratories, etc.) are considerably larger. Areas with many small offices are

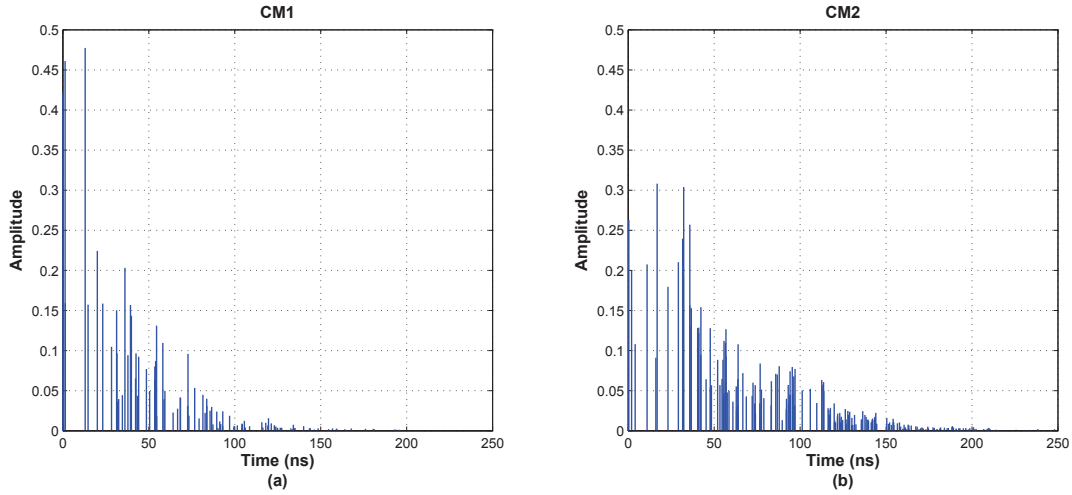


Figure 3.4.1: Power delay profile of the impulse responses for (a) CM1: IEEE 802.15.4a residential LOS and (b) CM2: IEEE 802.15.4a residential NLOS.

typically linked by long corridors. Each of the offices typically contains furniture, bookshelves on the walls, etc., which adds to the attenuation given by the (often thin) office partitionings [17, 93]. Table 3.4.2 presents the list of parameters of these channel types and figure 3.4.2 shows the power delay profile of the impulse responses.

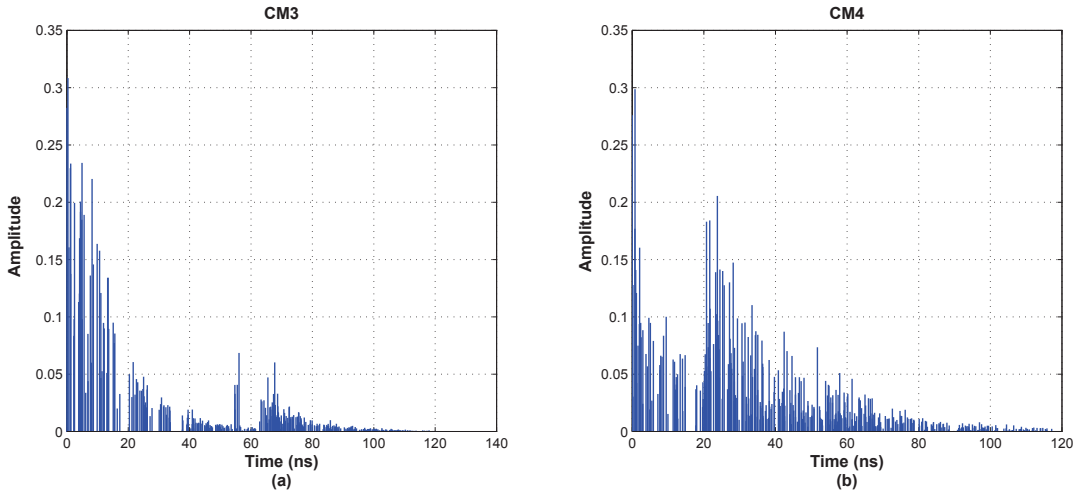


Figure 3.4.2: Power delay profile of the impulse responses for (a) CM3: IEEE 802.15.4a office LOS and (b) CM4: IEEE 802.15.4a office NLOS.

3.5 Receiver Structure

UWB multiple access system is studied over a multipath indoor wireless channel, thus addressing the IEEE 802.15.4a final report for UWB channel models [17]. The multipath distortion occurs when a radio frequency (RF) signal takes different paths from a transmitter to a receiver due to reflection, refraction and scattering [94]. As a result, the signal power is divided among

Table 3.4.1: Parameters for residential channel models CM1 and CM2.

Channel model	CM1	CM2
Environment	Residential LOS	Residential NLOS
Valid range [m]	7-20	7-20
Pathloss		
PL_0 [dB]	-43.9	-48.7
n	1.79	4.58
κ	1.12	1.53
Power delay profile		
$\bar{L}$	3	3.5
Λ_l [1/ns]	0.047	0.12
λ_1 [1/ns]	1.54	1.77
λ_2 [1/ns]	0.15	0.15
β	0.095	0.045
ζ [ns]	22.61	26.27
k_γ	0	0
γ_0 [ns]	12.53	17.50
$\sigma_{cluster}$ [dB]	2.75	2.93
Small-scale fading		
m_0 [dB]	0.67	0.69
$\hat{m}_0$ [dB]	0.28	0.32

these paths, these portions of the signal will encounter delays and travel longer paths to the destination. This can cause many critical phenomenon such as fading, inter-symbol interference (ISI), amplitude variation and signal nulling. For the signal to survive in a fading environment, one solution is to increase the transmitted power. However, this is not a viable solution for UWB systems due to the limitation on power mandated by the FCC. In cellular systems, the wireless signal travel from the source to the destination in different paths that can be distinguished by complex amplitudes and arriving delays. It is possible through numerical methods to estimate the multipath components of the received signal and then combine them coherently to maximize the received signal strength. This technique is referred to as a Rake receiver. This receiver exploits the multipath diversity by combining different signal components that have propagated through diverse links and thus enhances the signal-to noise ratio (SNR).

Table 3.4.2: Parameters for office channel models CM1 and CM2.

Channel model	CM1	CM2
Environment	Office LOS	Office NLOS
Valid range [m]	3-28	3-28
Pathloss		
PL_0 [dB]	-35.4	-59.9
n	1.63	3.07
κ	0.03	0.71
Power delay profile		
$\bar{L}$	5.4	1
Λ_l [1/ns]	0.016	NA
λ_1 [1/ns]	0.19	NA
λ_2 [1/ns]	2.97	NA
β	0.0184	NA
ζ [ns]	14.6	NA
k_γ	0	NA
γ_0 [ns]	6.4	NA
$\sigma_{cluster}$ [dB]	3	NA
Small-scale fading		
m_0 [dB]	0.42	0.50
$\hat{m}_0$ [dB]	0.31	0.25

3.5.1 Rake Receiver

The Rake receiver consists of a bank of correlators, or matched filters called fingers. Each finger uses a delayed version of the pulse shape which is time adjusted to match the delay of a particular multipath component. Many of the multipath components, in a typical Rake combiner, are bounded by design complexity issues. If the receiver uses all the L received paths, it is called all-Rake (A-Rake). The major drawbacks of using an A-Rake receiver are the increased complexity of circuits and channel estimation as well as power consumption [95]. Since UWB signals have very wide bandwidth, then the number of resolvable MPCs is usually very large. Even if it is possible for a RAKE receiver to provide so many taps, this can increase the complexity of the design. Hence, A-Rake receiver is not feasible for UWB systems due to its complexity. On the other hand, according to the IEEE 802.15.4a channel model, the

multipath components undergoes different channel distortion. Hence, it might become difficult to correctly estimate the channel parameters, so degradation in performance could be observed due to imperfect channel estimation and synchronization [96]. A practical implementation of multipath diversity can be obtained by a partial-Rake (P-Rake) and a selective-Rake (S-Rake) receiver. The P-Rake receiver uses the first M arriving paths out of L resolvable MPCs; while S-Rake seeks for the M best paths out of L received MPCs, those M best components are determined by a finger selection algorithm [95].

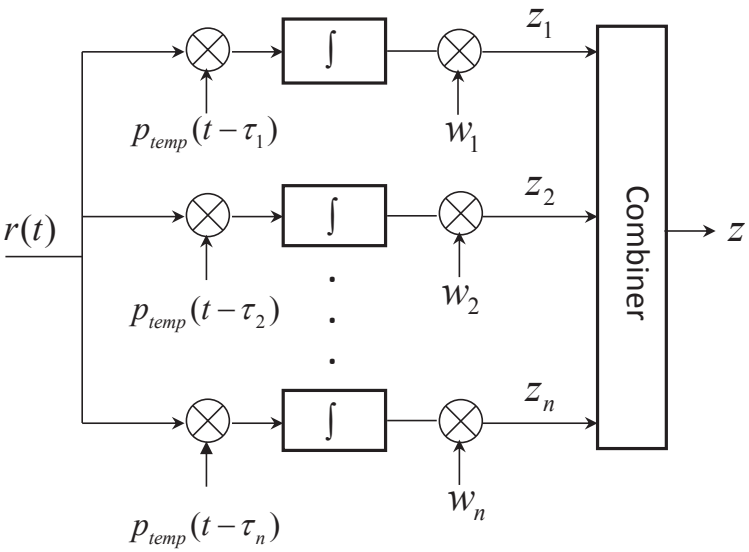


Figure 3.5.1: Block diagram of Rake Receiver.

Each finger of the Rake receiver correlates the received signal with the reference waveform. Due to the high resolution of UWB signals, chip-rate and frame-rate sampling are not very practical. In order to have a lower sampling rate, the received signal can be correlated with symbol-length template signals that enable symbol-rate sampling of the correlator output [97]. The template waveform used at the Rake fingers for the kth user that matches the whole pulse sequence of an information symbol is given by:

$$r^k_{temp}(t) = \sum_{j=0}^{N_f-1} p_{temp}(t - jT_c) \tag{3.5.1}$$

where the energy of $r^k_{temp}(t)$ is normalized to one, i.e., $\int_{-\infty}^{\infty} \left[r^k_{temp}(t)\right]^2 dt = 1$.

If we identify the output of the ith finger of the Rake by z_n, the output of the Rake receiver, after combination, is given by:

$$z = \sum_{n=1}^{N_{Fingers}} w_n z_n \tag{3.5.2}$$

where $N_{Fingers}$is the number of the Rake fingers and $w_n$is the weight assigned to the nth finger,

regardless the combination method. For the kth user, the correlator output of the nth finger with a delay τ_n is

$$z_n^k = \int_{\tau_n}^{\tau_n+T_s} r(t) r_{temp}^k (t-\tau_n) \tag{3.5.3}$$

3.5.2 Channel estimation

For the well demodulation of the received UWB signal, the template signal and the target path of the received signal must be perfectly aligned at each of the Rake correlators. The aim is to determine the relative delay of the received signal tap with respect to the template signal. Channel estimation, in UWB system, is a critical issue due to the precise channel characteristics. There are several used algorithms to estimate the channel taps with different complexity degree. One of the most used algorithms is the data-aided (DA) approach that is based on using a number of known pilot symbols called (training sequence) in the beginning of the data packet, while the rest of the packet is interpreted based on the acquired channel characteristics. After sampling, the received signal is correlated with the sampled impulses train of the well known training symbols. The channel estimator is then scans the value of the correlation and compares them with a threshold to find out the significant peaks. It is the time position of these peaks that are used as delay of the template waveform for the correlators of the Rake fingers. If the receiver knows the properties of the transmitted signal, it may also estimate the amplitudes of the path components corresponding to each of the selected delays.

Two suboptimal estimation algorithms with reduced complexity are examined in some papers. The first is denoted by sliding window (SW) algorithm and the second is the successive channel (SC) estimation [98]. The sliding window algorithm cross-correlates an identified pilot with the received pilot sequence and calculates gains and delays for all channel taps at the same time. The sliding window is optimal for a one-tap or if the shifted versions of the received signal are mutually orthogonal. The SC algorithm enhances the performance of SW algorithm by employing the iterative notion. The algorithm begins by using the sliding window to uncover the coefficients of the strongest tap, then the delayed version of the transmitted signal corresponding to the estimated tap is subtracted from the received sequence and the algorithm is repeated by a number of iterations equal to the number of taps to be estimated. Even though SC algorithm introduces more delay than the simple sliding window algorithm, the estimation error is significantly lower.

3.5.3 Maximum Ratio Combining (MRC)

The outputs of the Rake fingers is the signal power components extracted from all or a subset of the received path components. The linear combination of these outputs can be done in several

ways. The conventional Rake receiver, as defined by Turin in 1980 [99], uses the maximum ratio combining (MRC) to combine the finger outputs. With MRC, the diversity branches are weighted, cophased and combined in order to achieve the maximal signal strength. This require a perfect knowledge of the CSI at the receiver side, and it achieves the best performance among other combining schemes. However, the other combining techniques such as equal-gain combining (EGC) and selective combining are simpler than MRC due to the reduced need of CSI.

3.6 Conclusions

We have presented in this chapter our system model that uses IR-UWB transmission for cooperative communication. we have introduced the Rake receivers which has been implemented in our simulation. The BER performance of this system will be demonstrated in chapters IV and V for TH-PPM and DS-BPSK respectively.

Chapter 4

System Performance - TH-PPM

Contents

4.1 Introduction 76
4.2 Cooperative TH-PPM Impulse Radio UWB system 76
4.3 Decision Variable Statistics 79
4.4 BER Performance Analysis 82
4.5 Simulation Results And Discussion 82
4.6 Conclusions 89

4.1 Introduction

In this chapter, we study the performance of TH-PPM for impulse radio ultra wideband (IR-UWB). We consider the relay network presented in the previous chapter. The relaying protocol is DF and the channels between nodes adopt the IEEE 802.15.4a specifications. The BER performance is analyzed considering the effect of interference. Our results show significant improvement due to the diversity gain provided by the relay nodes. However, the performance is limited when MAI is present. To combat the MAI effect and further improve the detection reliability, we propose to use antenna selection at the relay. The relay receiver is assumed to be equipped with multiple antennas and only the best antenna is selected. This is shown to improve the performance in the presence of MAI and improve the diversity gain.

4.2 Cooperative TH-PPM Impulse Radio UWB system

The TH-PPM modulation scheme is designed to achieve multiuser capacity in UWB multiuser networks. The key motivations for using TH scheme are the ability to highly resolve multi-path, as well as the relative low complexity of the generation and implementation of UWB signals. The fine time resolution properties make TH technology a viable candidate for UWB communication in dense multipath environments such as short-range or indoor wireless communication [100]. Time hopping multiple access is implemented in both cooperative phases with equal hopping sequences sets, and which are selected randomly. In reality, some sort of pseudo random generator must provide the cooperative nodes with previously agreed time-hopping sequences for each communication links. The basic of TH is to regulate the time of transmitting pulses, where each pulse is positioned within each frame according to a user-specific TH sequence; hence the multiple accesses are accomplished by allocating different time slots "chips" for each user. Employing TH and PPM, the signaling interval T_s is divided into N_f frames each of duration T_f. The frame duration is also decomposed into N_h sub-interval of the chip duration T_c. N_h indicates the frame time over which TH is allowed, it is assumed that $N_h T_c \leq T_f$ in order to avoid pulse collision. The equiprobable binary data stream $b_m^x \in \{0,1\}_{m=0}^{M}$ of user x modulates the pulse $p(t)$ considering PPM modulation. That is, $b_m^x = 0$ is mapped to $p(t)$ and $b_m^u = 1$ is mapped to $p(t+\delta)$, where δ is a PPM time shift. Then by using the TH sequence assigned to user x, each pulse position is time shifted at multiple of T_c. Hence, the typical modulation functions from 3.3.1 are given by

$$\begin{aligned} F(n,x) &= 1 \\ G(n,x) &= nT_f + c_{m,n}^x T_c + b_m^x \delta \end{aligned} \tag{4.2.1}$$

Thus, the transmitted signal of the xth user becomes

$$s_x(t) = \sqrt{\frac{E_x}{N_f}} \sum_{m=0}^{M} \sum_{n=0}^{N_f-1} p(t\text{-}t_x - mT_s\text{-}nT_f - c_{m,n}^x T_c - b_m^x \delta) \tag{4.2.2}$$

where E_x is the bit energy, $c_{m,n}^x$ is the TH pseudo random sequence with i.i.d random variables taken in the interval $[0, N_h - 1]$, and we assume that $T_c = T_p + \delta$.

We consider the 3-nodes communication model depicted in 3.3.1 and the channel between each pair of nodes adopts the UWB IEEE 802.15.4a general channel model. Thus, the received signals at the destination and the relay during the first time slot are given in (4.2.3) and (4.2.4), respectively. In the second time slot, the relay first decodes the source signal, re-encodes and then transmits the source estimated data to the destination. The received signal at destination in the second time slot is given in (4.2.5).

$$\begin{aligned} r_{d_1}(t) = &\sqrt{\frac{E_s}{N_f}} \sum_{l=0}^{L_1-1} \sum_{k=0}^{K_1-1} \sum_{m=0}^{M} \sum_{n=0}^{N_f-1} \alpha_{k,l}^{sd} p(t\text{-}mT_s\text{-}nT_f - c_{m,n}^s T_c - b_m^s \delta - T_l^{sd} - \tau_{k,l}^{sd}) \\ &+ \sum_{i=1}^{N_I} s_i(t) \otimes h_{id}(t) + n_{d_1}(t) \end{aligned} \tag{4.2.3}$$

$$\begin{aligned} r_r(t) = &\sqrt{\frac{E_s}{N_f}} \sum_{l=0}^{L_2-1} \sum_{k=0}^{K_2-1} \sum_{m=0}^{M} \sum_{n=0}^{N_f-1} \alpha_{k,l}^{sr} p(t\text{-}mT_s\text{-}nT_f - c_{m,n}^s T_c - b_m^s \delta - T_l^{rd} - \tau_{k,l}^{rd}) \\ &+ \sum_{i=1}^{N_I} s_i(t) \otimes h_{ir}(t) + n_r(t) \end{aligned} \tag{4.2.4}$$

$$\begin{aligned} r_{d_2}(t) = &\sqrt{\frac{E_r}{N_f}} \sum_{l=0}^{L_3-1} \sum_{k=0}^{K_3-1} \sum_{m=0}^{M} \sum_{n=0}^{N_f-1} \alpha_{k,l}^{rd} p(t\text{-}mT_s\text{-}nT_f - c_{m,n}^r T_c - b_m^r \delta - T_l^{rd} - \tau_{k,l}^{rd}) \\ &+ \sum_{i=1}^{N_I} s_i(t) \otimes h_{id}(t) + n_{d_2}(t) \end{aligned} \tag{4.2.5}$$

Where $\otimes$ denote convolution. In (4.2.3)-(4.2.5), the first, second and third terms are respectively, the received signal, the MAI and the complex AWGN with zero mean and variance $\sigma^2 = N_0/2$. Here, we consider N_I interferers in each time slot with transmitted signals $s_i(t)$ where $i = 1, 2, ..., N_I$, $h_{id}(t)$ and $h_{ir}(t)$ are the complex channel coefficients of the i-D and i-R links.

We look for simple low complexity receiver with acceptable performance, so we choose to implement Partial Rake with MRC (P-Rake-MRC) at relays and destination. Under the assumption that CSI is available to receiver for all proposed schemes, P-Rake-MRC receiver will process

only a subset of the total number of resolvable paths, then combine them using MRC technique to attain multipath diversity, whereas, to accomplish diversity through cooperation, the receiver combine the detected data from S-D, and R-D links. In what follow, we use $K^{'}$-finger P-Rake receiver that captures the first $K^{'}$ rays from the first cluster of the targeted UWB link. The template waveforms used in the correlators at the destination and the relay in the first time slot and at the destination in the second time slot are given respectively by

$$\vartheta_{d_1}^{k^{'}}(t) = \alpha_{k^{'},0}^{sd^*} \sum_{n=0}^{N_f-1} q(t - nT_f - c_n^s T_c - T_0^{sd} - \tau_{k^{'},0}^{sd}) \tag{4.2.6}$$

$$\vartheta_{r}^{k^{'}}(t) = \alpha_{k^{'},0}^{sr^*} \sum_{n=0}^{N_f-1} q(t - nT_f - c_n^s T_c - T_0^{sr} - \tau_{k^{'},0}^{sr}) \tag{4.2.7}$$

$$\vartheta_{d_2}^{k^{'}}(t) = \alpha_{k^{'},0}^{rd^*} \sum_{n=0}^{N_f-1} q(t - nT_f - c_n^r T_c - T_0^{rd} - \tau_{k^{'},0}^{rd}) \tag{4.2.8}$$

where $0 \leq k^{'} \leq K^{'} - 1$, $q(t) = p(t) - p(t - \delta)$. It is assumed that the channel is time invariant during at least one frame. This assumption is justified by the fact that UWB channel is slow time varying in most WPAN applications [101].

In theory, TH codes are designed to ensure simultaneous and orthogonal UWB transmission in multiuser environments. However, perfect orthogonal transmission cannot be achieved in practice due to multipath propagation, asynchronous transmission, and the imperfect auto and cross-correlation of the TH codes. Thus, the received signals from different users are non-orthogonal resulting in MAI [89]. Another known source of interference is due to the self multipath interference which results from the correlation among adjacent paths.

Without loss of generality, we limit our interest to the detection of the first information bit b_s^0 in the observation interval $[0, T_s]$ and drop the symbol index 0. Also, in order to preclude intersymbol and intrasymbol interference; the frame duration is chosen to be sufficiently large $(T_f > max(T_{m1}, T_{m2}, T_{m3}) + (N_h - 1)T_c + T_p + \delta)$ [87, 102], where T_{mi} is the maximum excess delay spread of link i. Hence, the decision variables at the output of the Rake receivers at destination in the first and the second time slots are given respectively as

$$\hat{Z}_{d_1} = \sum_{k=0}^{K^{'}} \int_0^{T_s} r_{d_1}(t) \vartheta_{d_1}^{k}(t) dt \tag{4.2.9}$$

$$\hat{Z}_{d_2} = \sum_{k=0}^{K^{'}} \int_0^{T_s} r_{d_2}(t) \vartheta_{d_2}^{k}(t) dt. \tag{4.2.10}$$

At the destination, the receiver combines the two decision variables with a factor λ which controls the near-far effect. This effect consists of the pathloss difference and depends on the transmitted power and propagation distances. This type of detector has been refereed to as the λ-MRC [10]. The final decision variable is then given by

$$\hat{Z} = \hat{Z}_{d_1} + \lambda \hat{Z}_{d_2}. \tag{4.2.11}$$

The receiver then makes hard decision following

$$Z = \begin{cases} 0 & if\ \Re\left[\hat{Z}\right] > 0 \\ 1 & if\ \Re\left[\hat{Z}\right] \leq 0 \end{cases}. \tag{4.2.12}$$

Note that the receiver extracts the energy from a limited number of paths and that decision errors may occur due to the self interference, multiple access interference, and noise which render the receiver non-optimal. Next, we derive the statistics of $Z_{d_1} \triangleq \Re[\hat{Z_{d_1}}]$.

4.3 Decision Variable Statistics

By substituting (4.2.3) and (4.2.6) in (4.2.9), the decision variable at the output of the Rake receiver at the destination in the first time slot can be written as

$$\begin{aligned}
\hat{Z}_{d_1} = & \int_0^{T_s} \sum_{l=0}^{L_1-1} \sum_{k=0}^{K_1-1} \sum_{n=0}^{N_f-1} \sum_{k'=0}^{K'-1} \sqrt{\frac{E_s}{N_f}} \alpha_{k,l}^{sd} \alpha_{k',0}^{sd^*} p(t\text{-}nT_f - c_n^s T_c - b^s \delta - T_l^{sd} - \tau_{k,l}^{sd}) q(t\text{-}nT_f - c_n^s T_c - T_0^{sd} - \tau_{k',0}^{sd}) dt \\
& + \int_0^{T_s} \sum_{i=1}^{N_I} \sum_{l=0}^{L_i-1} \sum_{k=0}^{K_i-1} \sum_{n=0}^{N_f-1} \sum_{k'=0}^{K'-1} \sqrt{\frac{E_s}{N_f}} \alpha_{k,l}^{id} \alpha_{k',0}^{sd^*} p(t\text{-}nT_f - c_n^i T_c - b^s \delta - T_l^{id} - \tau_{k,l}^{id}) q(t\text{-}nT_f - c_n^s T_c - T_0^{sd} - \tau_{k',0}^{sd}) dt \\
& + \int_0^{T_s} n_{d_1}(t) \sum_{n=0}^{N_f-1} \sum_{k'=0}^{K'-1} \alpha_{k',0}^{sd^*} q(t\text{-}nT_f - c_n^s T_c - T_0^{sd} - \tau_{k',0}^{sd}) dt
\end{aligned} \tag{4.3.1}$$

Hence, $\hat{Z}_{d_1}$ can be decomposed into four terms, the desired signal, the self multipath interference, multi-access interference and the AWGN noise as

$$\hat{Z}_{d_1} = D + \hat{I}_s + \hat{I}_{MAI} + \eta. \tag{4.3.2}$$

Given the cross-correlation

$$R(x) \triangleq \int_{-\infty}^{+\infty} p(t-x) q(t) dt, \tag{4.3.3}$$

the desired signal component can be written as

$$D = \sqrt{N_f E_s} \sum_{k'=0}^{K'-1} |\alpha_{k,0}^{sd}|^2 . R(b^s \delta), \tag{4.3.4}$$

Note that the self multipath interference results from the correlation between the waveform template at each finger and all other multipath components. Thus, the total self interference is the sum of the self interference of all fingers, given by

$$\hat{I}_s = \sqrt{N_f E_s} \sum_{k'=0}^{K'-1} \sum_{k'=0, k\neq k'}^{K'-1} \alpha_{k,0}^{sd} \alpha_{k',0}^{sd^*} . R(\tau_{k,0}^{sd} - \tau_{k',0}^{sd} + b^s \delta)$$
$$+ \sqrt{N_f E_s} \sum_{k'=0}^{K'-1} \sum_{l=1}^{L_1-1} \sum_{k=0}^{K_1-1} \alpha_{k,l}^{sd} \alpha_{k',0}^{sd^*} . R(\tau_{k,l}^{sd} - \tau_{k',0}^{sd} + T_l^{sd} - T_0^{sd} + b^s \delta). \quad (4.3.5)$$

The first term in (4.3.5) corresponds to the interference of the rays of the 0th cluster where the second term represents the interference of the rays of other clusters. Based on the parametrization of the IEEE 802.15.4a subgroup [17], and from [87], the rays that are not adjacent arrive at intervals larger than the pulse duration T_p, which is less than a nanosecond. Therefore, we can assume that the correlation between any non-adjacent pair of rays is equal to zero i.e. $R(x) = 0$ out of $[-T_p, T_p + \delta]$. Therefore, the interference of the rays that do not belong to the 0th cluster is zero, and thus, the second term in (4.3.5) is ignored. With the same reasoning, we also find that $R(\tau_{k,0}^{sd} - \tau_{k',0}^{sd} + b^s \delta) = 0$ for $|k - k'| \neq 1$. That means the correlation between non-adjacent rays in the 0th clusters is equal to zero [87]. Thus, the real part of (4.3.5) is simplified to

$$I_s = \Re\left\{\hat{I}_s\right\} = \sum_{K'=0}^{K'-1} I_{s_{k'}} \quad (4.3.6)$$

where, $I_{sk'}$ is given in (20) and (21) for $0 \leq k' < K'-2$ and for $K'-1$, respectively,

$$I_{s_{k'}} = \sqrt{N_f E_s} \left(\Re\left\{ \alpha_{k'+1,0}^{sd} \alpha_{k',0}^{sd^*} \right\} R(v_{k'+1,0}^{sd} + b^s \delta) + \Re\left\{ \alpha_{k',0}^{sd} \alpha_{k'+1,0}^{sd^*} \right\} R(-v_{k'+1,0}^{sd} + b^s \delta) \right) \quad (4.3.7)$$

$$I_{s_{K'-1}} = \sqrt{N_f E_s} \Re\left\{ \alpha_{K',0}^{sd} \alpha_{K'-1,0}^{sd^*} \right\} R(v_{K'+1,0}^{sd} + b^s \delta). \quad (4.3.8)$$

In arriving to (4.3.7), (4.3.8), the arrival time of the kth ray in the lth cluster $\tau_{k,l}^{sd}$ has been replaced with $\sum_{j=1}^{k} v_{j,l}^{sd}$, where $v_{j,l}^{sd}$ is the inter-arrival time between rays j and $j-1$ in the lth cluster [74].

In the proposed TH-UWB system, the frame duration is composed of N_h sub-intervals of the chip duration T_c. Each frame can hold up to N_h users which can access the transmission medium sequentially using TH sequences. Each element $c_{m,n}^x \in [0, N_h - 1]$ in the TH sequence of user x provides time shift of $c_{m,n}^x T_c$ second. For UWB channels, as modeled in [17], the maximum excess delay spread T_m is much larger than the chip duration $T_c = T_p + \delta$. Therefore, paths with arrival time greater than T_c will overlay the intervals of other users. Due to the imperfect cross-correlation of the TH codes of different users, MAI will appear at the output of the Rake receiver. In our case, for the detection of the first information bit b_0^s of the source message, the MAI, denoted by $\hat{I}_{MAI}$, is the sum of MAI of all fingers due to the simultaneous transmission of $(N_i + 1)$ users. From (4.3.1), one can show that the MAI is given by

$$\hat{I}_{MAI} = \sum_{i=1}^{N_I} \sum_{l=0}^{L_i-1} \sum_{k=0}^{K_i-1} \sum_{n=0}^{N_f-1} \sum_{k'=0}^{K'-1} \sqrt{N_f E_i} \alpha_{k,l}^{id} \alpha_{k',0}^{sd^*} . R(\Lambda_{k',0}^{g,l_i}) \tag{4.3.9}$$

with

$$\Lambda_{k',0}^{g,l_i} = c_n^i T_c + T_{l_i}^{id} + \tau_{g,l_i}^{id} + b^i \delta - (c_n^s T_c + T_0^{sd} + \tau_{k',0}^{sd}), \tag{4.3.10}$$

where $\Lambda_{k',0}^{g,l_i}$ is the inter-arrival time between ray k' of the 0th cluster of the desired signal and ray g of the l_ith cluster of the interferer i.

Following the previous reasoning for the self interference, at each Rake finger, the correlation between the desired signal ray and all interferer's rays that arrive with intervals larger than the pulse duration is zero, i.e. $R(x) = 0$ for $\Lambda_{k',0}^{g,l_i} \notin [-T_p, T_p + \delta]$.

As it has been shown in [89], for most TH code designs, if a pulse is being corrupted by interference, it is highly possible that only one interfering pulse collides with the pulse position of the desired user. Therefore, in what follows, we consider only one interferer, $i(n)$, within the frame duration T_f, and note that the interferer might change from one frame to another. The MAI term can then be written as

$$\hat{I}_{MAI} = \sum_{n=0}^{N_f-1} \sum_{k'=0}^{K'-1} \sum_{g=1}^{G} \sqrt{N_f E_i} \alpha_{g,l_{i(n)}}^{i(n)d} \alpha_{k',0}^{sd^*} . R(\Lambda_{k',0}^{g,l_i(n)}) \tag{4.3.11}$$

given

$$\Lambda_{k',0}^{g,l_i(n)} \in [-T_p, T_p + \delta], \tag{4.3.12}$$

where G is the number of interferer's pulse rays that corrupt the desired signal ray at each of the Rake fingers. As discussed before, the inter-arrival time of non-adjacent rays is larger than the pulse duration. Therefore, the number of interferer's pulse rays, G, at each finger is at most equal two. Hence, the real part of (4.3.11) can be written as

$$I_{MAI} = \Re\left\{\hat{I}_{MAI}\right\} = \sum_{n=0}^{N_f-1} \sum_{k'=0}^{K'-1} I_{i(n),k'}, \tag{4.3.13}$$

with

$$I_{i(n),k'} = \sqrt{N_f E_{i(n)}} \sum_{g=1}^{G} \Re\left\{\alpha_{g,l_{i(n)}}^{i(n)d} \alpha_{k',0}^{sd^*}\right\} R(\Lambda_{k',0}^{g,l_i(n)}), \tag{4.3.14}$$

From (4.3.1), the AWGN component, $\hat{\eta}$, at the output of the Rake receiver is given by

$$\hat{\eta} = \int_0^{T_s} n_{d_1}(t) \sum_{k'=0}^{K'-1} \sum_{n=0}^{N_f-1} \alpha_{k',0}^{sd^*} q(t - nT_f - c_n^s T_c - T_0^{sd} - \tau_{k',0}^{sd}) dt, \tag{4.3.15}$$

with $\mathbb{E}\{\hat{\eta}\} = 0$ and $\sigma_{\hat{\eta}}^2 = 2N_f R(0) \sum_{k'=0}^{K'-1} \left|\alpha_{k',0}^{sd}\right|^2$. The real part, η, of $\hat{\eta}$ is Gaussian variable with zero mean and variance

$$\sigma_\eta^2 = \frac{1}{2}\sigma_{\hat{\eta}}^2 = N_f R(0) N_0 \sum_{k'=0}^{K'-1} \left|\alpha_{k',0}^{sd}\right|^2. \tag{4.3.16}$$

4.4 BER Performance Analysis

In this section, we analyze the BER performance of our relay network based TH-PPM IR-UWB system. From (4.2.11) and (4.3.2), the decision variable can be written as

$$\hat{Z} = D^{sd} + I_s^{sd} + I_{MAI}^{sd} + \eta^{sd} + \lambda \left(D^{rd} + I_s^{rd} + I_{MAI}^{rd} + \eta^{rd} \right) \tag{4.4.1}$$

where the statistics of D^{sd}, I_s^{sd}, I_{MAI}^{sd} and η^{sd} have been obtained in the previous section. The statistics of D^{rd}, I_s^{rd}, I_{MAI}^{rd} and η^{rd} can be obtained similar to (4.3.4), (4.3.6), (4.3.13) and (4.3.16), respectively. Hence, the conditional probability of bit error is given by

$$\begin{aligned} P_e &= \frac{1}{2} P\left(\Re\left\{\hat{Z}\right\} \le 0 |_{b^s=0}\right) + \frac{1}{2} P\left(\Re\left\{\hat{Z}\right\} \ge 0 |_{b^s=1}\right) \\ &= P\left(\Re\left\{\hat{Z}\right\} \le 0 |_{b^s=0}\right) \end{aligned} \tag{4.4.2}$$

$$P_e = P\left(I_s^{sd} + I_{MAI}^{sd} + \eta^{sd} + \lambda I_s^{rd} + \lambda I_{MAI}^{rd} + \lambda \eta^{rd} \le -D^{sd} - \lambda D^{rd} |_{b^s=1} \right) \tag{4.4.3}$$

4.5 Simulation Results And Discussion

Here, we present simulation results for the BER performance of a TH-PPM UWB transmission system with relay cooperation. Monte Carlo simulations have been carried out with and without MAI. The transmitted pulse is the second derivative of a Gaussian pulse with a duration of $0.7ns$, and the pulse shift δ of the PPM modulation is set to $0.15ns$. In all simulation, the transmission

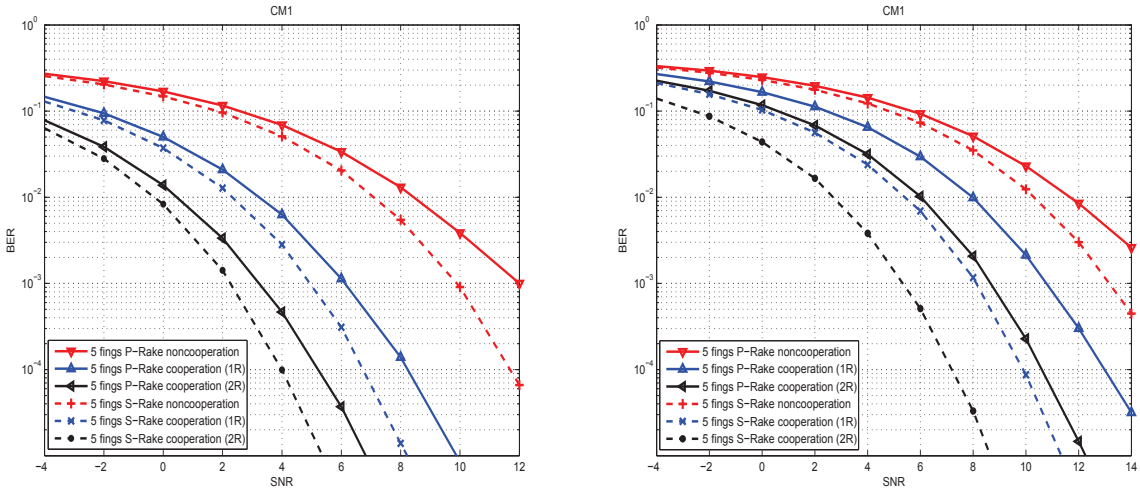
links (source to relay, source to destination, and relay to destination) are modeled according to the IEEE 802.15.4a channel models where the fading coefficients are fixed within a frame and change independently from one frame to another. The simulations are carried out in four types of UWB channels, namely CM1, CM2, CM3 and CM4. The power delay profile of the impulse responses of these channels and the list of their parameters are presented in chapter III. The values of the channel parameters have been taken from [17]. In the simulation, the UWB channels have been chosen randomly from a set of 500 channel realizations and the BER performance has been averaged over at least 100 channels. Furthermore, we have assumed equal average fading power of 1 for all S-R, S-D and R-D links. The chip duration equals to the sum of pulse duration and the time shift of the PPM modulation, $T_c = 0.85ns$. Each frame consists of 100 bits of the chip duration where each bit is presented by a single pulse. The channel bandwidth is set to 3 GHz. The pathloss is considered a function of distance and its frequency dependency is ignored. The transmitter power decays following the power law described in 2.7.3 where the reference distance d_0 is set to 1 m. We consider equal transmitted energies for the different nodes and at most equal to the FCC maximum emission power limit, i.e., $E_s = E_r = E_b = -41.3\,dBm/MHz$. Without loss of generality, we assume that the S-D distance is d_{sd} and the relay node is exactly at the middle point between the source and destination nodes. With respect to this assumption in the analysis, we assume that the average SNRs for all sub-channels between the source and the relay nodes as well as between the relay and the destination are equal, but they are different from the average SNRs for the channel between the source and destination. This difference in the average SNRs is calculated as the pathloss difference in dB according to the link distance using 2.7.3 and its values are given in table 4.5.1 for the different types of UWB channel models.

Table 4.5.1: Difference in the average SNRs Between S-R or R-D and S-D links when the relay node is exactly located at the middle point between the source and the destination.

Channel model	SNR Difference [dB]
CM1	5.3884
CM2	13.7872
CM3	4.9068
CM4	9.2416

Primarily we study the influence of relay cooperation with different number of relay for perfect S-R links, thus no errors propagation in the forwarded signal at relay. The Rake receiver is supposed to have a perfect knowledge of the channel coefficients. A five-finger P-Rake receiver is employed with a combination factor $\lambda = PL_{rd}/PL_{sd}$, where PL_{rd} and PL_{sd} are the pathloss in dB of the R-D and S-D links, respectively. Increasing the number of fingers in a Rake receiver will enhance the system performance but will increase the complexity of the design. In order

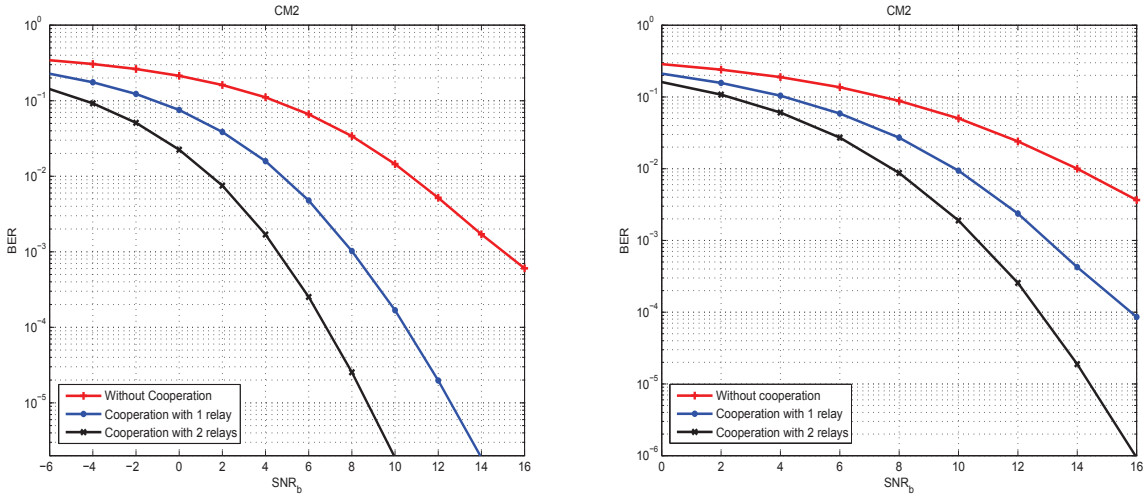
to enhance the performance without increasing the number of Rake correlators, we can use S-Rake-MRC, which combines the K' best, MPCs. Those K' best components are determined by a finger selection algorithm. In figure 4.5.1, we evaluate the difference between S-Rake-MRC and P-Rake-MRC performances for CM1, where each with 5 fingers.



(a) (b)

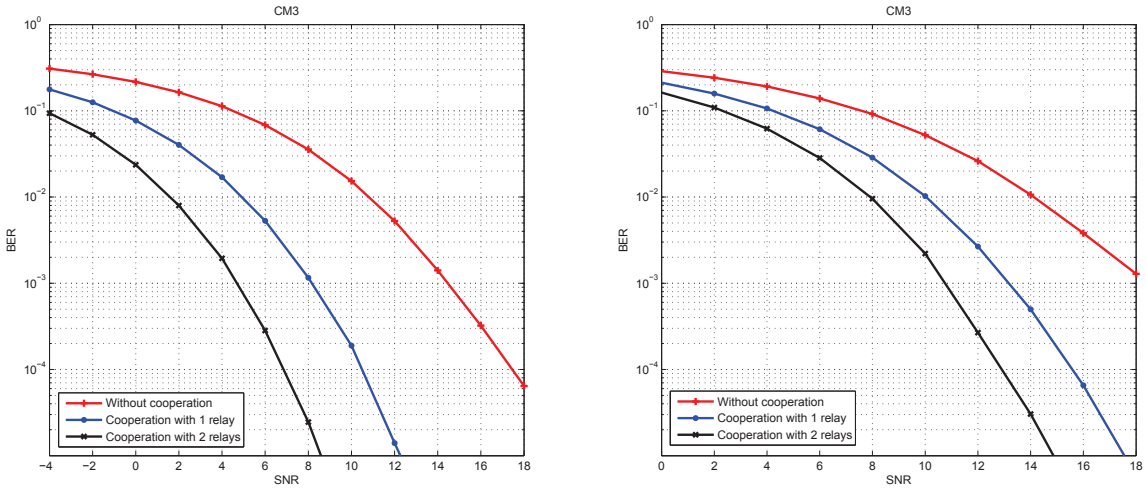
FIGURE 4.5.1 – BER performance of TH-PPM UWB non-cooperative and cooperative (with 1 and 2 relays) system with error-free detection at relay nodes for 5 P-Rake and 5 S-Rake under CM1 . (a) Without MAI. (b) In presence of MAI of one additional user.

Figs. 4.5.2-4.5.4 show the BER performance of the system using 5 fingers P-Rake receiver for CM2, CM3 and CM4 channels, respectively. Each of these figures plot the BER performance of TH-PPM UWB versus the SNR per bit under the dedicated UWB channel in two cases; free transmission without MAI (Figs. 4.5.2-4.5.4, a) and in presence of MAI (Figs. 4.5.2-4.5.4, b). In each figure, we compare the BER performance for different scenarios; the direct transmission without cooperation over the S-D link, cooperation with one relay and cooperation with two relay.



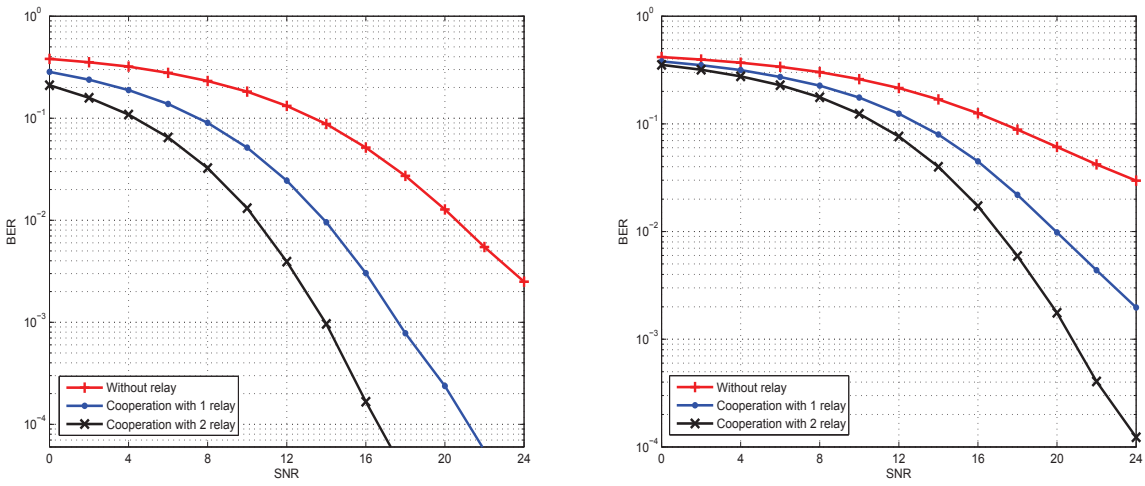
(a) (b)

FIGURE 4.5.2 – The BER performance of TH-PPM UWB system with relay cooperation under CM2 with error-free detection at relay nodes. (a) Without MAI. (b) In presence of MAI of one additional user.



(a) (b)

FIGURE 4.5.3 – The BER performance of TH-PPM UWB system with relay cooperation under CM3 with error-free detection at relay nodes. (a) Without MAI. (b) In presence of MAI of one additional user.

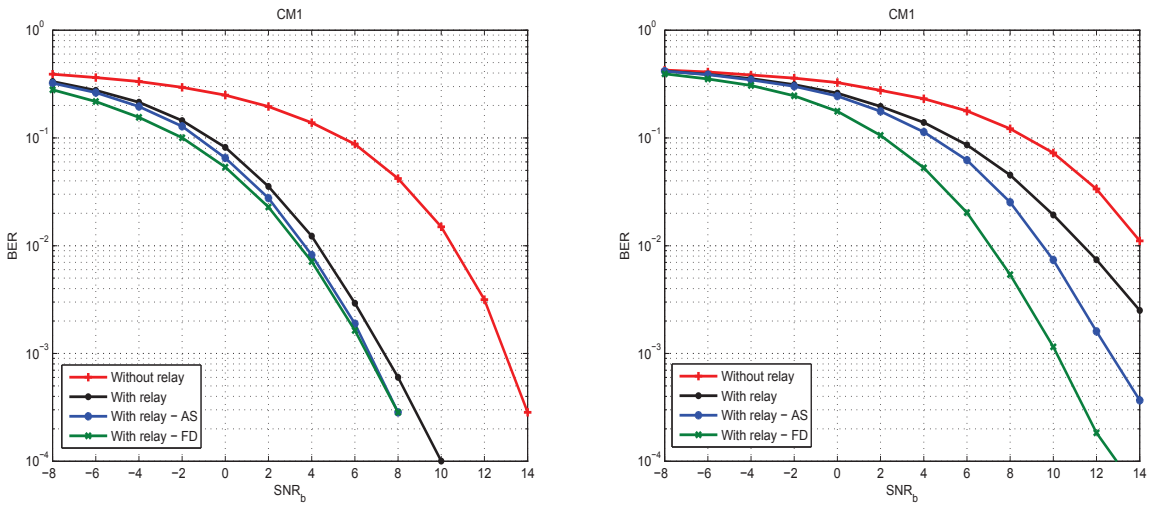


(a) (b)

FIGURE 4.5.4 – The BER performance of TH-PPM UWB system with relay cooperation under CM4 with error-free detection at relay nodes. (a) Without MAI. (b) In presence of MAI of one additional user.

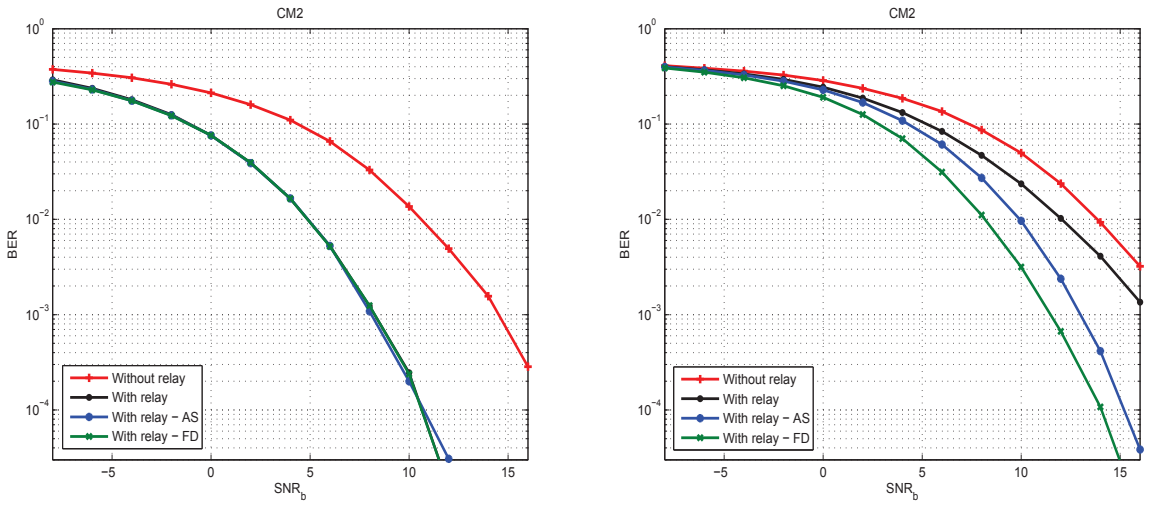
As shown in the previous figures, in absence of MAI and for perfect S-R links, the benefit of cooperation can take place and the diversity gain increases proportionally with the number of cooperative relays. However, once, the UWB channel is frequency selective fading channel, the orthogonality cannot be retained. Therefore, MAI exists at the output of the Rake correlators and the performance deteriorates. The results suggest that, in presence of MAI at the reception, the overall system performance degrades significantly, but the benefit of cooperation is still effective and the gain of diversity increases proportionally with the number of relay nodes. MAI can be minimized if proper coordination between relays can be achieved. If more than one relay use the same time slot, the destination will not be able to detect either of the signals properly. For such cases, error correction schemes must be applied.

Figs. 4.5.5-4.5.8 show the BER performance of the system for CM1, CM2, CM3 and CM4 channels, respectively. The BER performance is compared considering four cases; without relay (non-cooperative), relay equipped with a single antenna, relay equipped with four antennas and only the best antenna is selected (referred to as (AS)), and relay with four antennas where no antenna selection is employed (referred to as a full diversity (FD)). The last case corresponds to a SIMO system for the S-R link, where the receiver coherently combines the received signals from the four antennas. This requires four RF chains at the relay node and results in cost increment. However, this case has been considered in our results for comparison purposes.



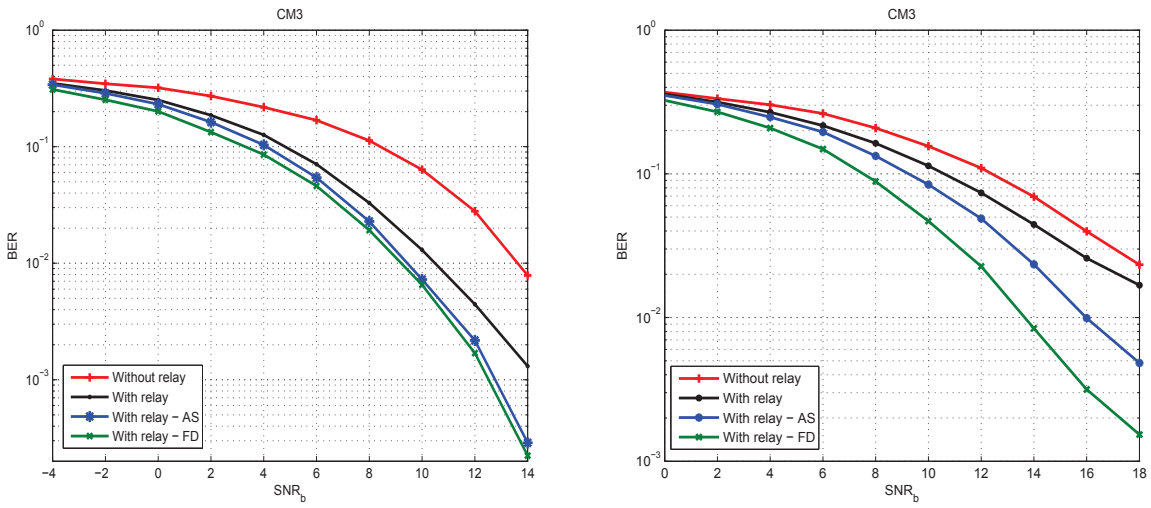
(a) (b)

FIGURE 4.5.5 – The BER performance of TH-PPM UWB system with relay cooperation under CM1 with error at relay nodes. (a) Without MAI. (b) In presence of MAI of one additional user.



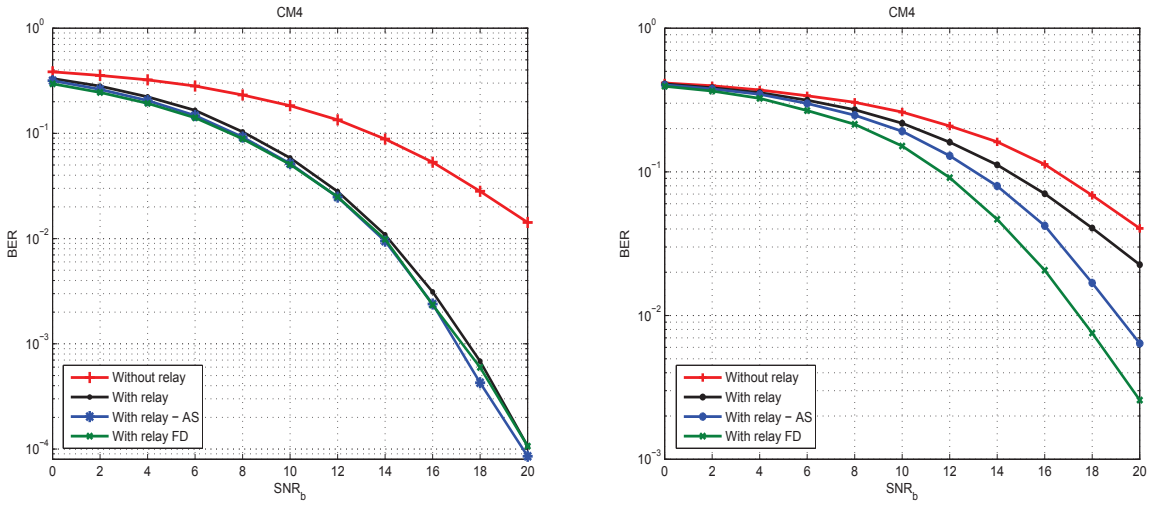
(a) (b)

FIGURE 4.5.6 – The BER performance of TH-PPM UWB system with relay cooperation under CM2 with error at relay nodes. (a) Without MAI. (b) In presence of MAI of one additional user.



(a) (b)

FIGURE 4.5.7 – The BER performance of TH-PPM UWB system with relay cooperation under CM3 with error at relay nodes. (a) Without MAI. (b) In presence of MAI of one additional user.



(a) (b)

FIGURE 4.5.8 – The BER performance of TH-PPM UWB system with relay cooperation under CM4 with error at relay nodes. (a) Without MAI. (b) In presence of MAI of one additional user.

From these results, we note that in the absence of MAI, a significant performance improvement is obtained by the use of a relay node. On the other hand, when MAI is present, the system performance degrades even when with relay cooperation. This is due to the fact that the received signals at the destination in both time slots suffer from high levels of interference. As a result,

the overall system performance degrades significantly, and the benefits of a single antenna relay node is minimum. To reach the benefit of cooperation, and to overcome the MAI effect, we propose to use antenna selection at the relay (kindly see Chapter 1, section 1.6). This is shown to improve the performance in the presence of MAI. We note that, while antenna selection maintains the full diversity order, there exist a SNR loss relative to the full complexity case (i.e. 4 RF chains).

Comparing Figs. 4.5.5 to 4.5.6, and Figs. 4.5.7 to 4.5.8, we note that the LOS channels lead to better performance than NLOS channels. This is due to the fact that in LOS channels, a fewer number of paths hold more energy than that in NLOS ones. Thus, in LOS channels, a five-finger Rake receiver captures more power out of five paths than that of the same number of paths in NLOS channels. However, the antenna selection strategy performs more efficiently as it brings better performance improvement in NLOS channels. The reason is that, the Rake receiver seeks the first K' arriving paths. Thus, in LOS channels, the most reliable path which is the LOS arrives with the minimum propagation delay and is always captured by the first Rake finger. In this case, the variance in power among the different antennas is not important. Unlike the case of NLOS channels, the most reliable path might arrive with delay that is out of the first K' paths, and might not be captured by any of the Rake fingers. Thus, the variance in signal power at the different antennas becomes more important.

4.6 Conclusions

We have studied in this chapter the DF cooperation strategy for a relay network considering the effect of MAI with contrast to the free access (ignoring MAI) and the direct non-cooperative transmission; we have also proposed to use antenna selection at the relay in order to mitigate the MAI effect. In the presence of MAI, we state that the overall system performance is significantly degraded and is dominated by the source-relay S-R link, especially, when the source-destination S-D link exhibits poor channel conditions. Relay cooperation combined with antenna selection is not only enhancing the system performance, but also significantly reduces the MAI effect. When employing multiple antennas at the relay, the use of antenna selection strategy reduces the complexity/cost of the system. This permits us to take advantage of the available antennas, while using single RF chain.

Chapter 5

System Performance - DS-BPSK

Contents

5.1 Introduction 92
5.2 Cooperative DS-BPSK IR-UWB system 92
5.3 Decision Variable Statistics 95
5.4 BER Performance Analysis 98
5.5 Simulation Results And Discussion 98
5.6 Conclusions 107

5.1 Introduction

In this chapter, we consider a relay network applying DF protocol and evaluate the performance of DS-BPSK modulation for IR-UWB transmission. The channels between nodes adopt the IEEE 802.15.4a subgroup specification. The BER performance is analyzed considering the effect of MAI. Our results show significant improvement due to the diversity gain provided by the relay nodes. However, the performance is limited when MAI is present. To combat the MAI effect and improve the detection reliability, we use antenna selection at the relay. The relay receiver is assumed to be equipped with multiple antennas and only the best antenna is selected.

5.2 Cooperative DS-BPSK IR-UWB system

DSSS is a well-known multiple access technique in digital wireless communications. When using the DSSS technique, several users are allowed to share the same frequency band instantaneously [103]. The multiple access capability is set up by assigning each user a unique PN spreading sequence out of family of orthogonal sequences. We consider a multiuser wireless network signaling through multipath UWB channels, where each user employs DS-BPSK modulation. The cooperative network is mainly consists of three nodes: S, R and D. The relay assists the S-D transmission using DF protocol in order to improve the detection reliability at the destination. In this scenario, two time slots with equal signaling intervals are used to accomplish the transmission. DS multiple access is deployed in both cooperative phases with equal spreading sequences sets, where each bit consists of train of pulses embody the spreading sequence, and each chip include one pulse. In the first time slot, the source broadcasts its signal to the destination and the relay node through S-D and S-R links. In the second time slot, the relay decodes the source signal, re-encodes and retransmits an estimate of the source signal to the destination through R-D link, whereas the source is silent. The DS-BPSK UWB transmission scheme is illustrated in Fig. 5.2.1.

In a DS-BPSK, users employ BPSK and DSSS to ensure multiple access capability. The equiprobable binary bit stream $b_m^x \in \{1,-1\}_{m=-\infty}^{\infty}$ of user x, is BPSK modulated by the pulse $p(t)$. That is, $b_m^x = 1$ is mapped to $p(t)$ and $b_m^x = -1$ is mapped to $-p(t)$ with $Pb_m^x = +1 = Pb_m^x = -1 = 1/2$. Hence, the typical modulation functions from 3.3.1 are given by

$$\begin{aligned} F(n,x) &= b_m^x c_n^x \\ G(n,x) &= mT_b - nT_c \end{aligned} \tag{5.2.1}$$

The transmitted signal generated by the xth user is given by

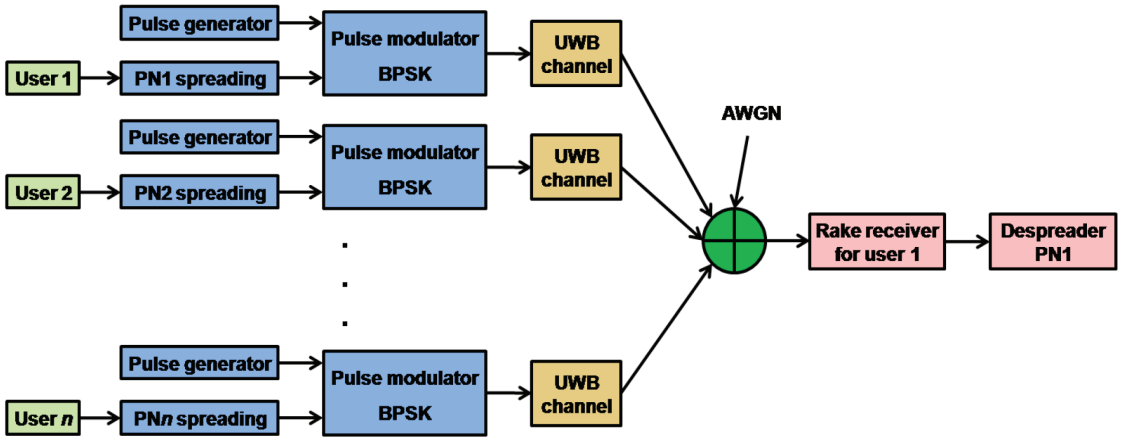


Figure 5.2.1: General cooperative system model.

$$s_x(t) = \sqrt{\frac{E_x}{N_c}} \sum_{m=-\infty}^{\infty} \sum_{n=0}^{N_c-1} b_m^x c_n^x p(t - t_x - mT_b - nT_c) \tag{5.2.2}$$

where E_x is the bit energy of user x, t_x is the relative transmission time difference compared to the desired user, with $t_s = 0$ and $t_r = 0$ are the desired users in the first and the second time slots, respectively. N_c is the number of chip per bit, also called the processing gain. $T_b = N_c T_c$, where T_c is the chip duration and T_b is the bit duration. c_n^x is the PN spreading sequence. To avoid pulses overlapping and reduce the effect of intersymbol and intrasymbol interference; the chip interval is chosen to be comparable to the delay spread of the typical IEEE 802.15.4a channel $(T_c > T_p + max(T_{m1}, T_{m2}, T_{m3}))$ [87, 102, 104], where T_{mi} is the maximum excess delay spread of link i.

The channel between each pair of nodes adopts the UWB IEEE 802.15.4a general channel model. Under multiple access scenario the simultaneous transmission of multiple signals is a typical source of interference for wireless signals. When using the DSSS multiple access technique, the data stream is combined with a high-speed digital code where each data bit is mapped into the user's unique PN code. This code is known only to the transmitter and the corresponding receiver. In a frequency-selective multipath fading UWB channel, MAI and self multipath interference are caused by multipath dispersion. The received signals at the destination and the relay during the first time slot are given in 5.2.3 and 5.2.4, respectively. In the second time slot, the relay first decodes the source signal, re-encodes and then transmits the source estimated data to the destination. The received signal at destination in the second time slot is given in 5.2.5. where $\otimes$ denotes convolution and b_m^r is the estimation at the relay receiver of b_m^s, the mth transmitted data signal of the source generated at a rate of $1/T_b$. In 5.2.3-5.2.5, the first, second and third terms are respectively, the desired signal, the MAI and the AWGN with zero mean and variance $\sigma^2 = N_0/2$. Here, we consider N_I simultaneous, asynchronous interfering users in each time slot with transmitted signals $s_i(t)$; $h_{id}(t)$ and $h_{ir}(t)$ are the complex channel coefficients of the i-D and i-R links.

$$r_{d_1}(t) = \sqrt{\frac{E_s}{N_c}} \sum_{l=0}^{L_1-1} \sum_{k=0}^{K_1-1} \sum_{m=-\infty}^{\infty} \sum_{n=0}^{N_c-1} \alpha_{k,l}^{sd} b_m^s c_n^s p(t - mT_b - nT_c - T_l^{sd} - \tau_{k,l}^{sd}) + \sum_{i=1}^{N_I} s_i(t) \otimes h_{id}(t) + n_{d_1}(t) \tag{5.2.3}$$

$$r_r(t) = \sqrt{\frac{E_s}{N_c}} \sum_{l=0}^{L_2-1} \sum_{k=0}^{K_2-1} \sum_{m=-\infty}^{\infty} \sum_{n=0}^{N_c-1} \alpha_{k,l}^{sr} b_m^s c_n^s p(t - mT_b - nT_c - T_l^{sr} - \tau_{k,l}^{sr}) + \sum_{i=1}^{N_I} s_i(t) \otimes h_{ir}(t) + n_r(t) \tag{5.2.4}$$

$$r_{d_2}(t) = \sqrt{\frac{E_r}{N_c}} \sum_{l=0}^{L_3-1} \sum_{k=0}^{K_3-1} \sum_{m=-\infty}^{\infty} \sum_{n=0}^{N_c-1} \alpha_{k,l}^{rd} b_m^r c_n^s p(t - mT_b - nT_c - T_l^{rd} - \tau_{k,l}^{rd}) + \sum_{i=1}^{N_I} s_i(t) \otimes h_{id}(t) + n_{d_2}(t) \tag{5.2.5}$$

We consider that the relay and the destination are equipped with $K^{'}$-fingers practical Rake receivers that has a prior knowledge of the CSI. The template waveform used in the correlators at the destination and relay are then given respectively by

$$v_{d_1}^{k^{'}}(t) = \alpha_{k^{'},0}^{sd^*} \sum_{n=0}^{N_c-1} c_n^s p(t - nT_c - T_0^{sd} - \tau_{k^{'},0}^{sd}) \tag{5.2.6}$$

$$v_r^{k^{'}}(t) = \alpha_{k^{'},0}^{sr^*} \sum_{n=0}^{N_c-1} c_n^s p(t - nT_c - T_0^{sr} - \tau_{k^{'},0}^{sr}) \tag{5.2.7}$$

$$v_{d_2}^{k^{'}}(t) = \alpha_{k^{'},0}^{rd^*} \sum_{n=0}^{N_c-1} c_n^s p(t - nT_c - T_0^{rd} - \tau_{k^{'},0}^{rd}) \tag{5.2.8}$$

where $0 \leq k^{'} \leq K^{'} - 1$. It is assumed that the channel impulse response remains the same over several consecutive data bits durations. This assumption is justified by the fact that UWB channel is slow time varying in most WPAN applications considering that the symbol duration is on the order of tens or hundreds of nanoseconds, and the coherent time of an indoor wireless channel is on the order of tens of milliseconds [101, 104, 105].

Without loss of generality, we limit our interest to the detection of the information bit b_0^s in the observation interval $[0, T_b]$ and drop the symbol index 0. Hence, the decision variables at the output of the Rake receivers at destination in the first and the second time slots are given respectively as

$$\hat{Z}_{d_1} = \sum_{k=0}^{K^{'}} \int_0^{T_s} r_{d_1}(t) v_{d_1}^k(t) dt \tag{5.2.9}$$

$$\hat{Z}_{d_2} = \sum_{k=0}^{K'} \int_0^{T_s} r_{d_2}(t) v_{d_2}^k(t) dt \tag{5.2.10}$$

Employing the λ-MRC [10]. The final decision variable is then given by

$$\hat{Z} = \hat{Z}_{d_1} + \lambda \hat{Z}_{d_2}. \tag{5.2.11}$$

This is followed by the hard decision employing

$$Z = \begin{cases} 0 & if\, \Re\left[\hat{Z}\right] > 0 \\ 1 & if\, \Re\left[\hat{Z}\right] \leq 0 \end{cases}. \tag{5.2.12}$$

Note that the receiver extracts the energy from a limited number of paths and that decision errors may occur due to the self multipath interference, multiple access interference, and noise which render the receiver non-optimal. Next, we derive the statistics of $Z_{d_1} \stackrel{\triangle}{=} \Re[\hat{Z}_{d_1}]$.

5.3 Decision Variable Statistics

By substituting 5.2.3 and 5.2.6 in 5.2.9, the decision variable at the output of the Rake receiver at the destination in the first time slot can be written as 5.3.1.

$$\begin{aligned}
\hat{Z}_{d_1} = & \int_0^{T_b} \sum_{l=0}^{L_1-1} \sum_{k=0}^{K_1-1} \sum_{k'=0}^{K'-1} \sum_{n=0}^{N_c-1} \sum_{n'=0}^{N_c-1} \sqrt{\frac{E_s}{N_c}} \alpha_{k,l}^{sd} \alpha_{k',0}^{sd^*} b^s c_n^s c_{n'}^s p(t - nT_c - T_l^{sd} - \tau_{k,l}^{sd}) p(t - n'T_c - T_0^{sd} - \tau_{k',0}^{sd}) dt \\
& + \int_0^{T_b} \sum_{i=1}^{N_I} \sum_{-\infty}^{\infty} \sum_{l=0}^{L_i-1} \sum_{k=0}^{K_i-1} \sum_{k'=0}^{K'-1} \sum_{n=0}^{N_c-1} \sum_{n'=0}^{N_c-1} \sqrt{\frac{E_i}{N_c}} \alpha_{k,l}^{id} \alpha_{k',0}^{sd^*} b_m^i c_n^i c_{n'}^s p(t - t_i - nT_c - T_l^{id} - \tau_{k,l}^{id}) p(t - n'T_c - T_0^{sd} - \tau_{k',0}^{sd}) dt \\
& + \int_0^{T_b} n_{d_1}(t) \sum_{k'=0}^{K'-1} \sum_{n'=0}^{N_c-1} \alpha_{k',0}^{sd^*} c_{n'}^s p(t - n'T_c - T_0^{sd} - \tau_{k',0}^{sd}) dt
\end{aligned} \tag{5.3.1}$$

Hence, $\hat{Z}_{d_1}$ can be decomposed into four terms, the desired signal, the self multipath interference, multi-access interference and the AWGN noise as

$$\hat{Z}_{d_1} = D + \hat{I}_s + \hat{I}_{MAI} + \hat{\eta} \tag{5.3.2}$$

Given the autocorrelation function for the DS-BPSK modulation

$$R(x) \stackrel{\triangle}{=} \int_{-\infty}^{+\infty} p(t - x) p(t) dt \tag{5.3.3}$$

the desired signal component can be written as

$$D = \sqrt{N_c E_s} b^s \sum_{k'=0}^{K'-1} \left|\alpha_{k,0}^{sd}\right|^2 . R(0) \tag{5.3.4}$$

where $R(0) = \int_{-\infty}^{+\infty} p^2(t)dt$, considering the fact that $c_n^s c_n^s = 1$. According to our assumption, the chips are transmitted with intervals that are comparable to the delay spread of the typical UWB channel impulse response. Thus, the self-inter-chip interference is ignored. The effect of the self multipath interference results from the correlation between the waveform template at each finger and all other multipath components. Thus, the total self multipath interference is the sum of the self multipath interference of all fingers, given by

$$\hat{I}_s = \sqrt{N_c E_s}\, b^s \sum_{k'=0}^{K'-1} \sum_{k=0, k\neq k'}^{K_1-1} \alpha_{k,0}^{sd} \alpha_{k',0}^{sd^*} . R(\tau_{k,0}^{sd} - \tau_{k',0}^{sd}) + \sqrt{N_c E_s}\, b^s \sum_{l=1}^{L_1-1} \sum_{k'=0}^{K'-1} \sum_{k=0}^{K_1-1} \alpha_{k,l}^{sd} \alpha_{k',0}^{sd^*} . R(T_l^{sd} + \tau_{k,l}^{sd} - T_0^{sd} - \tau_{k',0}^{sd}). \quad (5.3.5)$$

The first term in 5.3.5 corresponds to the interference of the rays of the 0th cluster where the second term represents the interference of the rays of other clusters. Based on the parametrization of the IEEE 802.15.4a subgroup [17], and from [87], the rays that are not adjacent arrive at intervals larger than the pulse duration T_p, which is less than a nanosecond. Therefore, we can assume that the correlation between any non-adjacent pair of rays is equal to zero i.e. $R(x) = 0$ out of $[-T_p, T_p]$. Therefore, the interference of the rays that do not belong to the 0th cluster is zero, and thus, the second term in 5.3.5 is ignored. With the same reasoning, we also find that $R(\tau_{k,0}^{sd} - \tau_{k',0}^{sd}) = 0$ for $|k - k'| \neq 1$. That means the correlation between non-adjacent rays in the 0th clusters is equal to zero [87].

Thus, the real part of 5.3.5 is simplified to

$$I_s = \Re\left\{\hat{I}_s\right\} = \sum_{k'=0}^{K'-1} I_{s_{k'}} \quad (5.3.6)$$

where, $I_{s_{k'}}$ is given in 5.3.7 and 5.3.8 for $0 \leq k' < K' - 2$ and for $K' - 1$, respectively,

$$I_{s_{k'}} = \sqrt{N_c E_s}\, b^s \left(\Re\left\{ \alpha_{k'+1,0}^{sd} \alpha_{k',0}^{sd^*} \right\} + \Re\left\{ \alpha_{k',0}^{sd} \alpha_{k'+1,0}^{sd^*} \right\} \right) R(v_{k'+1,0}^{sd}) \quad (5.3.7)$$

$$I_{s_{K'-1}} = \sqrt{N_c E_s}\, b^s \Re\left\{ \alpha_{k',0}^{sd} \alpha_{k'-1,0}^{sd^*} \right\} R(v_{k'+1,0}^{sd}) \quad (5.3.8)$$

where $R(x) = R(-x)$. Indeed, equations 5.3.7 and 5.3.8 are obtained by replacing the arrival time of the kth ray in the lth cluster $\tau_{k,l}^{sd}$ by $\sum_{j=1}^{k} v_{j,l}^{sd}$, where $v_{j,l}^{sd}$ is the inter-arrival time between rays j and $j-1$ in the lth cluster [106].

In the proposed DS-BPSK UWB system, the multiple access capability is set up using equal spreading sequences sets, where each bit consists of a train of pulses embody the spreading sequence, and each chip includes one pulse. If there is an interference or jammer in the same band, it will be spread out by a factor equal to the processing gain. The spreading increases

the signal's resistance to interference. Because of the extremely short duration of the UWB impulse, there are a lot of multipath components at the receiver. Indeed, in DS system, MAI is caused by multipath dispersion and the conventional Rake receivers cannot efficiently deal with this problem. The MAI caused by one interfering user is usually small, but as the number of interferers increases, the effect of MAI becomes noticeable. In our case, the MAI term in the decision variable at the output of the rake receiver, denoted by $\hat{I}_{MAI}$, is the sum of MAI at all fingers due to the simultaneous transmission of $(N_i + 1)$ users including the source.

To simplify the analysis, we denote the pair of consecutive data bits of the ith interfering signal in the range $[0, T_b]$ as b_1^i and b_2^i [104]. The channel response is considered invariant during the transmission of several consecutive data bits. Notice that the time difference t_i may span many chip durations, such that

$$t_i = q_i T_c + \varepsilon_i \tag{5.3.9}$$

where q_i is the nearest integer of $\frac{t_i}{T_c}$, and ε_i is the round error, uniformly distributed over $[-\frac{T_c}{2}, \frac{T_c}{2}]$. From 5.3.1, the MAI can be done by

$$\hat{I}_{MAI} = \sum_{i=1}^{N_I} \sum_{l=0}^{L_i-1} \sum_{k=0}^{K_i-1} \sum_{k'=0}^{K'-1} \sqrt{\frac{E_i}{N_c}} \alpha_{k,l}^{id} \alpha_{k',0}^{sd^*} \psi_i \tag{5.3.10}$$

with

$$\psi_i = \sum_{n=N_c-q_i}^{N_c-1} \sum_{n'=0}^{q_i-1} b_1^i c_n^i c_{n'}^s R(\Lambda_{k',0}^{g,l_i} - N_c T_c) + \sum_{n=0}^{N_c-1-q_i} \sum_{n'=q_i}^{N_c-1} b_2^i c_n^i c_{n'}^s R(\Lambda_{k',0}^{g,l_i}) \tag{5.3.11}$$

and

$$\Lambda_{k',0}^{g,l_i} = (q_i + n) T_c + \varepsilon_i + T_{l_i}^{id} + \tau_{g,l_i}^{id} - (n' T_c + T_0^{sd} + \tau_{k',0}^{sd}) \tag{5.3.12}$$

where $\Lambda_{k',0}^{g,l_i}$ is the inter-arrival time between ray k' of the 0th cluster of the desired signal and ray g of the l_ith cluster of the interferer i.

Following the previous reasoning for the self multipath interference, at each Rake finger, the correlation between the desired signal ray and all interferer's rays that arrive with intervals larger than the pulse duration is zero, i.e. $R(x) = 0$ for $\Lambda_{k',0}^{g,l_u} \notin [-T_p, T_p + \delta]$.

Considering G the number of interferer's pulse rays that corrupt the desired signal ray at each Rake fingers. As discussed before, the inter-arrival time of non-adjacent rays is larger than the pulse duration. Therefore, G equal ,at most, two. The MAI term can then be done by

$$\hat{I}_{MAI} = \sum_{i=1}^{N_I} \sum_{k'=0}^{K'-1} \sum_{g=1}^{G} \sqrt{\frac{E_i}{N_c}} \alpha_{g,l_i}^{id} \alpha_{k',0}^{sd^*} \psi_i \tag{5.3.13}$$

given

$$\Lambda_{k',0}^{g,l_i} \in [-T_p, T_p], \tag{5.3.14}$$

The real part of 5.3.13 can be written as

$$I_{MAI} = \Re\left\{\hat{I}_i\right\} = \sum_{i=1}^{N_I}\sum_{k'=0}^{K'-1} I_{i,k'}, \tag{5.3.15}$$

with

$$I_{i,k'} = \sqrt{\frac{E_i}{N_c}}\sum_{g=1}^{G}\Re\left\{\alpha_{g,l_i}^{id}\alpha_{k',0}^{sd^*}\right\}\psi_i. \tag{5.3.16}$$

From 5.3.1, the AWGN component, $\hat{\eta}$, at the output of the Rake receiver is given by

$$\hat{\eta} = \int_0^{T_b} n_{d_1}(t)\sum_{k'=0}^{K'-1}\sum_{n'=0}^{N_c-1}\alpha_{k',0}^{sd^*}c_{n'}^{s}p(t-n'T_c-T_0^{sd}-\tau_{k',0}^{sd})dt \tag{5.3.17}$$

with $\mathbb{E}\{\hat{\eta}\}=0$ and $\sigma_{\hat{\eta}}^2 = N_cN_0\sum_{k'=0}^{K'-1}\left|\alpha_{k',0}^{sd}\right|^2$. The real part, η, of $\hat{\eta}$ is Gaussian variable with zero mean and variance

$$\sigma_\eta^2 = \frac{1}{2}\sigma_{\hat{\eta}}^2 = \frac{N_cN_0}{2}\sum_{k'=0}^{K'-1}\left|\alpha_{k',0}^{sd}\right|^2. \tag{5.3.18}$$

5.4 BER Performance Analysis

In this section, we analyze the BER performance of our relay network based DS-BPSK IR-UWB system. From 5.2.11and 5.3.2, the decision variable can be written as

$$\hat{Z} = D^{sd} + I_s^{sd} + I_{MAI}^{sd} + \eta^{sd} + \lambda(D^{rd} + I_s^{rd} + I_{MAI}^{rd} + \eta^{rd}) \tag{5.4.1}$$

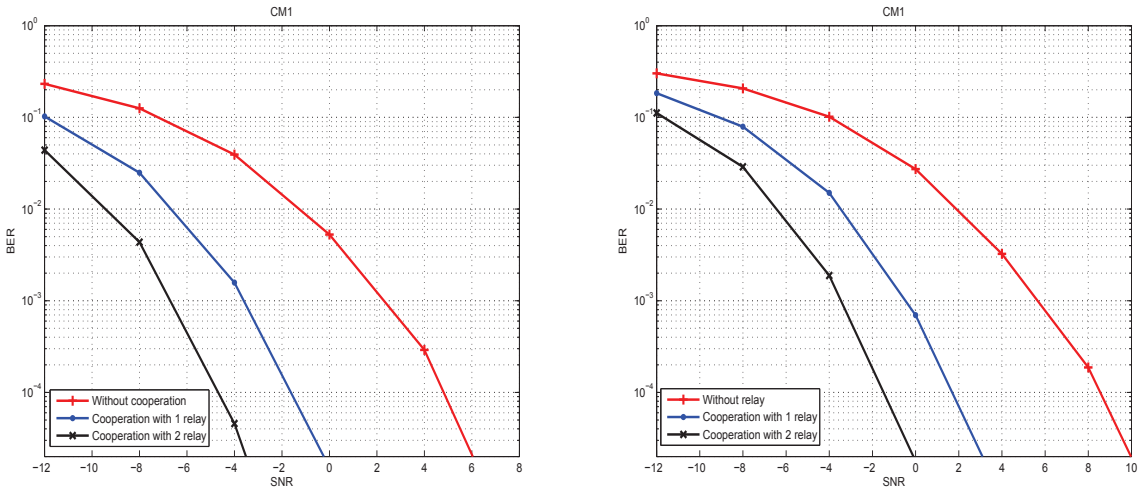
where the statistics of D^{sd}, I_s^{sd}, I_{MAI}^{sd} and η^{sd} have been obtained in the previous section. The statistics of D^{rd}, I_s^{rd}, I_{MAI}^{rd} and η^{rd} can be obtained similar to 5.3.4, 5.3.6, 5.3.15 and 5.3.18, respectively. Hence, the conditional probability of bit error is given by

$$P_e = P\left(I_s^{sd} + I_{MAI}^{sd} + \eta^{sd} + \lambda I_s^{rd} + \lambda I_{MAI}^{rd} + \lambda\eta^{rd} \le -D^{sd} - \lambda D^{rd}\mid_{b^s=0}\right) \tag{5.4.2}$$

5.5 Simulation Results And Discussion

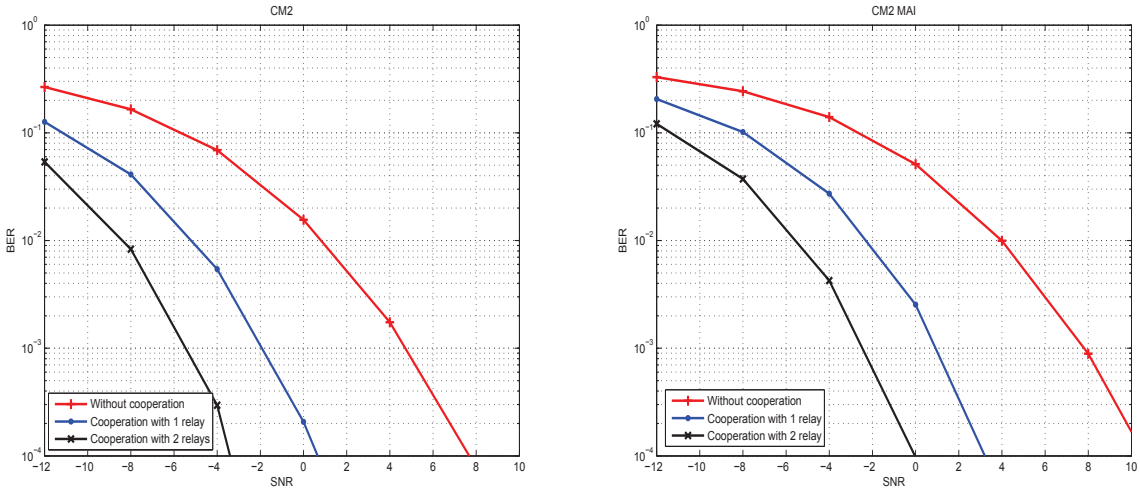
In this section, we present simulation results for the BER performance of a DS-BPSK UWB system with relay cooperation. Monte Carlo simulations have been carried out with and without MAI. We employ the second derivative of a Gaussian pulse with a duration of $0.7ns$. We adopt the UWB IEEE 802.15.4a channel models between nodes. The UWB channels have been chosen randomly from a set of 500 channel realizations and the BER performance has been averaged over at least 100 channels. The channel bandwidth is set to 3 GHz. The pathloss is

considered as function of distance and its frequency dependency is ignored. The transmitter power decays following the power law described in ([17], eq. (5)). We also assume equal transmitted powers at all nodes and at most equal to the FCC maximum emission power limit. A five-finger P-Rake receiver is employed with a combination factor $\lambda = PL_{rd}/PL_{SD}$, where PL_{rd} and PL_{sd} are the pathloss in dB of the R-D and S-D links, respectively. In the simulations, each frame consists of 100 bits; where each bit is spread into a set of 7-chips PN code. The chip duration T_c equals $10ns$ and thus the bit rate equals $14.28Mbits/s$. Higher data rate can be obtained by making the chip duration shorter. This may leads to inter-chip interference when the chip intervals becomes smaller than the delay spread of the UWB channel impulse response. Each chip is presented by a single pulse. In all results, we show the BER performance versus the SNR per bit under UWB IEEE802.15.4a channel models for (*i*) residential LOS and NLOS environments referred to CM1 and CM2 respectively and for (*ii*) office LOS and NLOS environments referred to CM3 and CM4, respectively. We assume that the relay node is exactly at the middle point between the source and destination. With respect to this assumption, the difference in the average SNRs are given in table 4.5.1 for the different types of UWB channel models.



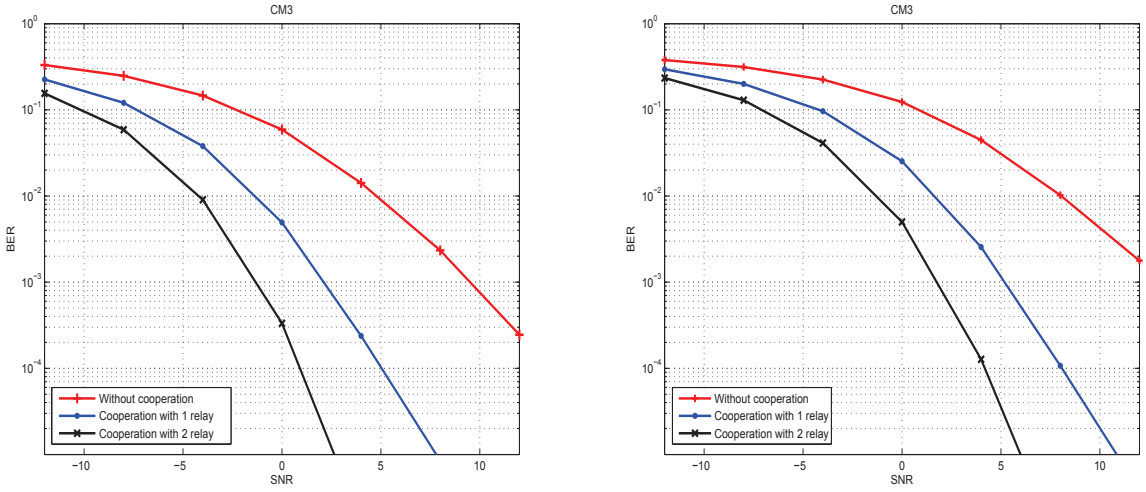
(a) (b)

FIGURE 5.5.1 – BER performance of DS-BPSK UWB non-cooperative and cooperative (with 1 and 2 relays) system with error-free detection at relay nodes using 5 P-Rake receiver under CM1 . (a) Without MAI. (b) In presence of MAI of one additional user.



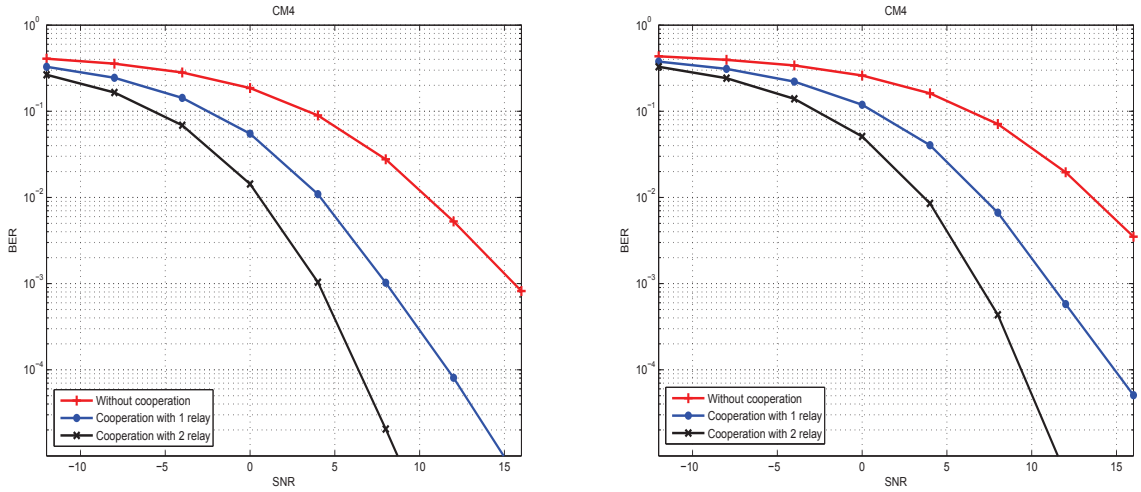
(a) (b)

FIGURE 5.5.2 – BER performance of DS-BPSK UWB non-cooperative and cooperative (with 1 and 2 relays) system with error-free detection at relay nodes using 5 P-Rake receiver under CM2 . (a) Without MAI. (b) In presence of MAI of one additional user.



(a) (b)

FIGURE 5.5.3 – BER performance of DS-BPSK UWB non-cooperative and cooperative (with 1 and 2 relays) system with error-free detection at relay nodes using 5 P-Rake receiver under CM3 . (a) Without MAI. (b) In presence of MAI of one additional user.



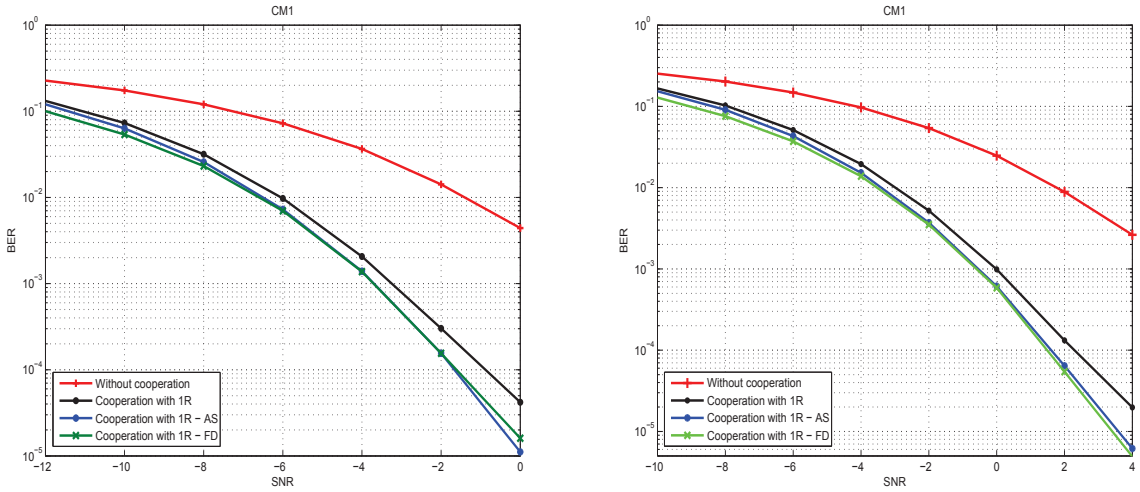
(a) (b)

FIGURE 5.5.4 – BER performance of DS-BPSK UWB non-cooperative and cooperative (with 1 and 2 relays) system with error-free detection at relay nodes using 5 P-Rake receiver under CM4 . (a) Without MAI. (b) In presence of MAI of one additional user.

Figs. 5.5.1-5.5.4 shows the BER performance of the system considering perfect S-R channels. We note that in the absence of MAI (fig. 5.5.1-5.5.4-a), a significant BER performance improvement is obtained by the use of one relay node. This is due to the diversity gain provided by that relay. When cooperating with two nodes to relay the source message, an additional performance improvement is obtained. Intuitively, when the links between the source and relays are error-free, full diversity is always achieved (assuming independent fading channels) and the system is similar to MIMO with $N_r + 1$ transmit antennas, where N_r is the number of relays.

Since the symbol period is equal to 7 chips durations, which is larger than the delay spread UWB channel models, then the effect of ISI in DS-BPSK UWB system will be neglected. Obviously, the benefits of cooperation are asserted, and the performance improved when the number of cooperative relays is increased.

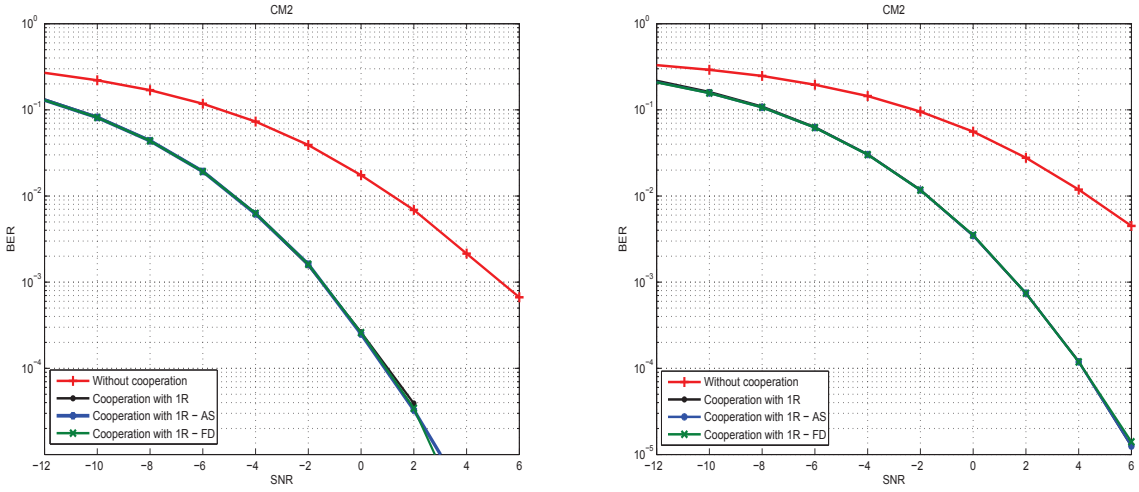
Fig. 5.5.1-b illustrates the BER performance of the system with the existence of interfering signal considering perfect S-R channels. In comparison to the former case, we note that the overall system performance is significantly degraded when MAI is present even when using relay cooperation. This is due to the fact that the received signals at the destination from the source and the relay nodes suffer from MAI interference. But, the cooperation with one and two relays in this case brings the same diversity gain which improve the detection reliability.



47

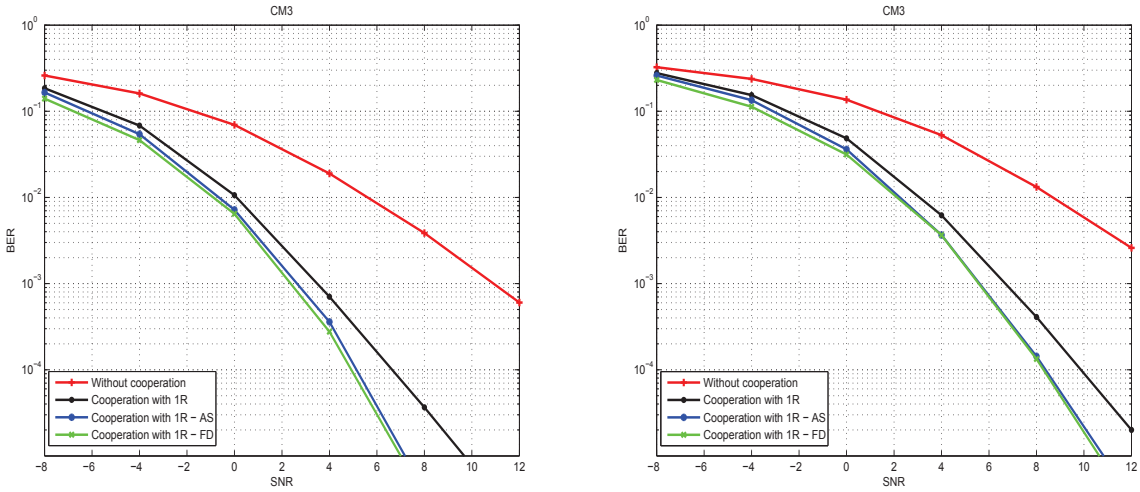
(a) (b)

FIGURE 5.5.5 – BER performance of DS-BPSK UWB system with relay cooperation under CM1 with error at relay nodes. (a) Without MAI. (b) In presence of MAI of one additional user.



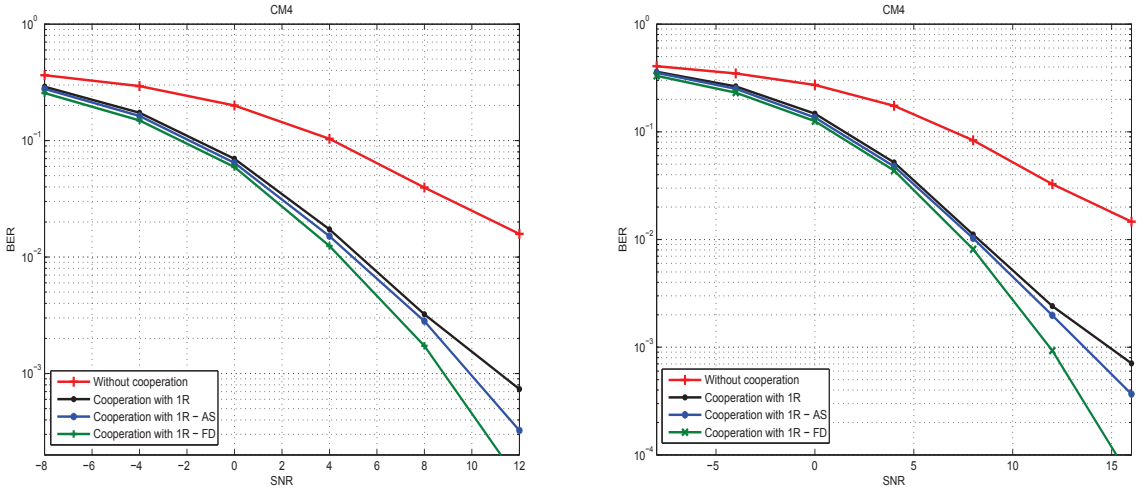
(a) (b)

FIGURE 5.5.6 – BER performance of DS-BPSK UWB system with relay cooperation under CM2 with error at relay nodes. (a) Without MAI. (b) In presence of MAI of one additional user



(a) (b)

FIGURE 5.5.7 – BER performance of DS-BPSK UWB system with relay cooperation under CM3 with error at relay nodes. (a) Without MAI. (b) In presence of MAI of one additional user



(a) (b)

FIGURE 5.5.8 – BER performance of DS-BPSK UWB system with relay cooperation under CM4 with error at relay nodes. (a) Without MAI. (b) In presence of MAI of one additional user

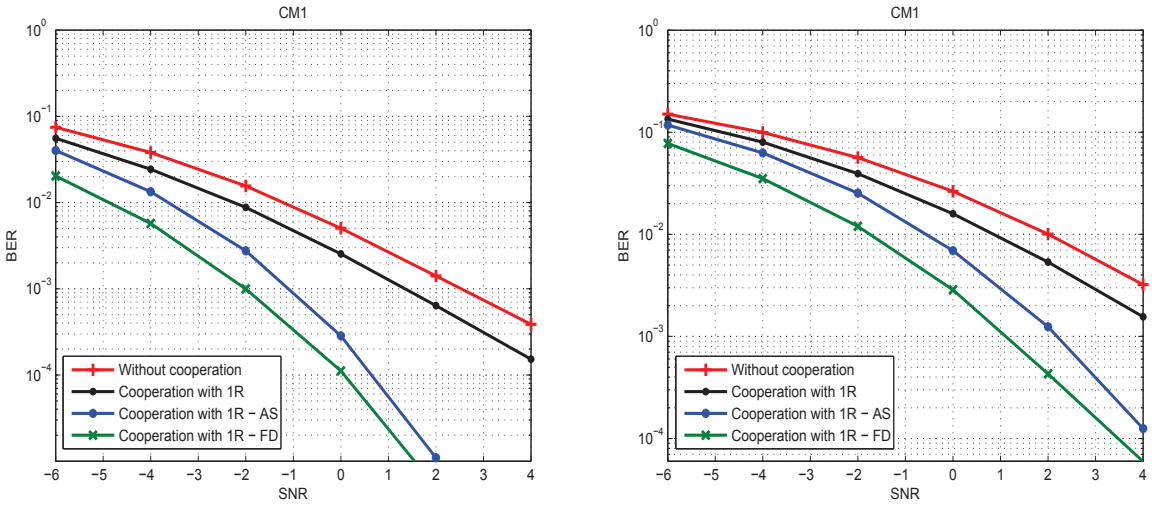
Figs. 5.5.5-5.5.8 show the BER performance of the system for CM1, CM2, CM3 and CM4 channels, respectively. The BER performance is compared considering four cases; without relay (noncooperative), relay equipped with a single antenna, relay equipped with four antennas and only the best antenna is selected (referred to as (AS)), and relay with four antennas where

no antenna selection is employed (referred to as a full diversity (FD)). The last case corresponds to a single input multiple outputs (SIMO) system for the S-R link, where the receiver coherently combines the received signals from the four antennas. This requires four RF chains at the relay node and results in cost increment. However, this case has been considered in our results for comparison purposes. From these results, we note that in both cases (presence and absence of MAI), performance improvement is obtained due to relay cooperation in contrast to noncooperative performance even when considering errors at the relay.

In DS-BPSK, each bit is presented by N_c pulses, thus the energy per bit is N_c times the energy per pulse. In our simulation, the power of each transmitted pulse is at most equal to the maximum allowed power determined by FCC. In this case the energy per bit can be increased by increasing N_c and thus we reach better performance while the FCC regulation is still met. In addition, the use of PN codes increase the signal resistance to noise and interference and thus improve the performance of the overall system as well as the benefits of cooperation.

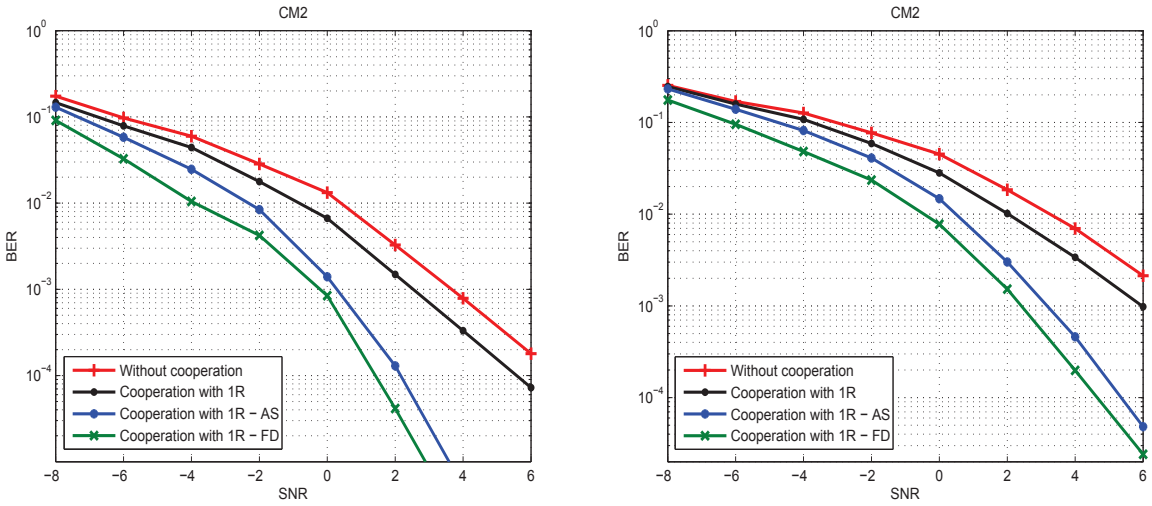
Actually, the imperfect S-R channel causes errors of detection at the relay node which propagate to the destination in the second time slot and deteriorates the diversity gain of cooperation. Our solution is to use antenna selection at the relay in order to enhance the S-R link reliability and mitigate error propagation. This makes S-R links more reliable than S-D link since the average SNR of the $r_r(t)$ signal is higher than $r_{d_2}(t)$, see table 4.5.1. Recall also that, each bit is encoded into N_c pulses which increase the received energy per bit and enhance detection reliability. This makes the differentiation between the different antennas less effective, and the advantages of antenna selection strategy cannot bring considerable enhancement to the BER performance of cooperation transmission.

In order to show the utilities of antenna selection, we consider in what follow another scenario of network topology. We assume a relay network of three nodes (S, R and D) that form an equilateral triangle. This yields equal received power from all users since the three nodes are located at equal distances from each others. We also change the combination factor to be 1, whereas all other parameters remain unchanged. Figs.5.5.9-5.5.12 show the BER performance of the system for CM1, CM2, CM3 and CM4 channels, respectively.



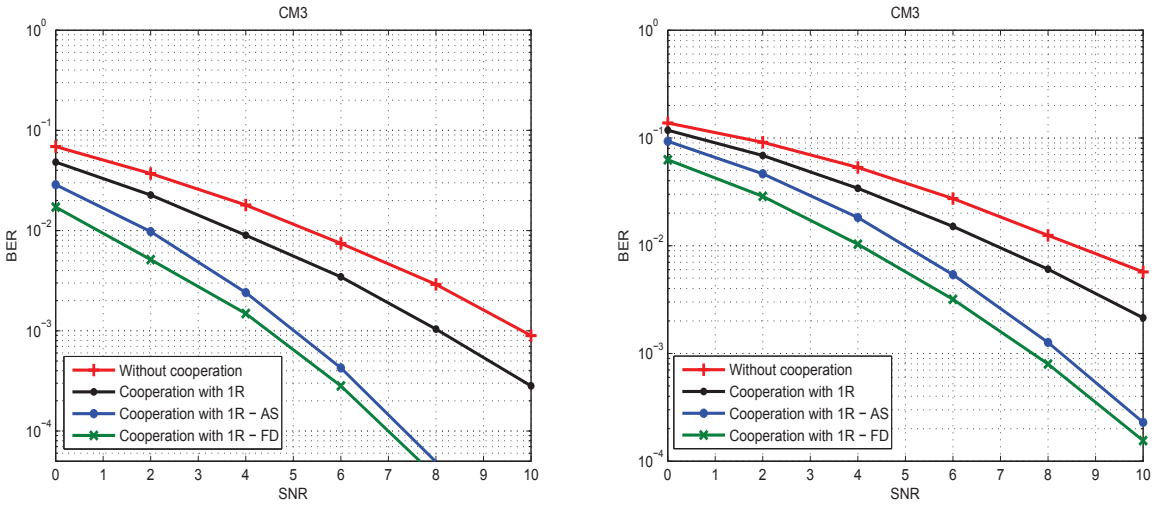
(a) (b)

FIGURE 5.5.9 – BER performance of DS-BPSK UWB system with relay cooperation under CM1 with error at relay nodes. (a) Without MAI. (b) In presence of MAI of one additional user.



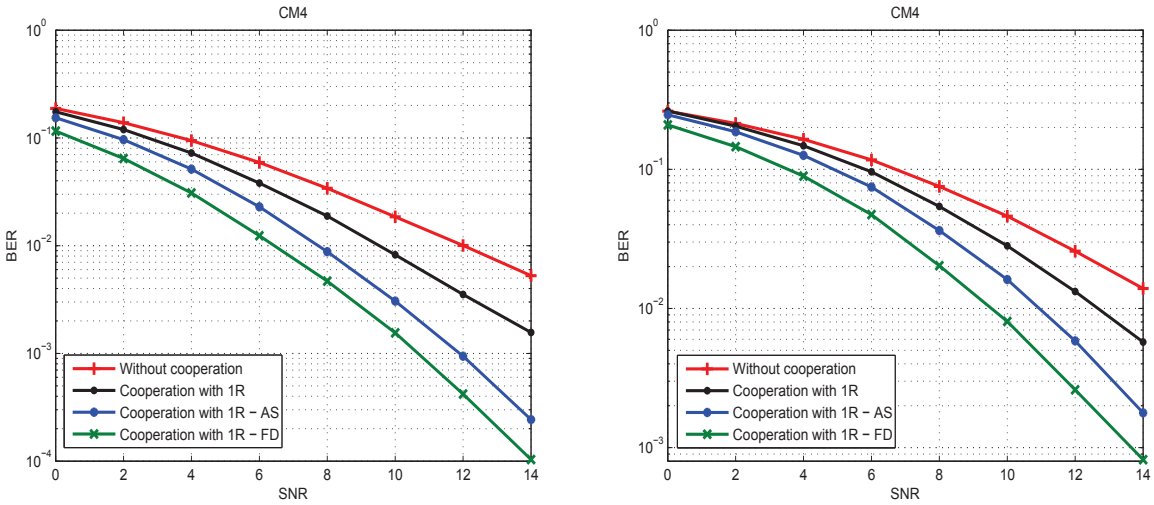
(a) (b)

FIGURE 5.5.10 – BER performance of DS-BPSK UWB system with relay cooperation under CM2 with error at relay nodes. (a) Without MAI. (b) In presence of MAI of one additional user



(a) (b)

FIGURE 5.5.11 – BER performance of DS-BPSK UWB system with relay cooperation under CM3 with error at relay nodes. (a) Without MAI. (b) In presence of MAI of one additional user



(a) (b)

FIGURE 5.5.12 – BER performance of DS-BPSK UWB system with relay cooperation under CM4 with error at relay nodes. (a) Without MAI. (b) In presence of MAI of one additional user

The BER performances presented in figs.5.5.9-5.5.12 confirm the benefits of relay cooperation in all channel types. However, the performance of cooperation with one relay is curbed due to the moderated unreliability of S-R link which increases the probability of error propagation to the destination. Moreover, when considering MAI interference, the link becomes worse, and

more errors will occur at the relay. This significantly degrades the overall system performance and the benefits of a single antenna relay node is minimum. The solution to reach the benefit of relay cooperation and to overcome MAI effect is to apply antenna selection at the relay. This is shown to significantly improve the system performance even when considering MAI interference. We note that, while antenna selection maintains the full diversity order, there exist a SNR loss relative to the full complexity case (i.e. 4 RF chains).

5.6 Conclusions

In this chapter, we have examined the performance of a relay network for DS-BPSK IR-UWB system. Our results for different UWB channels were presented to demonstrate the effectiveness of cooperation and antenna selection for relay network. We showed that, without MAI, a performance improvement is obtained due to the diversity gain provided by the relay nodes. However, due to the self-interference and MAI, the overall system performance is significantly degraded. To this end, we proposed a low complexity antenna selection at the relay to mitigate the interference effect and to improve the system performance. Simulation results show that employing antenna selection at the relay receiver significantly enhances the system performance and reduces.

General Conclusions and Future Works

The UWB technology represents a promising approach allowing the development of new types of wireless Local Area Networks (LANs) and Wireless Sensor Networks (WSNs). For twenty years, UWB has been an active field of research and it could be the physical layer for future multiple access wireless networks with very high bit rates, as well as low bit rate low power networks with high accuracy positioning abilities.

We presents here the conclusions of the accomplished study, and some future work propositions.

Conclusion

The essential idea of cooperative transmission in wireless systems is to exploit the broadcast nature and space diversity provided by the wireless medium. Deploying cooperative scheme in UWB TH-PPM and DS-BPSK multiple access systems, actually has accomplished considerable advantages. In this study, we have given a brief introduction to wireless channel and diversity techniques, especially cooperative diversity and relaying protocols in chapter I. In chapter II we have demonstrated the main UWB characteristics, the main UWB signal shapes, pulse modulation, multiple access techniques, and the UWB channel model. The system model, the characteristics of UWB channel for residential and office environments, the receiver structure were presented in chapter III. Consequently, in chapter IV, we have presented cooperative TH-PPM IR-UWB system and analyze the decision variable statistics at the output of the receiver. Then we have illustrated through simulation results the BER performance of this system in multiple user network. We have shown the benefits of relay cooperation on the system performance with contrast to the direct non-cooperative transmission. The overall system performance is significantly degraded in multiple access scenarios due to MAI but the benefits of cooperation still take place. Antenna selection at the relay node enhances the S-R link and thus offers further improvement of the BER performance especially when considering MAI interference. Our results also asserted that S-Rake receiver has better performance than conventional P-Rake receiver with additional complexity inherent in the need of finger selection algorithm. Cooperative DS-BPSK IR-UWB system has been studied in chapter V. Simulation results has been derived to demonstrate the benefits of relay cooperation and antenna selection on the BER performance

of the system considering different situations and under various UWB environments. The results has shown significant performance improvement due to the cooperation with one or more relays. However, the performance is deteriorated due to the self-interference and MAI, but the antenna selection strategy can be deployed when the relay is supposed to be equipped with multiple antennas to mitigate the interference effect and improve the system performance.

Perspectives

Beyond the work presented in this dissertation, this thesis may contribute to a number of open issues that need further investigations. Below, we list some topics that may be viewed as the natural continuity of our work:

- Communication between vehicles are intended to improve efficiency and safety of road traffic. An autonomous data collection and processing systems can exploit recent advances in UWB technology. In [107], we have proposed to apply cooperative diversity in vehicular communication using IR-UWB transmission.

In near future, vehicles will be equipped with wireless communication equipment that allow them to exchange messages with each other and also with a roadside infrastructure. A number of applications and services well be available including safety application, driver assistance, on board internet surfing, multimedia application and so on [108]. In vehicular communication, nearby vehicles will be able to communicate with each other without the need to backbone infrastructure or preinstalled base stations network. There are several proposals for data transmission between nodes. IEEE 802.11p is an international standard intended for both vehicle-to-vihicle (VTV) and vehicle-to-infrastructure (VTI) in the licensed band of 5.9 GHz ($5.85-5.925$ GHz). It defines enhancements to the popular WiFi standard (IEEE 802.11) required to support intelligent wireless transportation applications [109]. Based on the unlicensed IR-UWB system, we propose another alternative for wireless access in vehicular environments (WAVE). We use DSSS as a multiple access technique for the network nodes; in that, several nodes can share the same frequency band. We consider multiple vehicle transmitters signaling through the wireless access medium using IR-UWB signals, where each transmitter employs DS-BPSK modulation. The considered transmission scheme is illustrated in Fig. 5.6.1. For more details, we refer the reader to reference [107].

An ANR project (CRUISE) has just been deposited with both academic and industrial partners, in particular IFSTTAR. In this project, WSN based UWB could be one of radio interfaces.

- In our work, we have shown that the use of antenna selection at the relay node improves the BER performance of the overall system. It would be interesting to investigate the performance of a cross-layer (physical and MAC) design for the cooperative system that aims at maximizing

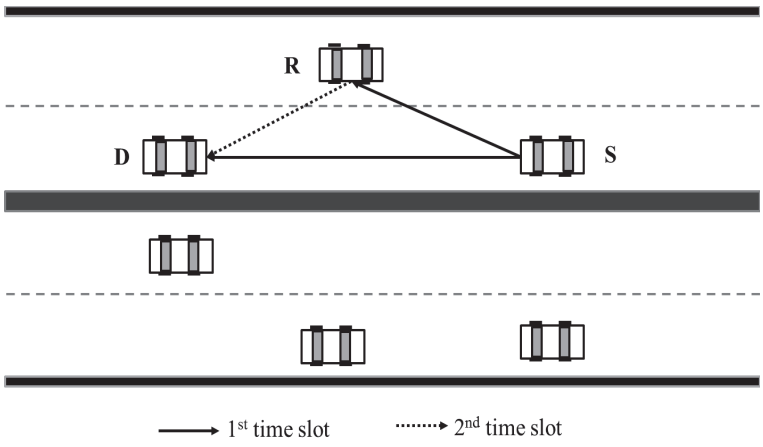


Figure 5.6.1: Relay inter-vehicle transmission scheme.

the throughput of the cooperative network by selecting the optimum antenna combination. This issue is currently under investigation by B. Bouraoui, a Ph.D. student is our team.

- The mathematical analysis of the theoretical BER performance of the two IR-UWB communication systems proposed in this thesis (i.e. TH-PPM and DS-BPSK) needs further investigations. Now, we encountered difficulties to find a proper expression of the MAI interference composition in the decision variable at the output of the Rake receiver.

- In the proposed UWB communication, the MAI interference results from the simultaneous transmission of multiple users that use the same wireless medium. Besides MAI, UWB signals will encounter interference from narrowband systems that inhabit the same frequency band. Therefore, its very interesting to investigate the performance of the system in more realistic propagation environment that includes narrowband interference.

- In this dissertation, we have assumed perfect synchronization at the receivers. Indeed, UWB communications use extremely short pulses making time synchronization a major challenge for this technology and requires further researches.

Bibliography

[1] T. Karygiannis and L. Owens, “Wireless network security 802.11, bluetooth and handheld devices,” National Institute of Standards and Technology, US Dept. of Commerce, Tech. Rep., 2002.

[2] S. M.-S. SADOUGH, “A tutorial on ultra wideband modulation and detection schemes,” Apr. 2009.

[3] M. Dohler, D.-E. Meddour, S.-M. Senouci, and H. Moustafa, “Cooperative communication system architectures for cellular networks,” *in M. Uysal (Edt), "Cooperative Communications for Improved Wireless Network Transmission: Frameworks for Virtual Antenna Array Applications," IGI-Global*, July 2009.

[4] K. Goel, A. Kaushik, S. Rani, and S. Goel, “Mobile ad-hoc and sensor network,” *IJSRET*, vol. 1, no. 1, pp. 047–051, Mar. 2012.

[5] J. Zhang, P. Orlik, Z. Sahinoglu, A. Molisch, and P. Kinney, “Uwb systems for wireless sensor networks,” *Proceedings of the IEEE*, vol. 97, no. 2, pp. 313–331, 2009.

[6] Y. Lim, H. Seo, and B. G. Lee, “Lifetime maximization under data convergence latency constraint in wireless sensor networks,” *IEEE Communications Society, Globecom*, 2004.

[7] D. W. Carman, P. S. Kruus, and B. J. Matt, “Constraints and approaches for distributed sensor network security,” NAI Labs, Tech. Rep., Sep. 2000.

[8] C. de M. Cordeiro and D. P. Agrawal, “Mobile ad hoc networking,” *Tutorial/short course in 20th brazilian symposium on computer networks*, pp. 125–186, May 2002.

[9] A. Sendonaris, E. Erkip, and B. Aazhang, “User cooperation diversity - part I System description,” *IEEE Trans. Communications*, vol. 51, no. 11, pp. 1927–1938, Nov. 2003.

[10] ——, “User cooperation diversity - part II implementation aspects and performance analysis,” *IEEE Trans. Communications*, vol. 51, no. 11, pp. 1939–1948, Nov. 2003.

[11] R. U. Nabar, H. Bölcskei, and F. W. Kneubühler, “Fading relay channels: Performance limits and space- time signal design,” *IEEE Journal on Selected Areas in Communications*, vol. 22, no. 6, pp. 1099–1109, Aug. 2004.

[12] J. N. Laneman, D. N. C. Tse, and G. W. Wornell, "Cooperative diversity in wireless networks: efficient protocols and outage behavior," *IEEE Trans. on Information Theory*, vol. 50, no. 12, pp. 3062–3080, Dec. 2004.

[13] R. U. Nabar and H. Bölcskei, "Space-time signal design for fading relay channels," in *Proc. of IEEE Global Telecommunications Conference (GLOBECOM)*, vol. 4, Dec. 2003, pp. 1952–1956.

[14] F. Shebli, "Réseaux de capteurs sans fil: minimisation de la consommation d'énergie et application à la localisation de cibles." Ph.D. dissertation, UVHC - IEMN - DOAE, 2008.

[15] A. Eid, W. Hamouda, and I. Dayoub, "Cooperative diversity in asynchronous CDMA over frequency-selective fading channel," *IET Proceedings-Communications*, vol. 5, no. 5, pp. 683–692, May 2011.

[16] H. B. Chikha, "Étude et amélioration de turbo-codage distribué pour les réseaux coopératifs," Ph.D. dissertation, UVHC, France and ENIT, Tunisia, 2012.

[17] A. F. Molisch, K. Balakrishnan, C.-C. Chong, S. Emami, A. Fort, J. Karedal, J. Kunisch, H. Schantz, U. Schuster, and K. Siwiak, "IEEE 802.15.4a channel model - final report," *IEEE doc.: IEEE 802.15-04-0662-02-004a*, July 2005.

[18] M. Hekeno, "Statistical modeling of small scale fading channels," Master's thesis, Florida State University FAMU - FSU college of engineering, Dec. 2007.

[19] G. E. Athanasiadou, A. R. Nix, and J. P. McGeehan, "A microcellular ray-tracing propagation model and evaluation of its narrowband and wideband predictions," *IEEE Journal on Selected Areas in Communications, Wireless Communications series*, Mar. 2000.

[20] M. R. Rao, "Statistical modeling of small scale fading channels," Master's thesis, Thapar University, Patiala-147004, Punjab, India, June 2010.

[21] V. Tarokh, N. Seshadri, and A. R. Calderbank, "Space-time codes for high data rate wireless communications : performance criterion and code construction," *IEEE Trans. on Inform. Theory*, March 1998.

[22] ——, "The art of signaling : Fifty years of coding theory," *IEEE Trans. on Inform. Theory*, Oct. 1998.

[23] S. Verdu, "Wireless bandwidth in the making," *IEEE Commun. Mag.*, July 2000.

[24] A. F. Naguib, N. Seshadri, and A. R. Calderbank, "Increasing data rate over wireless channels," *EEE Signal Processing Mag.*, May 2000.

[25] T. W. C. Brown, “Antenna diversity for mobile terminals,” Ph.D. dissertation, University of Surrey, Sep. 2002.

[26] M. Schwartz, W. R. Bennett, and S. Stein, *Communication systems and techniques*. New York: IEEE Press, 1966.

[27] K. Sulonen and P. Vainikainen, “Evaluation of handset antenna configurations,” *Dept. of Electrical and Communications Engineering, Helsinki University of Technology, Finland*, March 1999.

[28] A. Paulraj, R. Nabar, , and D. Gore, *Introduction to Space-Time Wireless Communications*. Cambridge University Press, May 2003.

[29] M. Jankiraman, *Space- Time Codes and MIMO System*. Artech House INC., 2004.

[30] C. E. Shannon, “A mathematical theory of communication,” *Bell System Technical Journal*, July 1948.

[31] G. J. Foschini, “Layered space-time architecture for wireless communication,” *Bell Labs Technical Journal*, Autumn 1996.

[32] I. E. Telatar, “Capacity of multi-antenna gaussian channels,” *Bell Labs Technical Memorandum*, 1995.

[33] D. Gesbert and J. Akhtar, “Breaking the barriers of shannon’s capacity: An overview of mimo wireless systems,” *Telektronikk*, 2002.

[34] D. Halperin, W. Hu, A. Sheth, and D. Wetherall, “802.11 with multiple antennas for dummies,” *ACM SIGCOMM Computer Communication Review*, Jan. 2010.

[35] A. F. Dana and B. Hassibi, “On the power efficiency of sensory and ad hoc wireless networks,” *IEEE Trans. on Inf. Theory*, vol. 52, no. 7, July 2006.

[36] J. N. Laneman and G. W. Wornel, “Distributed space-time-coded protocols for exploiting cooperative diversity in wireless network,” *IEEE Trans. on Information Theory*, vol. 49, pp. 2415–2425, Oct. 2003.

[37] T. M. Cover and A. E. Gamal, “Capacity theorems for the relay channel,” *IEEE Trans. on Information Theory*, vol. IT-25, no. 5, Sep. 1979.

[38] M. R. Souryal and B. R. Vojcic, “Performance of amplify-and-forward and decode-and-forward relaying in rayleigh fading with turbo codes,” in *IEEE International Conference on Acoustics, Speech, and Signal Processing (ICASSP)*, vol. 4, May 2006, p. IV.

[39] M. O. Hasna and M. S. Alouini, "A performance study of dual-hop transmissions with fixed gain relays," *IEEE Trans. on Wireless Commun.*, vol. 3, no. 6, pp. 1963–1968, Nov. 2004.

[40] K. Azarian, H. E. Gamal, and P. Schniter, "On the power efficiency of sensory and ad hoc wireless networks," *IEEE Trans. on Inf. Theory*, vol. 51, no. 12, pp. 4152–4172, Dec. 2005.

[41] B. Zhao and M. C. Valenti, "Cooperative diversity using distributed turbo codes," in *Proc. Virginia Tech Symp. on Wireless Personal Commun.*, June. 2003.

[42] R. Liu, P. Spasojevic, and E. Soljanin, "Punctured turbo code ensembles," in *IEEE Information Theory Workshop (ITW) Conf.*, Mar. 2003.

[43] M. Janani, A. Hedayat, T. E. Hunter, and A. Norsatinia, "Coded cooperation in wireless communications: Space-time transmission and iterative decoding," *IEEE Transaction On Signal Processing*, vol. 52, no. 2, pp. 362–371, Feb. 2004.

[44] A. Wittneben, "A new bandwidth efficient transmit antenna modulation diversity scheme for linear digital modulation," in *IEEE International Conf. Comm. (ICC93)*, vol. 3, May 1993, pp. 1630–1634.

[45] G. Kramer, M. Gastpar, and P. Gupta, "Cooperative strategies and capacity theorems for relay networks," *IEEE Trans. Inf. Theory*, vol. 51, no. 9, pp. 3037–3063, Sept. 2005.

[46] E. C. van der Meulen, "Three-terminal communication channels," *Advances in Applied Probability*, vol. 3, pp. 120–154, 1971.

[47] J. N. Laneman and G. W. Wornell, "Energy-efficient antenna sharing and relaying for wireless networks," in *IEEE Wireless Commun. Networking Conf. (WCNC)*, vol. 1, Oct. 2000, pp. 7–12.

[48] A. Nosratinia, T. E. Hunter, and A. Hedayat, "Cooperative communication in wireless networks," *IEEE Communications Magazine*, vol. 42, pp. 74–80, Oct. 2004.

[49] P. Liu, Z. Tao, Z. Lin, E. Erkip, and S. Panwar, "Cooperative wireless communications: A cross-layer approach," *IEEE Wireless Communications*, vol. 13, no. 4, pp. 84–92, Aug. 2006.

[50] H. B. Chikha, "Analysis and design of communication techniques in spectrally efficient wireless relaying systemnce and enit," Ph.D. dissertation, ETH Zurich, 2010.

[51] X. He, "Cooperative communications in wireless local area networks: Mac protocol design and multi-layer solutions," Ph.D. dissertation, Department of Information and Communication Technology, University of Agder, Norway, 2012.

[52] P. Sudarshan, H. Dai, and B. L. Hughes, "Statistics-based antenna selection for multiple-access mimo systems," in *Proc. Asilomar Conf. on Signals, Systems, and Computers*, Nov. 2004.

[53] S. Sanayei and A. Nosratinia, "Antenna selection in mimo systems," *IEEE Commun. Mag.*, vol. 42, no. 10, pp. 68–73, Oct. 2004.

[54] T. M. Duman and A. Ghrayeb, *Coding for MIMO Communication Systemsm*. John Wiley & Sons, Ltd, 2007.

[55] X. Zeng and A. Ghrayeb, "Performance bounds for space-time block codes with antenna selection," *IEEE Trans. on Inf. Theory*, vol. 50, no. 9, pp. 2130–2137, Sept. 2004.

[56] W. Hamouda and A. Ghrayeb, "Performance of combined channel coding and space time block coding systems with antenna selection," in *Proc. IEEE 59th Vehicular Technology Conference (VTC)*, vol. 2, May 2004, pp. 623– 627.

[57] D. A. Gore and A. Paulraj, "Mimo antenna subset selection with space-time coding," *IEEE Trans. Signal Proc.*, vol. 50, no. 10, pp. 2580–2588, Oct. 2002.

[58] C. Zhuo, Y. Jinhong, B. Vucetic, and Z. Zhendong, "Performance of alamouti scheme with transmit antenna selection," in *15th IEEE International Symposium on Personal, Indoor and Mobile Radio Communications*, vol. 2, Sept. 2004, pp. 1135–1141.

[59] *History of UltraWideBand (UWB) Radar & Communications: Pioneers and Innovators*, Cambridge, MA, July 2000.

[60] C. Fowler, J. Entzminger, and J. Corum, "Assessment of ultra-wideband UWB technology," *IEEE Aerospace and Electronic Systems Magazine*, vol. 5, no. 11, pp. 45 – 49, Nov. 1990.

[61] R. J. Fontana, "A brief history of uwb communications." [Online]. Available: http://www.jacksons.net/tac/First%20Term/A_Brief_History_of_UWB_Communications.pdf

[62] F. C. C. (FCC), "Revision of part 15 of the communication rules regarding ultra-wideband transmission systems, first report and order," ET Docket 98-153, Washington, Tech. Rep., Feb. 2002.

[63] N. Daniele, M. Pezzin, S. Derivaz, J. Keignart, and P. rouzet, "Principle and motivations of uwb technology for high data rate wpan applications," in *Smart Objects Conf.*, France, Grenoble, 2003.

[64] F. Nekoogar, *Ultra-Wideband Communications: Fundamentals and Applications*. Prentice Hall, 2005.

[65] D. S. Zeng, A. Annamalai, and A. I. Zaghloul, "Pulse shaping filter design in uwb system," in *Proc. of the IEEE Conf. on Ultra-Wideband Systems and Technologies (ICUWBST '03)*, Reston, Va, USA,, 2003, pp. 66–70.

[66] H. Sheng, P. Orlik, A. Haimovich, L. Cimini, and J. Zhang, "On the spectral and power requirements for ultra-wideband transmission," in *IEEE International Conf. on Comm. (ICC)*, vol. 1, 2003, pp. 738–742.

[67] L. B. Michael, M. Ghavami, and R. Kohno, "Multiple pulse generator for ultra-wideband communication using hermite polynomial based orthogonal pulses," in *Proc. of the IEEE Conf. on Ultra-Wideband Sys. and Technol.*, Mar. 2002, pp. 47–51.

[68] W. Gao, K. Veeramachaneni, and L. Osadciw, "Achieving spectrum efficiency through signal design for ultra wide band sensor networks," in *IEEE Swarm Intelligence Symposium (SIS) '09*, Mar.-Apr. 2009, pp. 122–128.

[69] M. G. D. Benedetto, T. Kaiser, A. F. Molish, I. Opperman, C. Politano, and D. Porcino, "Uwb communication systems a comprehensive overview," *EURASIP, Series on Signal Processing and Communications*, 2006.

[70] R. G. Aiello and G. D. Rogerson, "Ultra-wideband wireless systems," *IEEE. Microwave Magazine*, pp. 36–47, June 2003.

[71] M. Z. Win and R. A. Scholtz, "Ultra-wide bandwidth time-hopping spread-spectrum impulse radio for wireless multiple-access communications," *IEEE Trans. on Commun.*, vol. 48, no. 4, pp. 679–691, Apr. 2000.

[72] A. P. Adsul and S. K. Bodhe, "Performance comparison of bpsk, ppm and ppv modulation based uwb receiver using low band lna with and without noise cancellation," *International Journal of Information and Telecommunication Technology (IGITT)*, vol. 4, no. 1, May 2012.

[73] M. Ghavami, L. Michael, and R. Kohno, *Ultra Wideband Signals and Systems in Communication Engineering*. Wiley, 2004.

[74] W. P. Siriwongpairat and K. J. R. Liu, *Ultra-Wideband Communications Systems: Multiband OFDM Approach*. Wiley-IEEE Press, Nov. 2007.

[75] J. G. Proakis, *Digital Communications*. New York, NY, USA: McGraw-Hill, 1995.

[76] A. F. Molisch, J. R. Foerster, and M. Pendergrass, "Channel models for ultrawideband personal area networks," *IEEE Wireless Commun.*, vol. 10, no. 6, pp. 14–21, dec. 2003.

[77] M. Chiani, M. Fabbri, A. Giorgetti, C. Kupferschmidt, S. A. E. Din, and B. Tausieskul, "Integrated project-euwb: Application-specific channel modeling with spatial and temporal correlation analysis of the theoretical limits of mimo-uwb," Tech. Rep., Jan. 2009.

[78] A. F. Molisch, "Ultrawideband propagation channels-theory, measurement, and modeling," *IEEE Transactions on Vehicular Technology*, vol. 54, no. 5, pp. 1528–1545, 2005.

[79] L. Rusch, C. Prettie, D. Cheung, Q. Li, and M. Ho, "Characterization of uwb propagation from 2 to 8 ghz in a residential environment," *IEEE Journal on Selected Areas in Communications*, 2003.

[80] D. Cassioli, M. Z. Win, and A. F. Molisch, "A statistical model for the uwb indoor channel," in *Vehicular Technology Conference, 2001. VTC 2001 Spring. IEEE VTS 53rd*, vol. 2. IEEE, 2001, pp. 1159–1163.

[81] J. Foerster, "Channel modeling sub-committee report final," Tech. Rep., Feb. 2003. [Online]. Available: http://www.ieee802.org/15/pub/2003/Mar03/02490r1P802-15_SG3a-Channel-Modeling-Subcommittee-Report-Final.zip

[82] R. M. Buehrer, A. Safaai-Jazi, W. Davis, and D. Sweeney, "Ultra-wideband propagation measurements and modeling, final report,," Tech. Rep., 2004.

[83] "http://www.ieee802.org/15/pub/tg3a.html," Page available on 04/05/2011.

[84] R. C. Qiu and I.-T. Lu, "Wideband wireless multipath channel modeling with path frequency dependence," in *in IEEE International Conference on Communications (ICC'96)*, vol. 1, 1996, pp. 277–281.

[85] ——, "Multipath resolving with frequency dependence for broadband wireless channel modeling," *IEEE Trans. Veh. Tech.*, vol. 48, no. 1, pp. 273–285, 1999.

[86] A. A. M. Saleh and R. A. Valenzuela, "A statistical model for indoor multipath propagation," *IEEE J. on Selected Areas in Comm.*, vol. 5, no. 2, pp. 128–137, 1987.

[87] Z. Z. Yazdi, M. N. Kenari, and B. Aazhang, "Bit error probability analysis of uwb communications with a relay node," *IEEE Trans. Communications*, vol. 9, no. 2, Feb. 2010.

[88] Q. Li and L. A. Rusch, "Multiuser detection for ds-cdma uwb in the home environment," *IEEE J.Sel. Areas Commun.*, vol. 20, no. 9, pp. 1701–1711, Dec. 2002.

[89] H. Arslan, "Multi-access interference cancellation receiver for time-hopping ultra-wideband communication," *Wireless Personal Communications Journal (Springer)*, vol. 42, no. 4, pp. 479–490, Sep. 2007.

[90] C. C. Chong, Y. E. Kim, S. K. Yong, and S. S. Lee, "Statistical characterization of the uwb propagation channel in indoor residential environment," *Wireless Communications and Mobile Computing*, vol. 5, no. 5, pp. 503–512, 2005.

[91] B. Kannan et al, "Uwb channel characterization in office environments," Tech. Rep. Document IEEE 802.15-04-0439-00-004a, Tech. Rep., 2004.

[92] K. Haneda, J. Takada, and T. Kobayashi, "Spatio-temporal uwb propagation channel characterization," *IEEE 802.15-04-0112-01-004a*, Mar. 2004.

[93] A. F. Molisch, D. Cassioli, C. C. Chong, S. Emami, A. Fort, B. Kannan, J. Karedal, J. Kunisch, H. G. Schantz, K. Siwiak *et al.*, "A comprehensive standardized model for ultrawideband propagation channels," *Antennas and Propagation, IEEE Transactions on*, vol. 54, no. 11, pp. 3151–3166, 2006.

[94] G. L. Stüber, *Principles of mobile communication*. Springer, 2011.

[95] D. Cassioli, M. Z. Win, F. Vatalaro, and A. F. Molisch, "Performance of low-complexity rake reception in a realistic uwb channel," in *ICC 2002. IEEE International Conference on Communications.*, vol. 2. IEEE, 2002, pp. 763–767.

[96] Y. Zhao, "The study of multiple access techniques in ultra wideband impulse radio communications," Ph.D. dissertation, The University of Akron, 2005.

[97] A. F. Molisch, Y. P. Nakache, P. Orlik, J. Zhang, Y. Wu, S. Gezici, S. Y. Kung, H. Kobayashi, H. V. Poor, Y. G. Li *et al.*, "An efficient low-cost time-hopping impulse radio for high data rate transmission," in *Proc. IEEE 6th International Symposium on Wireless Personal Multimedia Communications (WPMC 2003)*, 2003, pp. 19–22.

[98] A. A. D'Amico, U. Mengali, and M. Morelli, "Multipath channel estimation for the uplink of a ds-cdma system," in *ICC 2002. IEEE International Conference on Communications*, vol. 1. IEEE, 2002, pp. 16–20.

[99] G. L. Turin, "Introduction to spread-spectrum antimultipath techniques and their application to urban digital radio," *Proceedings of the IEEE*, vol. 68, no. 3, pp. 328–353, 1980.

[100] M. Z. Win and R. A. Scholtz, "On the robustness of ultra-wide bandwidth signals in dense multipath environments," *IEEE Communications Letters*, vol. 2, no. 2, pp. 51–53, 1998.

[101] W. Cao, A. Nallanathan, and C. C. Chai, "Exact ber analysis of ds ppm uwb multiple access system in lognormal multipath fading channels," *in Proc. IEEE Globecom Conf.*, pp. 1–5, Nov. 2006.

[102] J. D. Choi and W. E. Stark, "Performance of ultra-wideband communications with sub-optimal receivers in multipath channels," *IEEE J.Sel. Areas Commun.*, vol. 20, no. 9, pp. 1758–1766, Dec. 2002.

[103] T. S. Rappaport, *Wireless Communications Principles and Practice*. Prentice Hall PTR, 1996.

[104] H. Ding, Y. Zhang, and X. Wu, "Performance evaluation of ds-bpsk uwb multiple-access systems in standard uwb channels," *IPCCC*, pp. 7 pp. – 348, Mai. 2006.

[105] S. Gezici, H. Kobayashi, H. V. Poor, and A. F. Molisch, "Evaluation of impulse radio uwb systems with pulse-based polarity randomization," *IEEE Trans. Signal Processing.*, vol. 53, no. 7, pp. 2537–2549, Jul. 2005.

[106] W. P. Siriwongpairat, W. Su, M. Olfat, and K. J. R. Liu, "Multiband-ofdm mimo coding framework for uwb communication systems," *IEEE Trans. Signal Process.*, vol. 54, no. 1, pp. 214–224, Jan. 2006.

[107] Y. Issa, I. Dayoub, and A. Bensrhair, "Performance of inter-vehicle relay network based ir-uwb," *springer*, vol. 7865, pp. 96–106, 2013.

[108] A. Festag, A. Hessler, R. Baldessari, L. Le, W. Zhang, and D. Westhoff, "Vehicle-to-vehicle and road-side sensor communication for enhanced road safety," *15th World Congress on Intelligent Transport Systems*, 2008.

[109] "IEEE p802.11p/d3.0, draft amendment for wireless access in vehicular environments (WAVE," July 2007.

Titre: Contributions à la diversité coopérative dans des systèmes ULB d'accès multiple

Résumé: Ce travail s'intéresse aux transmissions ultralarge bande (ULB) dans les réseaux sans fils. La diversité spatiale est introduite par l'utilisation du système multiple-input multiple-output (MIMO) comme une technique efficace pour lutter contre l'évanouissement dû aux trajets multiples dans les communications sans fils. Mais, souvent l'intégration d'antennes multiples au niveau de l'émetteur ou du récepteur est coûteuse. Comme alternative, nous proposons d'utiliser la diversité coopérative qui garantit des gains de diversité spatiale en exploitant les techniques MIMO traditionnelles sans avoir besoin d'antennes multiples. L'objectif est d'introduire la diversité coopérative aux systèmes de transmission ULB. Nous considérons deux techniques d'accès multiple avec des schémas de modulation différents (time hopping pulse position modulation TH-PPM et direct sequence binary phase shift keying DS-BPSK) avec le protocole de coopération decode-and-forward (DF). Nous utilisons le récepteur Rake afin d'exploiter la diversité de trajet multiple et analysons les statistiques de variable de décision à la sortie de ce récepteur. Nous présentons des résultats de simulation de la performance en termes de taux d'erreur binaire (TER) du système étudié sous différents canaux UWB compte tenu de la norme IEEE 802.15.4a. Ces résultats montrent que la coopération avec des relais améliore significativement les performances de transmission ULB, et que le gain de diversité augmente proportionnellement avec le nombre de relais. En présence d'IAM, la performance du système se dégrade de manière significative, mais l'avantage de la coopération est encore modérément efficace. La performance dans ce cas est limitée en termes de diversité achevée parce que le canal entre la source et le relais en présence d'IAM devient moins favorable. C'est pourquoi nous proposons d'utiliser la technique de sélection d'antenne au relais afin d'améliorer la fiabilité du canal source-relais. Cette solution permet d'améliorer la performance grâce au gain de la diversité d'antennes multiples disponibles au relais toute en n'utilisant qu'une seule chaîne radiofréquence (RF), qui conduit à une réduction des coûts et de la complexité.

Mots-clés: Diversité coopérative, ULB, MIMO virtuel, sélection d'antennes, récepteur Rake.

Title: Contributions to Cooperative Diversity in Multiple Access UWB Systems

Abstract: This work focuses on the ultra wideband (UWB) transmission in wireless networks. Spatial diversity is introduced by the use of multiple-input multiple-output (MIMO) system as an effective technique to overcome multipath fading in wireless communications. But the integration of multiple antennas at the transmitter or receiver is often costly. As an alternative, we propose to use the cooperative diversity that provides spatial diversity gains by exploiting the traditional MIMO techniques without the need for multiple antennas. The objective is to introduce cooperative diversity to UWB transmission systems. We consider two multiple access techniques with different modulation schemes (time hopping pulse position modulation TH-PPM and direct sequence binary Phase Shift Keying DS-BPSK) with the cooperation protocol decode-and-forward (DF). We use the Rake receiver to exploit multipath diversity and analyze the decision variable statistics at the output of the receiver. We present simulation results of the BER performance of the proposed system under different UWB channel given the IEEE 802.15.4a standard. Our results show that the cooperation with the relay significantly improves the performance of UWB transmission, and that the diversity gain increases with the number of relays. In the presence of MAI, the overall system performance degrades significantly, but the benefit of cooperation is still moderately effective. The performance in this case is limited in terms of attainable diversity that the source-relay link becomes worse when MAI is present. That is why we propose to use antenna selection at the relay receiver in order to improve the reliability of the source-relay link. This solution is shown to improve the performance by exploiting the diversity of the available antennas at the relay, while using a single Radio Frequency (RF) chains. This leads to reduced cost and complexity.

Keywords: *Cooperative diversity, UWB, virtual MIMO, antennas selection, Rake receiver.*